89-2062

TECHNICAL REPORT TO THE CALIFORNIA COASTAL COMMISSION

L. Physical and Chemical Oceanography

MARINE REVIEW COMMITTEE, INC.

William W. Murdoch, Chairman
University of California

Byron J. Mechalas
Southern California Edison Company

Rimmon C. Fay
Pacific Bio-Marine Labs, Inc.

Prepared by:
John Reitzel

Project Principal Investigators:
John Reitzel
Hany Elwany
Karel Zabloudil
M. Rustin Erdman

July 1989

This report analyzes and presents the results of studies by Ecosystems Management Associates, Inc. (ECO-M), which were done on behalf of the MRC over the period 1978-1988, under the direction of Mr. Karel Zabloudil. ECO-M's report to the MRC "SONGS Physical and Chemical Oceanography Final Report, Contract MRC 86-7" by Principal Investigators John Reitzel, Hany Elwany, Karel Zabloudil and M. Rustin Erdman provided the starting point for the analyses in the present report.

TECHNICAL REPORT
L. PHYSICAL-CHEMICAL OCEANOGRAPHY AT SONGS

CONTRIBUTING STAFF:
Hany Elwany
Bonnie M. Williamson

TABLE OF CONTENTS

APPENDICES

LIST OF FIGURES

This page intentionally left blank.

1.0 INTRODUCTION AND SUMMARY

1.1 Introduction

This Technical Report is a summary and discussion of studies in physical and chemical oceanography commissioned by MRC in support of the biological studies. It is written for technical readers, but not particularly for physical oceanographers, so some discursive textbook material is included here to provide background for the discussions of local conditions observed off San Onofre. The mathematical basis for some of the topics discussed is given, as a highly condensed outline, in Appendix B.

This report is mainly concerned with physical effects of SONGS that are of concern to MRC because they may produce or mediate changes in local marine populations. Section 2 is a description of natural conditions and processes that shape the marine ecosystems off San Onofre, and which are liable to be affected by SONGS; the observed interactions of the SONGS cooling system with these processes are considered in Section 3. Section 4 discusses particular potential effects of SONGS whose expected importance guided MRC's projects at various times. Section 5 is a summary and discussion of MRC's statistical studies of the effects of SONGS on underwater irradiance, which are described in detail in Appendix A, and Section 6 describes the statistically observed effects of SONGS on temperature and suspended particles.

Since this report does not set out to give an overview of all the physical and chemical data collected in MRC's programs, the reader can turn to the following references for discussions, statistical summaries, and plotted time-histories of

MRC's physical and chemical oceanographic observations off San Onofre: ECO-M 1988a, 1987d, 1987b.

1.2 Summary of the Physical Effects of SONGS

1.2.1 Water flow

SONGS Units 2 and 3 together discharge 100 m^3/sec of heated seawater through diffuser lines with multiple jets pointed offshore with an upward tilt; these jets entrain another 1000 m^3/sec, more or less, of ambient seawater within 300 m of the diffusers. The mixing of entrained water with the discharge dilutes the heat added by SONGS, to meet California thermal standards, and also produces a large seaward flow of discharged and entrained water, carrying about 1000 m^3/sec some 700 m offshore (on the average, and very approximately) in the plume of SONGS. This offshore flow is matched by an equal make-up flow toward SONGS from all directions in the sea, which brings some water from offshore to the vicinity of SONGS. The combination of plume and make-up flow amounts to a significant alteration of the natural local pattern of flow, which alters the natural distributions of suspended particles and other properties of the waters near San Onofre.

1.2.2. Suspended Particles and Underwater Light

Suspended particles in San Onofre waters are more concentrated near the bottom and near the shore, so near-bottom and nearshore waters are less transparent on the average than surface waters and midwaters further offshore. Recruitment of new kelp plants in the San Onofre kelp bed depends on the amount

of sunlight that reaches the bottom at 10 to 15 m depth, which depends on the transparency of the water overhead. The plume of SONGS goes through the San Onofre kelp bed much of the time, partly replacing ambient water with more turbid water originating closer to shore, which potentially reduces the average amount of light available to small new kelp plants on the bottom.

We estimated the actual changes induced by SONGS in average available light on the bottom by means of statistical BACIP tests comparing three stations in the San Onofre kelp bed downcoast from the diffusers with a control station in the San Mateo kelp bed 5 km upcoast, before and after Units 2 and 3 began operation. On days when the San Onofre stations were downcurrent from the diffusers for a majority of the daylight hours, the test showed a definite decrease in average light on the bottom at the San Onofre kelp bed stations, estimated at 26%. On days when the San Onofre stations were upcurrent from the diffusers, there was a statistically uncertain increase in light at the bottom which, on the balance of the evidence, could range from nearly zero up to nearly as large as the decrease on downcurrent days.

Downcurrent days outnumber upcurrent days by about 60 to 40, so the net effect over all days is a reduction of average light in the kelp bed downcoast of the diffusers, somewhere between 6% and 16% depending on the magnitude of the uncertain increase on upcurrent days. We do not have data from the part of the San Onofre kelp bed upcoast from the diffusers, but if everything except the current were symmetrical, the calculated overall effect upcoast would lie somewhere between a 12% reduction and a 6% increase.

We also made statistical comparisons between light on the bottom recorded hourly at pairs of stations, one in the plume and one outside in ambient water, as adjudged by a plume model based on the recent history of the current. Over two years with SONGS in operation, light at the plume stations averaged about 20% less than at the ambient stations in the same hour. This is not the same as the reductions estimated by the BACIP tests, which are relative to what the light would have been without SONGS, but the two kinds of estimate are in reasonable accord.

1.2.3. Temperature

SONGS is in compliance with the California thermal standard which prohibits temperature rise at the ocean surface exceeding 4°F beyond 1000 feet from the diffusers for more than half of any tidal cycle. We determined this by comparing hourly temperatures recorded during 1985 at plume and ambient stations 1000 to 1200 feet from the diffusers, using the same plume model that we used for light; plume temperature reached 4°F above ambient in only a single hour out of 972.

1.2.4. Nutrients

Much of the supply of nutrients to nearshore waters off San Onofre comes from natural upwelling of colder and richer water from greater depths offshore. SONGS may enhance this process by bringing in offshore water in the make-up flow and by lifting water entrained in the jets. There is a close relation between nitrate and temperature, so the actual effect of the make-up flow can be estimated from temperature records. BACIP tests at stations in the San Onofre kelp bed show no

evidence that SONGS has changed temperature or nutrients at the bottom in 10 to 15 m depth. The actual effect on surface nutrients due to the jets raising water from these depths to the surface is unknown and cannot be tested by temperature, but in principle it may increase the supply of nutrients to the surface canopy of the kelp at times of natural upwelling.

1.2.5. Plankton mortality and changes in abundance

SONGS kills most or all of the plankton and fish larvae that are drawn into the intakes, and may kill some other plankton and larvae by entraining them in the turbulent jets or by carrying them offshore out of their normal habitat. The depth and extent of depressions in abundances around SONGS due to these losses depends on the local long term diffusivity, which determines the capacity of the ocean to disperse new plankton to SONGS from unaffected waters. Other MRC reports show that the actual changes in average abundances found by BACIP tests on various planktonic organisms and groups are generally small, contrary to some early predictions. Physical studies of the currents recorded off San Onofre over periods of years have given approximate estimates of long term diffusivity which indicate that only small reductions in abundances due to SONGS-induced mortality are reasonably to be expected in the actual current regime.

1.2.6. Sedimentation

Reductions in water velocity across the diffusers and in the plume of SONGS are likely to cause suspended grains to settle out of the water and to be trapped in the vicinity of SONGS, perhaps to accumulate as sediments. The collection rates of

sediment traps give a rough measure of the concentration of suspended particles; a BACIP test on collection rates just above the bottom showed a 48% increase due to SONGS at a station in the San Onofre kelp bed 400 m downcoast from the diffusers, relative to a station 1400 m downcoast. A plume model test on the extinction of light near the bottom, which gives a different rough measure of particle concentration, also showed a significant increase at stations under the plume relative to ambient stations. Whether or not the operation of SONGS has actually changed the local rate or pattern of net sediment accumulation is the subject of a separate MRC study, which is treated in Technical Report B.

2.0 THE NATURAL ENVIRONMENT; PROCESSES AFFECTING LIFE IN COASTAL WATERS

This discussion of the physical environment off San Onofre concentrates on particular physical and chemical conditions that influence the abundance or range of local marine populations. The most fundamental conditions are those that affect marine plants, since nearly all marine animals ultimately depend on the plants at the bases of their food webs. The main physical problem of plant life in the sea, common to drifting marine plants and anchored giant kelp, is to bring together light from above and dissolved nutrients from below. At the surface of the sea, there is usually plenty of light, but nutrients are mostly locked up in the biomass of the existing plant populations. In deeper waters there is less light, but dissolved nutrients become available from a reservoir at depth, formed from organic matter that sank out of the light and decayed in darkness.

This section considers 1) how dissolved nutrients reach the shallow nearshore waters off San Onofre from the deep offshore reservoir; 2) how the light in these waters falls off with depth because of absorption by fine sediment particles suspended in the water; 3) the character and sources of the bottom sediments themselves, which are an important habitat in their own right; and 4) the processes of advection and turbulent dispersion in the sea, which bring together the factors required by marine life and play a large part in the response of a marine ecosystem to a local disturbance such as SONGS.

2.1 Nutrients

MRC's studies of dissolved nutrients have concentrated on nitrogen species, since these are generally considered to be the limiting nutrients in waters off Southern California, and the ratios of major nutrients are fairly stable. Of the nitrogen species, ammonia and nitrite are used by plants, and are also converted to nitrate by bacteria that can live in the dark. Nitrate is used by plants but not by aerobic bacteria, so it is taken up by phytoplankton in well-lit waters near the surface, the so called photic zone, but accumulates in deeper water below. Over the long history of marine life the continual fallout of organic matter from the photic zone has resulted in an enormous reservoir of nitrate in the deep sea, along with phosphate and other oxidized nutrients that are the end products of bacterial reactions.

In the shelf waters a few kilometers off San Onofre, the base of the photic zone (see 2.2 below) is at an average depth of something like 20 m, where the average temperature is something like 14°C. Within the photic zone there is generally a low concentration of total nitrogen, about 1 micromole/liter or less; below the photic zone is a zone called the nutricline, in which nitrate concentration rises steeply with increasing depth, to about 10 micromoles per liter at something like 35 m depth (ECO-M 1988a, Fig. 4-6a). This increase with depth indicates that nitrate is conducted upward from the deep-sea reservoir to the photic zone by turbulent mixing (see 2.4 below).

Profiles of nitrate with depth can vary a good deal over periods of hours because of internal waves, and over days, weeks and seasons because of other

processes discussed below. All these processes, though, have similar effects on temperature profiles, and it turns out that the relation of nitrate to temperature off San Onofre is fairly regular and stable. Figure 1 shows the results of all profiles of nitrate and temperature off San Onofre from 1981 through 1986, in water 10 to 100 m deep. The curve through the data points is the nitratetemperature relation from a simple physical model of upward turbulent dispersion within the nutricline and immediate uptake in the photic zone, with fluctuations in the temperature at the base of the photic zone (ECO-M 1987d). By this model, temperature accounts for 90% of the total variance of nitrate in this extensive data-set.

With this relation, we can say broadly that the availability of nutrients is adequate or good in water colder than 14°C, uncertain and variable in water between 14° and 16°C, and insufficient in water warmer than 16°C. It was not practical to make routine measurements of nutrients more often than about once a week, and this relation allows the history of nutrients to be followed in better detail from continuous records of temperature.

The inshore waters shallower than 20 m off San Onofre may receive some nutrients from runoff of streams and disturbance of bottom sediments, but the principal supply of nutrients to the inner shelf comes from events called upwellings, in which surface water near the shore is displaced by colder water from greater depths.

In shelf waters off California deeper than 20 m or so, upwelling generally results from winds blowing downcoast (that is, toward the southeast). In shallower waters close to shore, upwelling may result from any downcoast current with vertical

shear, flowing faster at the top than at the bottom, by the following mechanism (see Appendix B). The rotation of the earth gives moving water in north latitudes an acceleration proportional to its velocity, directed 90° to the right of the velocity. Acting on a vertically sheared downcoast current, this acceleration will be directed to seaward, and will be stronger at the top than at the bottom. In stratified water, with cold and dense water underlying hotter and lighter surface water, this seaward acceleration decreasing with depth can be hydrostatically balanced at all depths by a slope of the surface upward to seaward, together with an opposite slope of the isotherms upward toward shore. The slope of the isotherms upward toward the shore is the upwelling itself; the occasions when rearrangement of isotherms brings water colder than 14°C up to depths of 15 m or less in the nearshore zone are the times when this region receives most of its supply of nutrients.

The opposite process is downwelling, in which upcoast winds, or upcoast currents falling off with depth, may lead to slopes of the isotherms downward toward the shore. Downwellings that exclude water colder than 14° from the inner shelf are the times of minimal or near-zero nutrient supply to nearshore waters.

Upwellings and downwellings may happen in any season, but the seasonal changes of winds and thermal stratification combine to make nearshore upwellings most evident in the spring and early summer, and downwellings most evident in late summer and fall, as may be seen from the temperature records off San Onofre (ECO-M 1987d, 3.3). Thermal stratification begins from the top in spring, and the thin warm surface layer at that season is more easily displaced close to shore by an upwelling. This is also the season when insolation is rising rapidly to its summer peak, and enough light becomes available to allow the nutrients supplied by

upwelling to be used for rapid growth and reproduction of plants. In late summer, a thicker and warmer surface layer is established; upwellings may be confined to depths beyond the inner shelf, but downwellings may involve filling the whole nearshore water column to 20 m depth with water hotter than 16°, completely cutting off the nutrient supply.

The complications of nearshore upwelling and downwelling are brought up to make the point that these may have other causes besides longshore winds. Any longshore current in shallow water that persists for more than a day or two will be retarded by bottom friction and will tend toward a profile in which speed falls off with depth, whether it is driven by wind-stress or by a surface slope related to hydrographic conditions offshore. The mechanism producing upwelling or downwelling will work in about the same way whatever force drives the current.

The fluctuations of winds, currents, and subsurface temperatures in summer off San Onofre tend to track one another, with lower temperatures associated with downcoast winds and currents, as expected. There are times, though, when these relations break down badly; some of these times are occasions of intense upwellings and downwellings which must be ascribed to unpredictable events occurring offshore or elsewhere along the coast.

2.1.1. El Nino

At intervals of years, global events produce deep and persistent downwellings on the eastern shore of the Pacific, called El Nino events. These occur, broadly speaking, when the perennial easterly trade winds over the tropical Pacific slacken

off for a time, and the belts of westerly winds in the temperate zones encroach on the subtropics. Several consequences ensue: warm surface water piled up on the west side of the tropical Pacific by the trade winds flows back to the east as an internal wave on the main thermocline, producing massive downwelling on tropical eastern shores which may spread into the subtropics; the movement of westerly winds into lower latitudes also drives surface water to the east in lower mid-latitudes, which is probably the most immediate and important cause of downwelling off California during El Nino events; the appearance of westerly winds in lower latitudes also brings extreme storms and rainfall to coasts where wet winds from the ocean are normally rare.

Minor or moderate El Nino events recur at irregular intervals of about three to seven years. Major El Nino events in this century came in 1914-15, 1941-42, and 1957-58 (Chelton 1981), followed by the most recent and perhaps the greatest, which arrived in the fall of 1982 and remained through the summer of 1984.

Starting in August of 1982, the normal nearshore water off San Onofre was replaced in rapid stages by oceanic surface water from about five hundred kilometers to the west-southwest, identifiable by its low salinity (ECO-M 1988a, 4.1.3; Lynn *et al.* 1982). For the next two years, temperature was abnormally high in all seasons, and the nutricline was usually depressed to depths below 30 m, except for brief remissions during strong upwellings (ECO-M 1988a, 4.1.3). The winter of 1982-83 was a time of intense storms in Southern California, with very high waves, sometimes exceeding 3 m at San Onofre, and high runoff from streams in the region comparable to that in 1979-80 or the two wet winters preceding (see 2.3 below).

This El Nino event is an extreme example of the kind of natural change that can confound a simple Before-After study of the effects of SONGS on local population densities, making it necessary to use the more complex Before-After-Control-Impact design which deals with differences of abundance between an Impact location near SONGS and a Control location at distance (see Interim Technical Report: 2. Sampling design and Analytical procedures). With such a major event as the 1982-84 El Nino, nonuniformity of its impacts could masquerade as an effect of SONGS, so it is important to examine whether El Nino had markedly different physical effects at Impact and Control stations.

A high overall uniformity is shown by statistical comparisons of bottom temperature between stations in the San Onofre kelp bed (SOK) near SONGS and control stations in the San Mateo kelp (SMK) 5 km upcoast, and Barn kelp (BK) 10 km downcoast. In each of the three El Nino years 1982 through 1984, the correlation coefficients of bottom temperature between SMK and any of four stations in SOK ranged from 0.93 to 0.97, and those between BK and any of the SOK stations or SMK ranged from 0.91 to 0.96 (ECO-M 1987d, Tables 3-3-4, 9, 13). The changes in mean bottom temperature at SMK and at two SOK stations in the same depth of 13.7 m were very similar over the course of El Nino, as shown by the following table (from ECO-M 1988a, Table 4-1; the Barn kelp station is omitted here because it was deeper).

	SMK45	SOKU45 & SOKD45 (mean)
10/81 - 9/82	14.6°C	14.8°C
10/82 - 9/84	16.3°C	16.55°C
10/84 - 9/86	14.6°C	14.7°C

2.2 Irradiance

The measure of light intensity used in MRC's studies is called downward planar irradiance and represents the downward flux of photons available for photosynthetic reactions, in units of Einsteins per square meter per hour or day (E/m^2-hr or E/m^2-day; one Einstein is one mole of photons). The sunlight reaching the sea surface off San Onofre ranges from about 50 E/m^2-day in midsummer to 20 E/m^2-day in winter. Below the surface, irradiance decreases by a fraction of itself with each increment of depth, because of absorption by the water and by suspended particles of all kinds, which come together under the general name of seston. The fractional decrease per meter of depth is called the extinction coefficient K (m^{-1}); the irradiance at depth z is given by the relation $I = I_o\exp\{-Kz\}$, I_o being the surface irradiance and K the mean extinction coefficient from the surface to z. At the depth for which $Kz = 4.6$ the irradiance is 1% of the surface value, on the order of a few tenths of one E/m^2-day; this is the conventional lower boundary of the photic zone in which marine plants can grow and reproduce actively.

In nearshore waters off San Onofre, extinction ranges widely from a little above 0.1 m^{-1} to nearly 1.0 m^{-1}. The 1981-86 mean surface-to-bottom K at stations in 13.7 m depth of water was 0.25 m^{-1} plus or minus 0.12 m^{-1} standard deviation. The distribution is highly skewed, with few observed values below 0.12 m^{-1}. In the outer parts of the San Onofre kelp bed around 13.7 m depth, bottom irradiance fluctuates above and below 1% of the surface value as the mean surface-to-bottom extinction fluctuates below and above 0.34 m^{-1}; the history of extinction is likely to be a critical factor for recruitment of new kelp plants on the bottom.

Extinction is higher in the lowermost layer from the bottom to 2 m above, averaging 0.46 m^{-1} at the same stations (ECO-M 1987d, 3.2). Near the coast, average extinction generally falls off with distance from shore. Simultaneous recordings in April through July of 1980 showed average midwater extinction decreasing to seaward by about 0.10 m^{-1} per kilometer between 800 and 2800 m from shore (Reitzel 1980).

Absorption by the water and dissolved pigments accounts for the first 0.1 to 0.2 m^{-1} of extinction in San Onofre waters. The rest is due to varying concentrations of seston, which is made up of fine mineral grains, plus phytoplankton and organic detritus, suspended in the water column. These relations are shown by the regressions of extinction on seston characteristics from 82 samples taken off San Onofre in the summer of 1980 (Reitzel 1981, Table 1). The regression lines are:

$$K = 0.16 + 0.41\ A,\ r^2 = 0.81;\ \text{and}\ K = 0.19 + 0.060\ W,\ r^2 = 0.77,$$

in which A (m^{-1}) is the seston cross section (volume concentration divided by diameter) measured by Coulter counter, and W (mg/liter) is the seston concentration by dry weight. The linear relation to cross section shows that finer particles produce more extinction for a given concentration than coarser particles, in inverse proportion to their diameters.

The immediate source of mineral seston is the sediments on the bottom, which are suspended off the bottom by waves and then dispersed upward into the water column by turbulence due to currents. This process is highly selective with grain size: smaller grains with lower settling rates in water are dispersed higher into

the water column by a given level of turbulence, and remain suspended longer if the turbulence decreases. The observed relations between wave height and extinction off San Onofre are complicated and difficult to quantify. The highest extinctions are nearly always associated with high waves, but some episodes of high waves do not produce high extinctions; a given wave-episode may produce high extinction at one place but not at another. The most reasonable explanation is that the highest extinctions are associated with finer-than-normal sediments that are sporadic both in time and space. When suspended by one wave-episode, these sediments may be carried to deeper water or dispersed thinly by currents so that they are not available to cause high extinction in nearshore waters during the next wave-episode.

The ultimate sources of these fine grains are at the shoreline, either in runoff from streams or erosion of coastal bluffs, as discussed in more detail in 2.3 below. These grains make their way offshore in successive episodes of suspension by waves together with upward and lateral dispersion in the water column, and ultimately settle in water deep enough to prevent their further resuspension by waves. Any process of dispersion from a source involves a gradient of concentration toward the source (see 2.4), and a general increase of seston concentration toward the shoreline and toward the bottom is inseparable from this transport across the shelf. This is the general reason for the increase of average extinction with proximity to the shore and to the bottom off San Onofre noted above.

Advection and dispersion of seston along the shelf is faster than it is across the shelf, and extinction does not always come from local sources. The finest silt grains can remain in suspension for many days and travel many tens of miles. For some days after an episode of high waves, fine grains can sometimes remain in the

lower part of the water column even in weak currents, forming a turbid layer at the bottom that is often noted by divers off San Onofre.

The clearest mid-ocean water carries hardly any dissolved pigments or suspended particles, and can have extinction below 0.05 m^{-1}, so that 1% of surface light penetrates to 100 m or more. The massive influx of water to the shelf from hundreds of kilometers offshore that occurred in the El Nino years 1982-84 resulted in notably lower extinction and higher bottom irradiance off San Onofre in those years.

2.3 Sediments

The sediments of the inner shelf off San Onofre, beyond the surf zone and outside the localized cobble beds and reefs, are fine sands and silts, with median grain diameter decreasing gradually from about 0.09 mm in 8 m depth of water (the depth near the SONGS intakes) to about 0.06 mm in water of 18 m depth (the depth a few hundred meters offshore from the outer end of the SONGS diffusers). They are fairly well-sorted, with grain-size dispersion (the standard deviation of log diameter to the base 2) of about 0.5, meaning that about two-thirds of the grains at any place differ in size by no more than a factor of two. This general statement smooths over considerable variations between places, seasons, and years, which arise because these sediments are slowly dispersed over the shelf from sources at the shoreline that are highly localized and episodic.

The supply of fine sediments (silt and clay, with diameters of 0.06 mm or less) from distinct sources over the eleven years 1974-84 has been estimated as

follows (ECO-M 1988a, 4.6): creeks north of San Onofre up to Dana Point (San Juan and tributaries, San Mateo, and San Onofre), about 1.5 million metric tons; rivers south of San Onofre down to Oceanside (Santa Margarita and San Luis Rey), about 4 million metric tons; small watersheds near San Onofre and erosion of gullies and bluffs, about 1 million metric tons.

Over three-quarters of the total supply to this 50-kilometer stretch of coast came from the five river mouths mentioned, and nearly all of this came during short episodes of flooding in the winters 1977-78, 1978-79, 1979-80, and 1982-83. (San Juan Creek, for instance, supplied nearly half a million tons in the winter 1977-78, but only a few hundred tons in the driest winters.) The sources upcoast from San Onofre are probably the most important for San Onofre, because the prevailing drift is downcoast, both within and beyond the surf zone.

A ten-year history of sediment grain-size from quarterly samplings along the 8 m and 18 m isobaths from San Onofre to 10 km downcoast is shown in Figures 2 and 3, as contours of the percentage of silt and clay on plots whose axes are time and distance downcoast from SONGS (ECO-M 1987c). The major events of the history at 18 m depth are the rapid and localized increase from under 50% to over 70% silt and clay at about 1 km downcoast in early 1980, and the further increase to over 90% at about 2 km downcoast in early 1983. The same events appear on the history at 8 m depth as increases from about 20% to 40% silt and clay.

Changes of grain-size dispersion near SONGS indicate that the local increases of silt-clay percentage in 1980 were due to an influx of fine sediments from upcoast. Nearly all samples were well-sorted in November 1979; samples upcoast of

SONGS were poorly-sorted in March 1980; nearly all samples were poorly sorted in May 1980 (ECO-M 1987c). By far the most likely source of these sediments is the runoff of the creeks upcoast from SONGS in the wet winters of 1977-78 through 1979-80 (which followed a ten-year dry cycle). Some sediment from these sources may have appeared near SONGS in 1978 and 1979, but it is clearly minor compared to the influx of 1980. At 8 m depth these new fine sediments dispersed during 1981, but at 18 m depth they were still in place when more fine sediments arrived in 1983.

The delayed arrival at SONGS of sediment from the runoff of 1977-80, and the persistence of this sediment at 18 m depth for at least three years afterward, shows that the sediments of the inner shelf do not come to prompt equilibrium with the local regime of waves and currents. Sooner or later, fine particles entering the sea in runoff are carried across the inner shelf to settle out at depths beyond the reach of wave action, but this process can evidently take several years off San Onofre and can lead to irregular and changing distributions of fine sediments.

The increases of silt-clay percentage near SONGS in 1983 are most likely due to the high runoff in the winter of 1982-83, the first winter of the 1982-84 El Nino event. That winter had extreme high waves as well as high runoff, which may well explain the more prompt arrival of fine sediments off San Onofre in the following spring and summer.

MRC was concerned that the emplacement of the SONGS intakes and diffusers in the seabed during 1977-80 might have local effects on the bottom sediments that would die away during the period of MRC's BACIP studies, causing changes in bottom dwelling populations that might be confused with effects of

SONGS operation. In retrospect, we cannot distinguish construction effects from local natural changes due to extreme runoff in the same period 1977-80.

Later on, MRC was concerned that excavated material released to the sea by the removal of a sea wall from SONGS in the winter of 1984-85 might confound BACI studies in the same way. This material amounted to about 170,000 m^3, including about 10,000 m^3 of fine sand and 20,000 m^3 of silt and clay. (The weight of suspended silt and clay corresponding to this volume, with density of one or two metric tons per m^3, is much less than the natural sediment supply estimated for a wet year, but much more than the natural supply for a dry year.) This released material did not have effects on optical extinction large enough to stand out plainly above the natural variations, but bottom samples did show some evidence of its passage across the shelf. The silt-clay percentage at 18 m depth 1100 m and 1900 m downcoast from SONGS dropped abruptly from over 75% to a minimum of 25% in April 1985, and did not regain its original values until December. This was the most sudden and deep change reliably observed in the ten-year histories in Figures 2 and 3, and cannot be taken as an ordinary natural variation. (The high isolated peaks at 58% in Fig. 2 and 61% in Fig. 3 are each from a single sample; if not doubtful, they are certainly very local and ephemeral.)

From October of 1985 to the present, continuing or recurring deposits of unusually cohesive sediments have been observed at places in the vicinity of SONGS and the San Onofre kelp bed. MRC has undertaken a separate study of these deposits; the results of this study are given in Technical Report B, and are not reported here.

2.4 Oceanic Dispersion

To look at the different ways in which things are transported by ocean currents, it is useful to average the velocity in some way, dividing the total current into the mean flow and the fluctuations about the mean. The mean flow is relatively smooth and uniform, and carries any set of particles bodily downcurrent, in a process called advection. The fluctuations are more or less random and average to zero; they will not move a set of particles as a whole, but will scatter the particles over an ever increasing area, in a process called turbulent dispersion. These processes are important to the natural running of the local ecosystem and especially to its response to the SONGS discharge, so they need some specialized discussion here. The subject is complicated and the literature is large; a useful short account may be found in Fischer *et al.* (1979, Ch. 2 & 3), and the mathematical basis for some points discussed below is sketched briefly in Appendix B to this report. Here we shall only discuss some results that will be useful in later sections (3.3 and 4.1).

Turbulent dispersion carries particles away from each other, so it generally moves particles away from regions in which they are plentiful toward regions where they are sparse. More formally, the flux of any substance due to turbulent dispersion is directed down the gradient of concentration. This relation is so universal that we can confidently infer an upward flux of dissolved nitrate from the downward increase of nitrate concentration below the photic zone, as we did in 2.1 above.

The strength of dispersion is measured by a quantity called diffusivity, denoted by K, which is half the rate of increase of the mean-square displacement

σ^2 of the particles in a dispersing mass: $2K = \partial\sigma^2/\partial t$ (cm^2/sec). In many situations it is a useful and sufficiently accurate approximation to say that the relation between turbulent flux and concentration gradient is linear. In this case, the constant of proportionality between flux and gradient is -K. The linear relation of flux to gradient gives an approximate basis for estimating turbulent flux and the dilution of effluents from a source, if K can be measured or estimated from statistics of the current regime. Accurate measurement of K requires a large set of observations of dye-patches or groups of drifting objects, but very rough estimates can be obtained from theoretical arguments and ordinary current measurements.

In turbulent dispersion, K is not a property of the turbulent medium alone, but also increases with the spatial scale σ or the age t of the dispersing mass in question. The physical rationale for this is that the turbulence is made up of eddies both small and large; particles which are closer together may be in different small eddies, but are likelier to be moving together in the same large eddy; particles farther apart are likelier to be in different large eddies also, which carry them faster in different directions. In the limit of small scales or ages, it can be shown that K increases linearly with scale or age: $K = w\sigma$ or $K = w^2t$, in which w^2 is the variance of velocity of the particles in the dispersing mass.

For large values of the age or scale K ultimately levels off to a constant value that depends on w and on the time-lag for which the current fluctuations become uncorrelated. In many cases, turbulent dispersion at intermediate scales or ages may still be described approximately by a linear increase of K, replacing w by an empirical w'.

Both the numerical value and the physical meaning of turbulent diffusivity will depend on the set of dispersing particles that is considered, which determines how the total current is divided into mean flow and fluctuations. We will look at two important cases, based on very different conceptual experiments.

If the particles in the set are all released at the same instant, as in the release of a single dye-patch, the variance of particle-velocities w^2 that appears in the diffusivity only includes the differences of velocity between particles at the same instant, and excludes the slowly varying velocity common to all the particles which moves the patch as a whole. This kind of short-term or single-patch diffusivity is appropriate for estimating the expected dilution rate of a single instantaneous release into the sea (such as a toxic spill) without regard to where the dispersing cloud actually goes. A large body of data from different places compiled by Okubo (1974) shows patch-diffusivity in the sea behaving very regularly under a variety of conditions. The growth of patch-diffusivity for ages from a few hours to a few days can be fairly well represented by the linear approximation $K = w'^2 t$, with a dispersion velocity w' of about 1 cm/sec.

If, on the other hand, the particle-set comprises a large ensemble of dye-patches released at random instants over a long span of time (with the age t of each patch set to zero at the instant of release), the variance of particle velocities w^2 will include all the long-period variations of current which carry patches launched at different times to different places. This kind of long-term or ensemble diffusivity, with allowance for advection by the long-term mean flow, is the only suitable kind for estimating the long-term mean distribution of effluents from a continuous fixed source such as SONGS. As discussed below, it is likely to be a

good deal larger than single-patch diffusivity in a current regime with large long-period variations, as at San Onofre, so the uncritical use of short-term diffusivity can seriously underestimate mean effluent concentrations from a continuous discharge.

If the current statistics are steady in time and spatially uniform, the variance w^2 in the small-age approximation $K = w^2t$ will be the same as the total variance of velocity in a long current record from a fixed point. Off San Onofre, this long-term variance is about 100 cm^2/sec^2 for longshore currents and 25 cm^2/sec^2 for cross-shelf currents (ECO-M 1988a, Table 4-3). About 80% of the longshore variance and 50% of the cross-shelf variance comes from current fluctuations with periods longer than 30 hours (ECO-M 1988a, Table 4-6). For estimating long-term mean dilution of SONGS effluents, as discussed in 3.3 below, an allowance was made for the levelling off of diffusivity with age, leading to the smaller values of 50 and 10 cm^2/sec^2 for longshore and cross-shelf w'^2 (see ECO-M 1987f, pp. 8, 11). For a given age, these numbers give ensemble diffusivities one to two orders of magnitude higher than patch diffusivities, reflecting the great importance of long-period fluctuations in the regime of dispersion off San Onofre.

From the relation $K = w'\sigma$ for diffusivity as a function of spatial scale, patch-diffusivity with w' of about 1 cm/sec will be about 10^4 cm^2/sec on a scale of 100 m, 10^5 cm^2/sec on a scale of 1 km, and 10^6 cm^2/sec for 10 km. Ensemble diffusivities off San Onofre, with longshore and cross-shelf w' of 7 and 3 cm/sec, will correspondingly be 7 and 3 times larger at any scale.

3.0 INTERACTIONS OF SONGS UNITS 2 AND 3 WITH NATURAL PROCESSES

The cooling system of SONGS Units 2 and 3 together is designed to discharge 10^4 m^3/sec of seawater, heated to 10.7°C above the intake temperature, into the ocean without increasing the surface temperature by more than 2.2°C beyond 305 m from the discharge for more than half of any tidal cycle, as required by California standards for thermal discharges. These requirements make it necessary to dilute the discharge by a factor of at least five within 300 m, even at times when currents are very weak. This objective is attained by discharging the heated water through a line of jets directed offshore with an upward tilt; the entrainment of ambient water in the jets is enough to produce more than the necessary dilution within 300 m from the discharge ports (Fischer *et al.* 1979, 10.5.3). The analysis of temperature records given in 6.1 below shows that actual operation of SONGS does in fact meet the standard.

A consequence of this design, though, is that the cooling system adds a large flux of seaward momentum to the local environment. The effect of this on the local patterns of flow largely depends on the ratio of the SONGS-induced seaward momentum flux (volume flow times velocity) to the natural longshore momentum flux due to currents. The original offshore momentum flux of the discharge is 100 m^3/sec times the initial jet velocity of 4 m/sec, or 400 m^4/sec^2. This is about equal to the longshore momentum flux in a current of 14 cm/sec (0.14 m/sec) through a cross section extending 2.5 km out from the shore to the end of the diffusers: the cross section of 20,000 m^2 times 0.14 m/sec gives a volume flow of 2800 m^3/sec; this times 0.14 m/sec gives 392 m^4/sec^2. In moderate currents of about 10 cm/sec, the discharge will turn the total flow toward the offshore direction, and in weak currents

the total flow near the diffusers will be almost directly offshore. This redirection of the natural pattern of flow, involving a large and fairly rapid upward and seaward transport of water, with whatever suspended particles and passive organisms it contains, is the most obvious and probably the most important impact of SONGS on the local physical environment.

This section starts by considering the flow near the SONGS intakes in 3.1, and goes on in 3.2 to discuss the dilutions, depths, and velocities observed in the discharge plume, and the velocity in the make-up flow that replaces water carried away from SONGS in the plume. The last subsection, 3.3, gives estimates of the mean dilution at long ranges where dilution is not directly observed.

3.1 Intake Hydrodynamics

SONGS Units 2 and 3 have separate intakes, about 950 m from shore and 200 m apart alongshore. Each intake is essentially a vertical pipe 15 m in diameter, open at the top, but with a flat lid, the so-called velocity cap, mounted 2.1 m above the end of the pipe (ECO-M 1988b, Table 1), so that water is drawn in more or less horizontally through an opening that is a segment of a vertical cylinder 15 m in diameter and 2.1 m high, centered at a level 4 m above the bottom in water depth H = 10 m below mean sea level (mean sea level is about 1 m above Mean Lower Low Water). The area of this opening is 99 m^2 (π x 15 m x 2.1 m) and the pumping rate Q of each unit is 52 m^3/sec, so the average velocity at the entrance is 0.53 m/sec (1.7 fps or 53 cm/sec).

Continuity alone specifies that the vertically-averaged velocity due to each intake by itself (in the absence of current) must be radially inward, given by $V = -Q/2\pi HR$, so that the total flow of water into any region enclosing the intake is the same as the intake rate Q. With mean H = 10 m, the average velocity toward the intake falls off to less than 3 cm/sec at R = 30 m from the axis of the intake, and less than 1 cm/sec at R = 100 m. With no current, a particle would take about eight minutes on the average to reach the entrance from a distance R = 30 m and 100 minutes from R = 100 m.

The number of planktonic organisms drawn into each intake per second is the product of the pumping rate Q and the local population density of the organisms in question. MRC has sampled plankton throughout the water column in the neighborhood of the intakes in order to estimate this number, and it is important to consider in some detail whether water is withdrawn at equal rates from equal intervals of depth and plankton samples from different depths have equal weighting in the average.

We can in fact expect to a good approximation that withdrawal is the same at all depths except for a thin boundary layer at the bottom. Water at a distance is actually accelerated toward the intake by a hydrostatic pressure-gradient due to a drawdown of the surface toward the intake. The acceleration is horizontal and uniform from top to bottom (see Appendix B, 3), and can be balanced at every point by the advection of momentum in the steady vertically-uniform converging flow $V = -Q/2\pi HR$.

This balance is possible because the momentum generated by the surface slope is all carried into the intake. This situation is very different from an ordinary slope-driven current in shallow water, which can only reach a steady state when all the momentum generated throughout the water column by the slope is transferred to the bottom by turbulence and shear, to be destroyed by bottom friction. Such a current will accelerate until the necessary turbulence and shear are developed, and will end with a characteristic profile of velocity decreasing toward the bottom. Bottom friction is present also in the steady radial flow toward an intake, but here it is incidental rather than controlling; turbulence generated at the bottom by velocities exceeding a few cm/sec near the intake will itself be carried into the intake before it can spread a significant amount of shear upward into the water column.

In the presence of an ambient current of velocity U, the water entering the intake will come from a restricted sector upstream, whose cross-sectional area A perpendicular to the flow will approach the value Q/U at distance upstream (so that UA = Q). In slow currents this upstream cross section will be a rectangle encompassing the whole depth H of the water column over a width Q/UH. In currents so fast that this width falls to a value approaching H, the cross section may begin to rearrange itself so that the top and bottom of the water column are underrepresented, finally becoming a circle of radius $(Q/2\pi U)^{1/2}$ centered at the entrance depth. In a current of 25 cm/sec, which is rarely exceeded off San Onofre, the width for each SONGS intake will still be twice the water depth H = 10 m, so top and bottom water will hardly ever be excluded from the intakes.

If the ambient current velocity falls off with depth, as is usual, the upstream cross section is wider at the bottom than at the top. The wider bottom layers move more slowly toward the intake, though, and equality of withdrawal with depth is maintained.

In density-stratified waters, steady-state isotherms will not cross the streamlines of flow to an intake. In the extreme case of two layers separated by a sharp interface, an intake starting up in the upper layer will at first take water only from this layer. The drawdown of the surface, though, will accelerate top and bottom water equally toward the intake, and the interface will rise toward the intake until it reaches an equilibrium level within the entrance and top and bottom water enter with equal velocities.

3.2 Diffuser Hydrodynamics

SONGS Units 2 and 3 together discharge 104 m^3/sec through staged diffusers, which are assemblies of jets (126 in all) mounted on pipes in line offshore, starting about 1 km from shore in water 10 m deep and ending about 2.5 km from shore in water 15 m deep. The individual jets have an initial diameter of 0.5 m, discharging 0.8 m^3/sec each with an initial velocity of 4 m/sec; the ports are 2.2 m above the bottom, and are aimed 20° upward and 25° to either side of the offshore direction in alternation (Fischer *et al.* 1979, Table 10.8; ECO-M 1988b, Table 1). The layout of the intakes and diffuser lines, relative to the shoreline and the regions of cobble substrate that provide kelp habitat, is shown in Figure 4.

In the course of designing the diffusers, a hydraulic scale-model of the whole system was built to predict the dilutions and trajectories of the discharge plume in various conditions of current (Koh *et al.* 1974; Fischer *et al.* 1979, 10.5.3). After the actual system began operating, dilutions and trajectories in the ocean were observed in some dye-studies, and many aerial photographs were taken of plumes made visible by contrasts in color or turbidity. The field studies of the real plume (ECO-M 1987a; 1987e; 1988b) are the primary sources of data on its behavior, but the model studies remain highly relevant because they are in good general accord with the field studies and cover a wider range of currents.

3.2.1 Dilution

The most reliable field experiment with dye injected into the intake of Unit 3 (the unit with the inshore diffuser) showed the dilution (total flow divided by discharge) rising from 8 at 50 m distance downcurrent from the diffuser, to 10 at 400 m, 18 at 650 m, and 24 at 1100 m downcurrent. During this experiment, Unit 3 was pumping at 3/4 of its full rate, and the current outside the plume was about 7 cm/sec downcoast. On other occasions, minimum surface dilutions estimated very approximately from local disturbances of surface temperature near the diffusers were about 7 or 8 in three instances and about 14 in one instance, all at times when the current speed was 10 cm/sec or less (ECO-M 1987a).

Mappings of temperature-rise in runs of the hydraulic model with a longshore current of 2.5 cm/sec showed a minimum dilution a little less than 10 close to the inshore diffuser, and dilutions from 10 to 13 along the axis of the model plume out to nearly 1.5 km beyond the end of the outer diffuser. In a modelled

current of 5 cm/sec, the minimum dilution was still a little less than 10, but dilutions less than 13 did not occur beyond a few hundred meters from the diffusers. In a current of 13 cm/sec, the minimum dilution was about 13, observed only at a single point, and a large central region (about 1.5 km^2) of the model plume showed dilutions from 13 to 20; at 26 cm/sec, dilution over the whole model plume was greater than 20 (Koh *et al.* 1974, Figs. 6.15-6.18). The increase of dilution with current speed has not been quantitatively documented in the field by dye-studies in strong currents, but since the model results for weak and moderate currents are well confirmed in the field, the model results for strong currents can be used with fair confidence.

As an overall result in round numbers, we can say that the diffusers entrain something like 10 times the discharge within two or three hundred meters of the ports in weak currents, and that the entrainment close to the diffusers can rise to more than 20 times the discharge in strong currents. The relative prevalence of weak and strong currents is shown by the long-term cumulative distribution of longshore speeds: the hourly average speed is 5 cm/sec or less about 45% of the time, 10 cm/sec or less about 75% of the time, and 20 cm/sec or less about 95% of the time (ECO-M 1988a, 4.3, Fig. 4-17). Near-field dilutions of about 10, then, are representative of most of the time.

3.2.2 Plume Depth

The initial momentum and the upward tilt of each jet usually carry its discharge to the surface, where "boils" from the individual jets are often to be seen. At about this stage, the jets begin to run together into a plume, and the traces of

individual jets soon merge. Depending on the temperature stratification and the course of entrainment on the way, the newly-formed plume may or may not be denser than the surrounding surface water. In weakly-stratified water, the plume will spread at the surface; profiles of dye-concentration show surface plume thicknesses of 3-5 m within 1 km of the diffusers. When temperature stratification is unusually strong, the plume may reach the surface initially but then sink and spread at middepth, or in extreme cases it may fail to reach the surface at all (ECO-M 1987a, 1987e).

3.2.3 Plume Configurations

Field observations and dye-trajectories in the hydraulic model both show that the plume goes offshore along the diffusers in very weak longshore currents, diverging at a small angle and tending to spread in a pool beyond the outer end of the diffuser line. With increasing longshore current, the plume becomes wider because it makes an increasing initial angle to the diffusers, and continues to bend toward the longshore direction as it goes downcurrent. In longshore currents of 25 cm/sec or more, the plume makes only a small angle to the longshore direction, and is about as wide as the diffusers are long. Figure 5 shows schematic plumes for steady longshore currents at different speeds, drawn from photographs of the hydraulic model operating with a dyed discharge (Koh *et al.* 1974, Figs. 6.4-6.7). To indicate the prevalence of the different configurations we may note that the actual current speed off San Onofre is 5 cm/sec or less about 45% of the time, 13 cm/sec or less about 80% of the time, and 26 cm/sec or less over 97% of the time.

Figure 6 illustrates an actual plume flowing through and around the San Onofre kelp bed in an ambient current of speed varying between 8 and 12 cm/sec. The solid lines in this Figure are the trajectories of dye-patches released near the diffusers, marked by dots every half-hour (ECO-M 1987e).

There are some notable differences between actual plumes and model plumes. Actual plumes sometimes show distinct whorls and meanders on scales of several hundred meters or more, due to ambient turbulence on these scales that is present in the actual current but not in the modelled flow. Actual plumes sometimes show sharp fronts, either at the upcurrent and seaward boundary of a warm surface plume where the colder ambient flow dives under the plume, or occasionally downcurrent from the diffusers when an overdense plume, carried to the surface by its initial upward momentum, sinks beneath the warmer ambient surface water.

Perhaps the most important difference is that the actual plume, like the ambient current, is retarded and partly diverted by the San Onofre kelp in the beds on either side of the diffusers, as has been observed directly from trajectories of dye injected in an intake or released in the plume (ECO-M 1987a, 1987e). The dye-patches 9 and 15 in Figure 6 illustrate the slowing and diversion of the plume at the upcoast end of the kelp bed very clearly. In a different dye-study, a dyed plume was seen to flow inshore of the south kelp bed, with little penetration of the kelp, but on still another occasion the dyed plume flowed slowly through the kelp and more swiftly around both ends of the bed.

3.2.4 Offshore Velocity and Offshore Transport

Field observations and dye trajectories in the hydraulic model both show offshore velocities in the plume on the order of 10 cm/sec, with a maximum of about 20 cm/sec in weak longshore currents. If momentum were conserved, we would expect about 40 cm/sec from a dilution of the initial velocity of 400 cm/sec by a factor of 10. It is evident that some of the initial momentum is destroyed near the diffusers, probably because the jets disturb the free surface, making hydrostatic pressure-gradients that decelerate the flow. At later stages in the plume, buoyancy forces may destroy or create offshore momentum to an unknown and highly variable extent.

The uncertainty about how much offshore momentum is lost from the plume rather than exchanged with ambient water prevents any accurate prediction of offshore transport in the plume beyond the seaward end of the diffusers (the hydraulic model is limited by a seaward boundary about 4.8 km from shore, and there are no dye-studies of actual dilutions at long ranges offshore). We do have some useful field evidence on this point, though, from the joint distributions of cross-shelf and longshore currents (that is, current roses) shown in Figure 7 (ECO-M 1988b, 5). The distribution of currents at station 20, 500 m directly offshore from the end of the diffusers, shows a distinct and unique lobe of offshore velocities, up to 20 cm/sec, which are recorded when the plume swings past the station during current reversals. At station 02, 1.7 km beyond the end of the diffusers and 4.2 km from shore, there is no evidence of unusual local offshore velocities, and it can be taken that offshore transport of plume water beyond this distance is minor.

The different question of how far offshore the water in the plume is moved on the average cannot be answered accurately, but we can form a very rough estimate from the plume configurations in Figures 5 and 6. The idealized plume trajectory for a current of 13 cm/sec in Figure 5 moves somewhat more than 700 m offshore before the plume loses its identity by mixing into the sea. The dye-patches 14 and 15 in Figure 6, launched near the inshore diffuser, also moved about 700 m offshore, as did water at the plume front directly offshore from the outer diffuser. Plume water will move further offshore at lower current speeds, and since the actual current is 13 cm/sec or less for 80% of the time we can take 700 m or so as a rough lower estimate for the average offshore displacement of plume water.

3.2.5 The Make-up Flow

The total volume flow of one or two thousand cubic meters every second that the plume carries out of a region surrounding the intakes and diffusers clearly has to be matched by an equal influx to the region, or else the region would quickly run dry. This make-up flow is driven by a drawdown of the surface toward SONGS, like the flow to a single intake discussed in 3.1 above, and will be approximately uniform from top to bottom.

The configuration of the make-up flow can be approximately calculated by potential theory (ECO-M 1988b, 3). Near the diffusers, the vertically averaged flow will be toward the diffusers from either side, at about 3 cm/sec for a total flow Q in the plume of 1000 m^3/sec; at ranges beyond 3 km, the flow will be increasingly well approximated by a velocity $V = Q/2BR^2$ radially inward toward the point on the shoreline nearest the diffusers, R being the distance to that point and B the

average slope of the sea bottom in radians; with $Q = 1000\ m^3/sec$ and $B = 0.006$, this gives V of about 1 cm/sec at 3 km from the shoreline point. Because the water is shallower nearer shore, 70% of the transport in the make-up flow by itself comes from the sector within 45° to either side of the offshore direction.

The instantaneous total velocity at any point is approximately the vector sum of velocities in the current, the plume, and the make-up flow. In longshore currents of more than a few cm/sec, water that is withdrawn or entrained by SONGS comes immediately from upcurrent directions close to longshore. The shoreward component of the make-up flow persists through the reversals of current, however, so that all this water comes ultimately from some distance offshore. The extent to which it retains properties of offshore water, such as transparency, depends on the ratio of shoreward advection to turbulent dispersion, and cannot be closely predicted.

The reality of the make-up flow toward SONGS is shown for particular times by the shoreward movement of dye-patches upcurrent from the diffusers, and by dye-patch 16 in Figure 6, which was released between the separate plumes of Units 2 and 3 and remained in the same place for over four hours (ECO-M 1987e, 2.6). The long-term reality of the make-up flow is shown by the negative coefficient of correlation $r = -0.24$ between cross-shelf velocities at stations 01 and 19 (see Figure 7) on opposite sides of the diffusers (ECO-M 1988b, 5, Table 2): when the downcurrent station has an offshore velocity because of the plume, the upcurrent station tends to have an onshore velocity due to the make-up flow. (The correlation coefficient between stations 01 and 18, both upcoast of the diffusers, is +0.76.)

3.3 Long-term Mean Dilution at Long Range

Somewhere about two or three kilometers from the diffusers the contrasts in velocity and density between the plume and neighboring ambient waters fall to values comparable to the natural fluctuations, and further dilution of the plume becomes a matter of natural oceanic mixing and dispersion. Beyond this range we have no guidance from the hydraulic model or from quantitative dye-studies to estimate the dilution of the SONGS discharge; the only source for such an estimate is some kind of model for the advection and dispersion produced by the observed currents off San Onofre.

The question of dilution at a distance has been addressed by theoretical calculations of dispersion in the wedge-shaped space between the surface and the bottom of the sea, with longterm diffusivities (see 2.4 and Appendix B, 5) along and across the shelf derived from the time-averaged autocovariances of current (ECO-M 1987f). The results are shown in Figure 8, as contours of the long-term mean of relative concentration C/C_o of a conservative tracer released at concentration C_o in a continuous discharge of 100 m^3/sec of water at a point 2.5 km from shore (at the outer end of the diffuser lines). The Figure shows a maximum relative concentration of 1.5% on the shoreline at a point about 2 km downcoast from SONGS, corresponding to a dilution of about 65; the concentration at the shore falls off by a further factor of three at 9 km to either side of this maximum. The displacement of the whole pattern downcoast from SONGS is a result of the long-term mean current of 2.9 cm/sec downcoast; if the mean current were zero, the pattern would be centered at SONGS but otherwise essentially the same.

These estimates should be taken as order-of-magnitude results, in the sense that they might well be wrong by a factor of three or four either way, but are unlikely to be wrong by a factor of more than ten. The estimates are not reliable in the region around the diffusers where the discharge seriously alters the ambient flow, and they do not refer to instantaneous dilutions, so they cannot be neatly connected to the direct observations of dilution within a kilometer or so of the diffusers. Both approaches suggest long-term relative concentrations on the order of 1% in the range of 2 or 3 km from the diffusers where neither approach applies very well, and there is no evident disagreement as to order of magnitude.

4.0 POTENTIAL EFFECTS OF SONGS

MRC's investigations have necessarily been guided by hypotheses about potential effects of SONGS on marine life, simply because it is not possible to study everything in equal detail.

This section recounts the most important hypothetical physical effects of SONGS that were considered in designing MRC's projects at various times.

4.1 Direct Mortality of Plankton

It is not disputed that large numbers of plankton are drawn into the intakes of SONGS and that a large fraction of these are killed by heat and turbulence within the power plant. Turbulent entrainment in the heated diffuser jets close to the exit ports might also kill some fraction of the plankton in the entrained water, and still more plankton might possibly be killed if the plume carried them to an inhospitable habitat offshore. Testimony in the 1973-74 public hearings before the CCZCC predicted that such plankton deaths would lead to serious impacts on nearshore fauna (Minutes of October 18, 1973, p.13; see Annotated Interim Report of MRC, April 18, 1988, 3.2).

It is not immediately obvious, though, what effect these deaths would have on local population densities. The plume of water discharged and entrained by SONGS will show some deficit in the density of living plankton, for any or all of the reasons above; if this water did not mix at all with ambient water, it would form a pool of depleted water expanding without limit around the diffusers; if it were

scope of the model. This process gives entirely determinate fluctuations of current at periods and scales longer than those of the observing array, instead of the random long-term and large-scale fluctuations that make up a large part of the turbulent diffusivity in the actual current-field, as discussed above in 2.4.

4.2 Redistribution of Suspended Particles

The hydraulic model of SONGS showed that the discharge plume would often carry water offshore over the region occupied by the San Onofre Kelp. Since nearshore water generally carries a greater load of suspended particles and is less transparent than water further offshore, MRC considered that the partial replacement of ambient water in the kelp bed by plume water originating closer to shore might reduce the irradiance near the bottom in the kelp bed, with adverse effects on early lifestages of kelp plants. The field experiments of the Kelp Ecology Project included observations of irradiance and the flux of suspended particles, to assess the biological effects of these variables; eventually these observations were also used in BACIP analyses of irradiance itself, described in 5.1 below, and of seston flux, described in 6.3.

Experiments were carried out in 1980 to study the actual optical effects of suspended particles in waters off San Onofre. These led to the linear relations of extinction to seston given in 2.2, and showed that SONGS would redistribute extinction in about the same way that it redistributed actual suspended particles (Reitzel 1980, 2.0; Reitzel 1981). A numerical simulation of this redistribution was carried out, based on current-records, plume-behavior inferred from the hydraulic model, and the mean cross-shelf gradient of extinction observed in the summer of

1980 (Reitzel 1980, 4.0-5.0). This model predicted that SONGS would reduce average bottom irradiance in the outer part of the San Onofre Kelp by about half. The uncertainties of the model were large, and the force of this prediction was only to show that the potential reduction of irradiance by SONGS was a proper matter for concern and continued study.

As Units 2 and 3 approached a state of normal operation, MRC decided to keep up a running comparison of irradiance under the plume of SONGS (as defined by a kinematic model based on current records) with irradiance in ambient water at the same time; this was done by recording irradiance at pairs of stations on opposite sides of the diffusers. The results of these Plume-Ambient comparisons over the years 1985-86 are described below in 5.2.

A potential secondary effect of SONGS on irradiance comes from the make-up flow of water toward the intakes and diffusers that is necessary to replace the water withdrawn or entrained by SONGS and carried off in the plume (see 3.2). Part of this flow comes from offshore directions, bringing relatively clear offshore water to the vicinity of SONGS. The extent to which this influx may actually increase average irradiance near SONGS is another complicated problem in oceanic dispersion beyond the reach of accurate prediction.

4.3 Sedimentation

The water entrained by the diffuser jets is immediately supplied by a flow toward the diffusers from either side whose speed near the diffusers is about 3 cm/sec (see 3.2). Added to an ambient longshore current faster than 3 cm/sec, this

flow produces a drop of about 6 cm/sec in the speed of water that crosses the diffusers but escapes entrainment in the jets. The load of suspended material that a current can carry falls off steeply with the speed of the current, and material will tend to settle to the bottom at places where the speed is reduced. Material settling out downcurrent from the diffusers may or may not be resuspended and carried back across the diffusers when the current reverses, but in any case the drop in speed across the diffusers will increase the deposition rate of suspended particles near the diffusers and tend to trap particles in the vicinity. Suspended particles withdrawn or entrained by SONGS will also tend to settle out of the plume as its velocity falls off with distance, producing some deposition at places under the plume.

Slowing of currents by a good deal more than 6 cm/sec occurs frequently all over the region with the reversal of tidal currents. Since the nearshore shelf is not accreting over the years, grains that settle out when currents slow naturally must be removed by wave erosion, even if much of this happens episodically in winter storms. Since the slowing across the diffusers and within the plume does not rise above the natural background of changes in speed, it was expected that any resulting deposits would also be removed by wave erosion from time to time, so that continuous long-term accumulation of sediment due to SONGS was not to be expected.

This view did not foresee the possibility of cohesive deposits with unusually high resistance to erosion by waves. New deposition of cohesive sediment near the margin of the San Onofre Kelp bed was first noted in late 1985 and has persisted or recurred up to the present time. The nature and origin of this deposition, and

whether or not SONGS is a contributing cause, are considered at length in Technical Report B, and will not be dealt with here.

5.0 SONGS' EFFECTS ON IRRADIANCE

The effects of SONGS operation on underwater irradiance have been studied statistically by two independent methods. Appendix A describes the statistical designs and procedures in detail and gives a full tabulation of the results. Here we describe the statistical studies very briefly, repeat the summaries of results and the conclusions from Appendix A, and discuss the physical interpretation of the results.

5.1 BACIP Analyses

The Before-After/Control-Impact Pairs or BACIP design is the same as has been used for many of MRC's biostatistical studies of SONGS effects on marine populations. It examines time-series of measured differences between Impact and Control stations, to see whether the mean difference between Impact and Control in the time After SONGS started up is different from the mean difference in the time Before start-up. The main conditions for a valid BACIP result are that the Before differences should have a stationary mean and should be additive (that is, independent of the Before sums). When these conditions are met, it can be presumed that the natural mean difference in the Before period will remain the same after start-up, so that the difference of differences can be taken as the effect of SONGS. If the conditions are not met, a BACIP result may be seriously misleading.

Independent BACIP tests were applied to irradiance at two levels, on the bottom and at 2 m above. The Impact station was a composite of three stations in the San Onofre kelp bed (SOKU45, SOKD45, and SOKD35) and the Control was

station SMK45 in the San Mateo kelp bed, about 5 km upcoast from SONGS (see Fig. A-1 in Appendix A). Besides an overall test on the complete data-sets, separate tests were made for different sets of days distinguished by whether the SOK stations were downcurrent or upcurrent from the SONGS diffusers for a majority of the daylight hours (5 or more out of 9), or for all daylight hours (9 out of 9). The sets of downcurrent and upcurrent days for 5 or more out of 9 daylight hours together include all days on which current direction was recorded.

Irradiance itself proved to be additive in most of the data-sets, but its logarithm usually did not, so the BACIP results are properly expressed as absolute rather than fractional changes in irradiance.

The table below, taken from Appendix A, shows the results of all the BACIP tests for which p_A, the probability that the Before data-set was additive, roughly speaking, was greater than 0.10. Results with p_A less than 0.80 or so are more or less unreliable and should be discounted, but are included here for comparison with the clearly additive results. In this table, B is the SONGS effect, s.d. is its standard deviation, and p is its level of significance, the probability that the result would occur by chance in the absence of a real effect.

Data-set	Var.	Ht. (I in E/m²-day)	B	s.d.	p	p_A
Downcurrent						
9hr/9	I	0	-0.60	0.23	0.01	0.98
5+hr/9	I	0	-0.46	0.21	0.03	0.86
9hr/9	I	2	-0.39	0.32	0.22	0.50
5+hr/9	I	2	-0.43	0.29	0.14	0.20
Upcurrent						
9hr/9	I	0	+0.51	0.32	0.11	0.97
5+hr/9	I	0	+0.02	0.26	0.93	0.31
9hr/9	I	2		not additive		
5+hr/9	I	2	+0.41	0.42	0.33	0.82
All Days	I	0		not additive		
	I	2	-0.13	0.25	0.61	0.62

The significant and highly additive results for downcurrent days at level 0 compel the conclusion that average irradiance on the bottom at the SOK stations was reduced by approximately 0.5 E/m²-day on downcurrent days by the power plant (in the absence of demonstrated confounding effects). The whole body of BACIP results makes it highly reasonable to conclude that the power plant generally reduced average irradiance at and near the bottom in SOK by about 0.4 E/m²-day on all downcurrent days, and probably increased irradiance by a comparable but smaller amount on upcurrent days.

There are more downcurrent days than upcurrent days in these data-sets, in the ratio 59 to 41, so the net effect over all the days is a reduction of irradiance, ranging from about 0.27 E/m²-day if the SONGS effect B for upcurrent days is actually zero, to about 0.08 E/m²-day if the upcurrent value of B is equal and opposite to the downcurrent value. This accords with the tolerably additive but non-significant BACIP estimate of the net effect as B = -0.13 E/m²-day for all days at 2

m above the bottom. We have no data from the San Onofre kelp bed upcoast from the diffusers, but we can estimate that the asymmetry of the current would produce a net SONGS effect at comparable stations upcoast from the diffusers ranging from -0.19 to +0.08 E/m^2-day.

5.2 Plume-Model and Upstream-Downstream Analyses

An entirely separate set of analyses was carried out to see if irradiance at a station under the plume of Units 2 and 3 was different on the average from irradiance at the same time at a counterpart station in ambient water on the opposite side of the diffusers. A station was classified as in the plume (P) or ambient (A) in a particular hour by a kinematic model which used current records to backtrack water from the station to see if it had recently crossed the diffusers.

The SONGS effect found by this kind of analysis on pairs of stations is the average difference between Plume irradiance and Ambient irradiance over all hours, regardless of which station in the pair was (P) and which (A) in any given hour. This procedure separates SONGS effects from any natural effects of current direction that are uniform at both stations in a pair. It does not separate out any natural current effects that are not the same at both stations, and these remain as possible confounding effects.

The station-pairs analyzed were made up of four stations in the San Onofre kelp bed and another station 2.5 km downcoast from SONGS, together with counterpart stations upcoast from the diffusers (see Appendix A, Table A-2 and Fig. A-1 for station names and locations). The data-set for any pair comprised all

daylight hours in the years 1985 and 1986 for which irradiance was recorded at both stations in the pair.

For these analyses, there were no data-sets free of SONGS influence to be tested for additivity. It turned out, though, that analyses of irradiance and its logarithm gave concordant estimates of fractional changes in irradiance due to SONGS, showing that errors due to non-additivity were not important.

Here we summarize the results in terms of changes in absolute irradiance, noting that the fractional changes reported in Appendix A are concordant and equally valid.

Every Plume-Model analysis of irradiance showed a highly significant reduction of irradiance in the model plume relative to ambient water at the same time, with an average reduction of 0.056 E/m^2-hour. Integrated over nine daylight hours, this is equivalent to 0.50 E/m^{2}day. For the pairs including the three SOK stations analyzed by BACIP, the equivalent reduction was 0.54 E/m^2-day. The model classified the four SOK stations as in the plume (P) for percentages of all recorded hours ranging from 17% to 28%; it classified the stations 2.5 km distant from SONGS as (P) in only 6% or less of all hours.

The Plume-Model analyses used only the hours for which one station was (P) and the other (A), dropping the remaining hours. The dropped hours added up to about half the total; in all but a few of these the plume model classified both stations as (A). These hours were analyzed with an Upstream-Downstream model which simply classified a station and hour as (P) if the station was downcurrent from

the diffusers in that hour, or as (A) if it was upcurrent, so that one station in a pair would be (P) and the other (A) in every hour analyzed.

Every Upstream-Downstream analysis showed a significant reduction of irradiance at the downstream station relative to the upstream station, with an average reduction of 0.022 E/m^2-hour, equivalent to 0.20 E/m^2-day (0.21 E/m^2-day for the three SOK stations analyzed by BACIP). The Upstream-Downstream model classified the south station in a pair as (P) for a percentage of all analyzed hours ranging from 46% to 69%.

The reductions for pairs of stations about 500 m downcoast and upcoast from the diffusers (particularly the closest pair SOKU45-PL45) were somewhat smaller than those for pairs of stations at greater distances, as is shown in Figures A-2 and A-3 of Appendix A. The most plausible physical reason for such an effect is that the actual plume may sometimes have been redirected away from closer stations by kelp beds on both sides of the diffusers (see Fig. A-1), while the model plume was not. It is also possible that part of the nominal SONGS effect is due to a natural current effect that is not the same at both stations in a pair, as noted above. The difference of a natural current effect between two stations should decrease with the separation between the stations, falling off to zero when the stations are side-by-side. Supposing there actually is such a nonuniform natural effect, we can subtract it out by extrapolating the data on Figs. A-2 and A-3 inward to zero on the axis of distance. Reasonable extrapolations indicate that the possible natural current effect does not exceed about half the total.

5.3 Interpretation and Comparison of Results

There are two principal mechanisms by which SONGS might potentially affect irradiance. The most obvious mechanism for reducing irradiance in the plume or downcurrent from SONGS is that naturally turbid water from near the shore and near the bottom is carried upward and offshore in the plume, replacing surface water further offshore that is naturally clearer. It is not disputed that this process often takes place, and there is no good evidence for any other mechanism to make the plume turbid.

There is another mechanism which potentially has the opposite effect of making the water in the neighborhood of SONGS generally less turbid than it would be without SONGS. This mechanism is the make-up flow toward SONGS (see 3.2) which replaces the water carried away from SONGS in the plume. Some of this flow is composed of offshore water that is naturally clearer than the normal nearshore water around SONGS; if enough offshore water reaches the vicinity of SONGS by this means, it could perceptibly reduce the average turbidity of water near SONGS that is not in the plume. Here too there is good evidence that the make-up flow is actually at work (see 3.2), and no good evidence for other mechanisms that might reduce turbidity near SONGS.

The Plume-Model and Upstream-Downstream results are clear in showing that the water that leaves the diffusers in the plume is more turbid on the average than ambient water on the other side of the diffusers at the same time, resulting in a reduction of irradiance under the plume relative to ambient by roughly 0.4 E/m^2-day (averaging over all the hours comprised in both kinds of analysis). The ambient

water, however, may be less turbid than it would have been without SONGS, because of the make-up flow, so these analyses by themselves do not prove a net reduction of irradiance by SONGS relative to a purely natural state without SONGS.

The BACIP analyses show a definite SONGS-induced decrease of average irradiance at the SOK stations by 0.46 E/m^2-day for all days when the stations are downcurrent from SONGS, with a smaller and much less certain increase of irradiance for days when the stations are upcurrent from SONGS. Downcurrent days outnumber upcurrent days, and the net effect found by the BACIP analyses is a reduction of average irradiance over all days together by 0.08 to 0.27 E/m^2-day, relative to a natural state.

Speaking very broadly, the downcurrent BACIP decrease of irradiance by about 0.4 E/m^2-day can be attributed to the first mechanism discussed above, and the uncertain upcurrent increase can be attributed to the second. In the same way, the Plume-Ambient differences of about 0.4 E/m^2-day given by Plume-Model and Upstream-Downstream analyses can be attributed to the combined action of both.

The results of the different kinds of analysis rest on different bases and need not agree closely, but it is worth noting that they can easily be brought to reasonable agreement. For instance, an actual downcurrent decrease of 0.4 E/m^2-day due to the first effect and an upcurrent increase of zero due to the second effect would together give the observed Plume-Ambient difference of 0.4 E/m^2-day. This would accord closely with the BACIP estimates at the bottom for all upcurrent and all downcurrent days (5 or more out of 9 hours), but might unduly discount the

evidence of an upcurrent increase from the 9/9 upcurrent days at 0 m and the 5+/9 upcurrent days at 2 m above (see the table in 5.1). At the other extreme, a downcurrent decrease of 0.25 E/m²-day and an upcurrent increase of 0.15 E/m²-day would produce the same Plume-Ambient difference of 0.4 E/m²-day without stretching any BACIP result by more than one standard deviation.

6.0 EFFECTS OF SONGS ON TEMPERATURE AND SUSPENDED PARTICLES

The analyses in this section are BACIP or Plume-Model analyses, whose methods and terminology, except as noted, are the same as those for the analyses of irradiance treated in Section 5 and Appendix A.

6.1 Compliance with Thermal Standards

The minimum dilutions of about 8 discussed in 3.2 above imply a maximum temperature rise less than 2.5°F (1.4°C), indicating that SONGS is in compliance with the California thermal standard which requires temperature rise at the surface not to exceed 4°F (2.2°C) beyond 1000 feet (305 m) from the discharge for more than half of any tidal cycle. To investigate compliance more thoroughly, with an extended set of direct measurements of temperature rise, we applied the plume model of 5.2 to the measurements of temperature at 3 m depth at stations UVT01 and UVT19 during the year 1985. UVT01 is upcoast of the diffusers, 310 m from the nearest point on the Unit 2 diffuser; UVT19 is downcoast, 370 m from the nearest point on the Unit 3 diffuser (see Figure 7). We formed the set of all hourly temperature differences between these stations in hours when one station was classified as Plume by the model and the other was classified as Ambient. The difference Plume-minus-Ambient reached 2.2°C in only one hour out of 972, and exceeded 1.4°C (2.5°F) for only 34 hours out of 972 (3.5% of the time).

The shortest tidal cycle is 12.42 hours. The temperature rise definitely did not exceed 4°F for more than six hours within any consecutive set of twelve, so the temperature rise at either station was in full compliance. This data-set does not give

a perfect test, since temperatures were not measured right at the surface, but it is the best available set for the purpose. Since thermal stratification in the top 3 m will generally be less in the plume than in ambient water because the plume is better mixed, a temperature rise of plume above ambient will generally be less at the surface than at 3 m, so there is no reason to believe that the standard is exceeded at the surface. The Plume-Ambient difference defines an instantaneous temperature rise across the diffusers, rather than a rise relative to a hypothetical state without SONGS, but this is the only kind of definition that can be applied to any individual tidal cycle.

The California thermal standards also limit the temperature rise to 4°F at any point on the bottom or the shoreline. We do not have data to test for compliance on the bottom or the shore as we did at 3 m depth. However, we may fully expect that shoreline or bottom differences will be much less than those at 3 m depth at stations UVT01 and UVT19. The inshore end of the Unit 3 diffuser is over 1 km from the shore, and the plume goes seaward from there. Observed surface plumes are 5 m thick or less and do not reach the bottom, and subsurface plumes spread at the equilibrium depth where the densities and temperatures of plume and ambient water are the same.

6.2 SONGS-induced upwelling

Since the make-up flow discussed in 3.2 above brings some water to the neighborhood of SONGS and the San Onofre kelp bed from greater depths offshore, there is a possibility that this flow might act as an artificial upwelling to supply nutrients to this neighborhood. Because of the close relation of dissolved

nitrate to temperature (see 2.1 above), this potential effect can be studied by BACIP tests on bottom temperature. We carried out these tests on four individual stations in SOK with SMK45 as control, and found with one exception that the Before data-sets were not additive either for temperature or its logarithm (p_A of 0.07 or less). The test on the single additive data-set (p_A = 0.30), for temperature differences between SOKD35 and SMK45, showed a SONGS-induced warming by 0.04°C, of no statistical or physical significance (p = 0.83). These tests leave us with no evidence that SONGS changed the bottom temperature at any place, and a positive though weak indication that the average SONGS-induced change at SOKD35 was indeed very small. Besides showing that there is no evidence for significant artificial upwelling due to the make-up flow, these results also show no evidence that the data given in 2.1 supporting the uniformity of El Nino are affected by temperature changes due to SONGS.

Another form of artificial upwelling comes from the upward tilt and buoyancy of the discharge jets, which lift some entrained water to the surface from depths down to 10 or 15 m near the diffusers. In the data-set for the compliance test discussed above, the plume water at 3 m was cooler than ambient 59% of the time, and cooler by 0.5°C or more 26% of the time, as a result of entrainment of cooler water from below 3 m. The nitrate-temperature relation of 2.1 does not apply to plume water, which has been heated by SONGS and abruptly mixed from different depths and temperatures, so the actual enhancement of surface nitrate in the plume cannot be estimated from temperature. On some occasions of natural upwelling, though, when bottom temperature near the diffusers falls to 14°C or below, the SONGS jets may well lift some nutrients into the surface canopy of the San Onofre kelp.

6.3 Suspended Particles

As we noted, effects of SONGS on net sedimentation on the sea bottom are considered in Technical Report B and not here. This is a suitable place, though, to report statistical evidence of SONGS' effect on the local concentration of suspended particles near the bottom, which indicates that a process of particle-trapping by SONGS something like that outlined in 4.3 above is actually taking place, whether or not it leads to long-term net deposition of bottom sediments.

The accumulation-rate of seston in open-tube traps is roughly equal to the product of volume concentration and settling-rate for fast-settling coarse particles, rising to roughly twice this product for the slowest-settling fine particles (ECO-M 1987h, 4.5.1), so this rate can be taken as a rough index of seston concentration if the size-distribution does not vary greatly.

A BACIP test on the collection rates of traps close to the bottom at station SOKU45, 400 m downcoast from the diffusers, with SOKD45, 1400 m downcoast from the diffusers, as control, showed an increase in mean collection-rate by 48% at SOKU45 relative to SOKD45 after Units 2 and 3 began operating. The Before and After mean rates at SOKD45 and the Before mean at SOKU45 were all close to 7.5 mm/day; the After mean at SOKU45 was close to 11.1 mm/day. The result is highly significant ($p = 0.0012$) and the data-set of Before differences was reliably additive ($p_A = 0.82$). The result for log-transformed data (reported in Appendix A of Technical Report K) is essentially the same, and the SONGS effect may equally well be interpreted in terms of absolute or relative changes. Even though trap collection-rates are only an approximate index of seston concentration, and not an

accurate measure, this result is definite evidence of a significant SONGS-induced increase of seston concentration close to the bottom.

Some corroboration comes from a statistical test of optical extinction near the bottom, which can be taken as a rough index of seston concentration even though the close relations of extinction to seston concentration given in 2.2 above probably do not apply to seston just above the bottom. The effect of SONGS on extinction over the interval from the bottom to 2 m above was tested with a kind of Upstream-Downstream plume model (see 5.2) which classified a station as Plume on a given day if the current ran from the diffusers to the station for 9 out of 9 daylight hours, and otherwise as Ambient. The stations used in this test were a composite of SOKU45, SOKD45, and SOKD35 for the station downcoast of the diffusers, and a composite of P-N and PI-N for the station upcoast of the diffusers. The mean Plume-minus-Ambient difference in extinction was $+0.045\ m^{-1}$, with $p = 0.003$. (This test is also reported in Appendix A of Technical Report K.) This test only applies to a special set of days, rather than all days, but the result gives independent evidence that seston concentration near the bottom is higher on the downcurrent side of SONGS.

7.0 REFERENCES

Chelton, D.B. 1981. Interannual Variability of the California Current - Physical Factors, CalCoFi Reports Vol. XXII, 1981.

Ecosystems Management Associates, Inc. (ECO-M). 1987a SONGS Physical and Chemical Oceanography Final Report, Contract MRC 86-7, II-2: Synoptic Studies of the Plume of SONGS Units 2 and 3, April 30, 1987.

ECO-M. 1987b. SONGS Physical and Chemical Oceanography Final Report, Contract MRC 86-7, VI: Databases: Organization, Access, and Contents, April 30, 1987.

ECO-M. 1987c. SONGS Physical and Chemical Oceanography Final Report, Contract MRC 86-7, II-2: Construction Effects and Effects of the Sand-Release of 1984-5, June 1, 1987.

ECO-M. 1987d. SONGS Physical and Chemical Oceanography Final Report, Contract MRC 86-7, VI-3: Summaries of Data, June 1, 1987.

ECO-M. 1987e. SONGS Physical and Chemical Oceanography Final Report, Contract MRC 86-7, II-2: Addendum to Synoptic Studies of the Plume of SONGS Units 2 and 3, September 25, 1987.

ECO-M. 1987f. SONGS Physical and Chemical Oceanography Final Report, Contract MRC 86-7, II-2: Estimated Long-Term Mean Concentration of Effluents from SONGS, October 15, 1987.

ECO-M. 1987g. SONGS Physical and Chemical Oceanography Final Report, Contract MRC 86-7, V-2: The Relation of Dissolved Nitrate to Temperature off San Onofre, November 9, 1987.

ECO-M. 1987h. SONGS Physical and Chemical Oceanography Final Report, Contract MRC 86-7, IV-4: Instrumentation, July 31, 1987.

ECO-M. 1988a. SONGS Physical and Chemical Oceanography Final Report, Contract MRC 86-7, II-1: The Natural Environment near San Onofre, January 20, 1988.

ECO-M. 1988b. SONGS Physical and Chemical Oceanography Final Report, Contract MRC 86-7, II-2: Disturbances of the Flow-Field by the Cooling System of SONGS, January 26, 1988.

Fischer, H. B., E.J. List, R.C.Y. Koh, J. Imberger and N.H. Brooks. 1979. *Mixing in Inland and Coastal Waters*. Academic Press, New York, 1979. 483 pp.

Koh, R.C.Y., N.H. Brooks, E.J. List, E.J. Wolanski. 1974. Hydraulic Modelling of Thermal Outfall Diffusers for the San Onofre Nuclear Power Plant, Report No. KH-R-30, W.M. Keck Laboratory of Hydraulics and Water Resources, California Institute of Technology, January 1974.

Lynn, R.J., K.A. Bliss and L.E. Eber. 1982. Vertical and horizontal distributions of seasonal mean temperature, salinity sigma-T, stability, dynamic height, oxygen saturation in the California current 1950-1978. CalCoFi Atlas No. 30. A. Fleminger, ed.

Marine Review Committee, Inc. (MRC). 1988. Interim Technical Report 2. Sampling design and Analytical procedure (BACIP). Report submitted to the California Coastal Commission.

MRC. 1989. Final Technical Report B. Anomalous sediments in the San Onofre Kelp Bed. Report to the California Coastal Commission.

Okubo, A. 1974. Some Speculations on Oceanic Diffusion Diagrams, Rapp. P.-v. Reun. Con. Int. Explor. Mer. 167, 77-85, December 1974.

Reitzel, J. 1980. Final Report of the Turbidity Program: Predicted Changes in Irradiance at San Onofre Kelp, Report to MRC (MRC Document No. 80-05), November 15, 1980.

Reitzel, J. 1981. Addendum to the Final Report of the Turbidity Program: Further Observations of Seston and Extinction, Report to MRC (MRC Document No. 81-05), January 12, 1981.

8.0 FIGURES

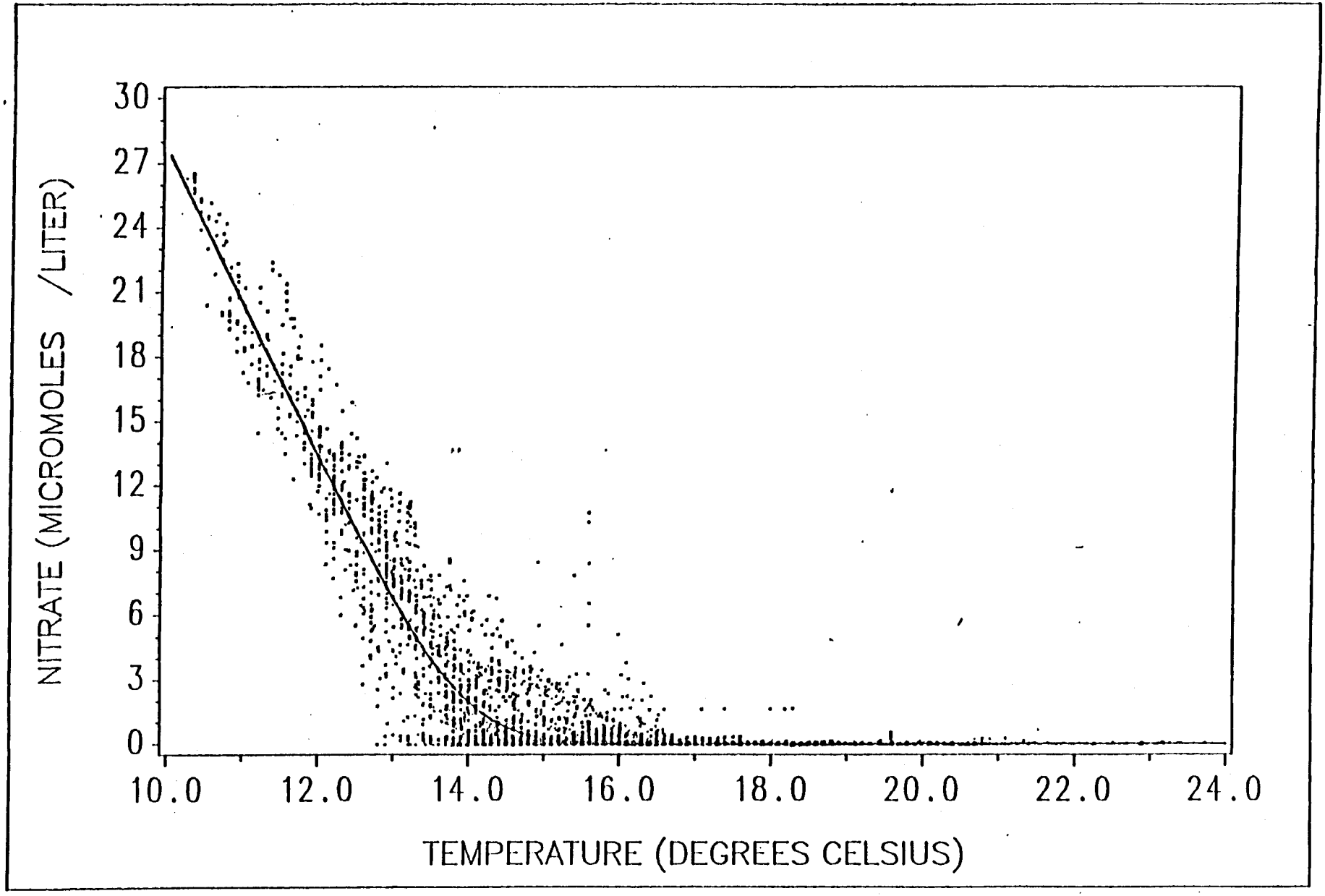

Figure 1: Plot of measured Nitrate versus Temperature with the solid line representing the N - T Relationship.

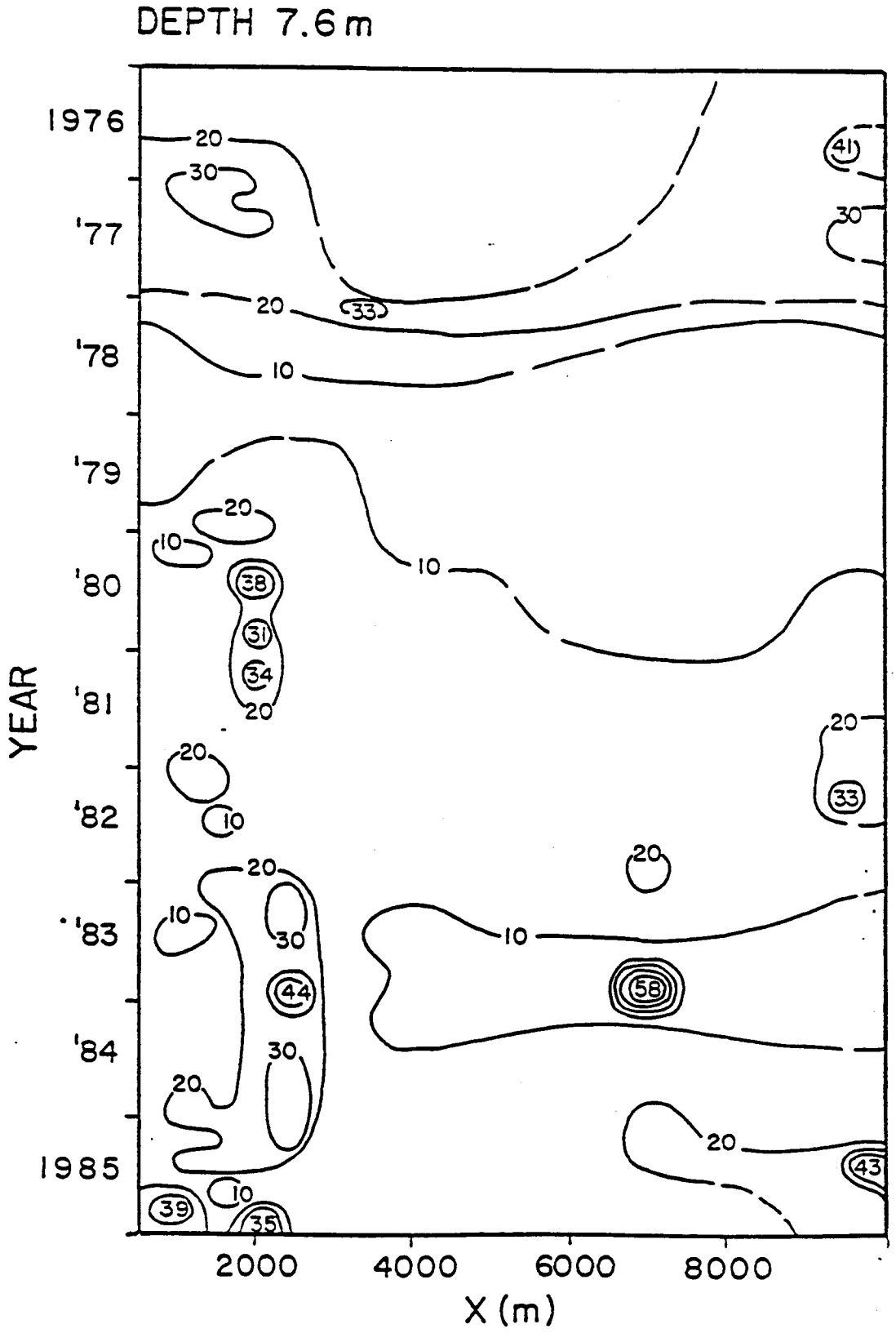

Figure 2: Percentage of silt and clay in sediments at 7.6 m depth of water, 1976-85

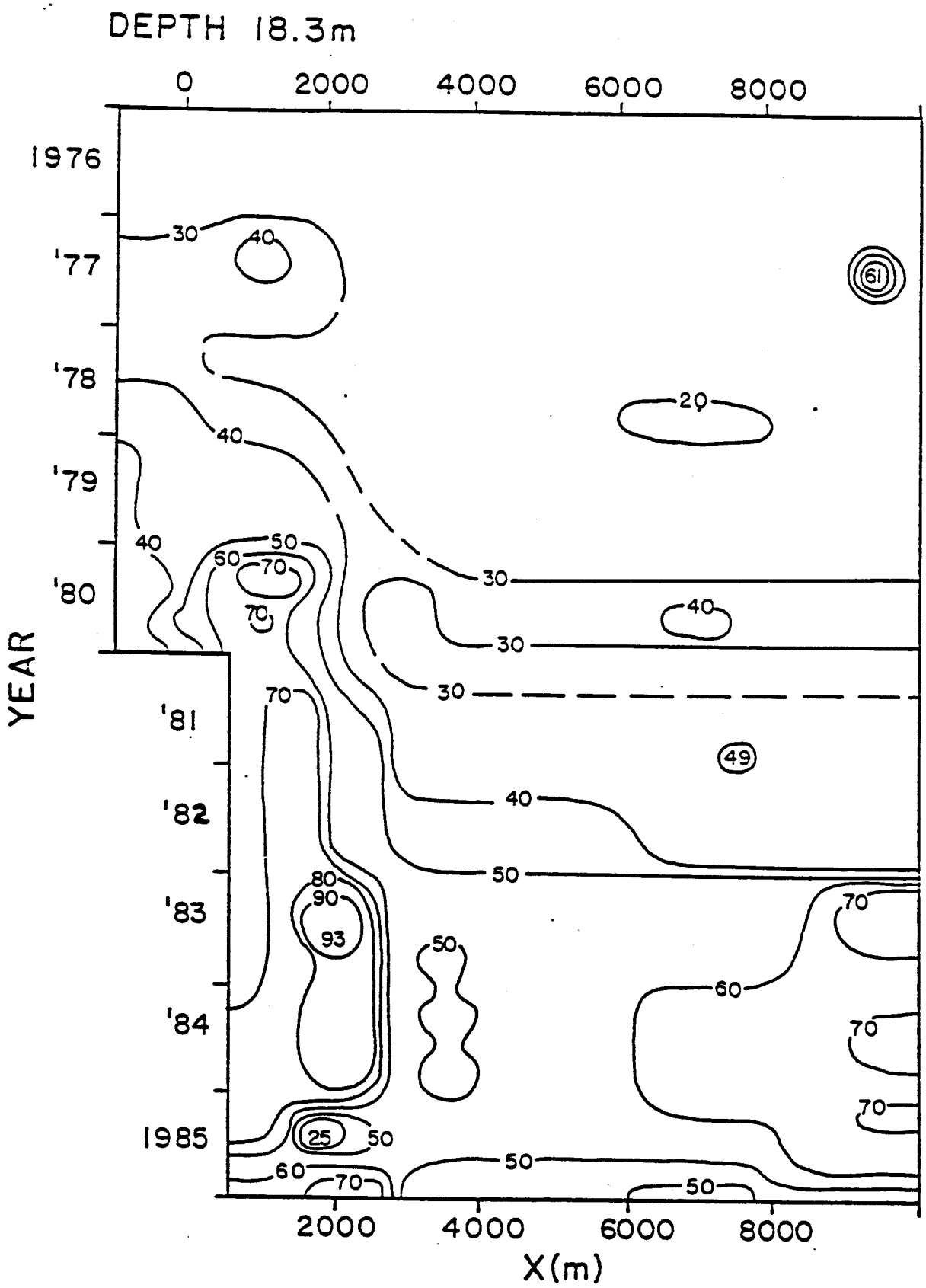

Figure 3: Percentage of silt and clay in sediments at 18.3 m depth of water, 1976-85

Upcoast

Figure 4: Study site and locations of Stations

Downcoast

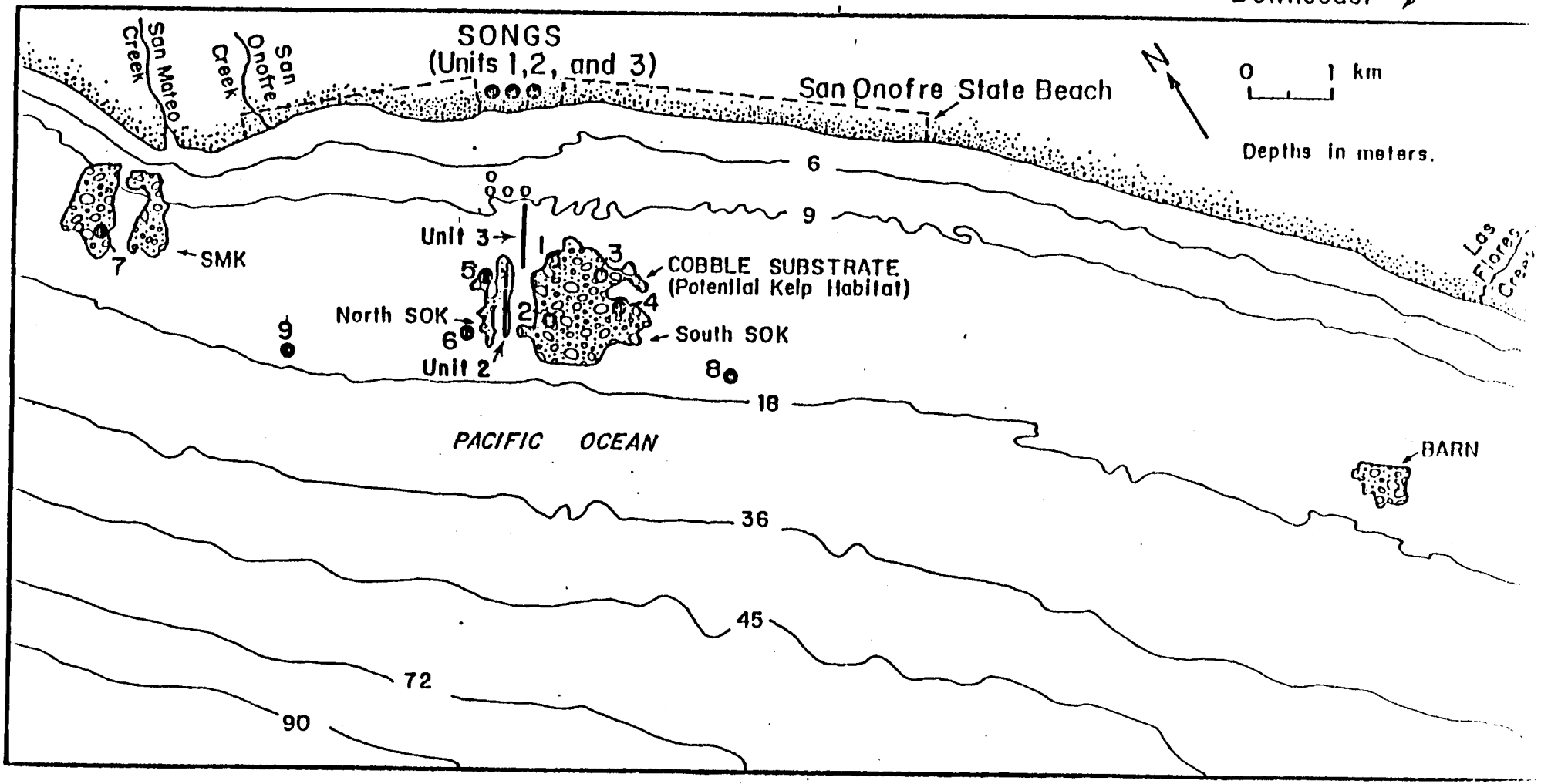

1. SOKU35
2. SOKU45
3. SOKD35
4. SOKD45
5. PN
6. PL45
7. SMK45
8. PMRS
9. PMRN

ooo = UNITS 1,2,and 3 INTAKES

o = UNIT 1 DISCHARGE

—— = DIFFUSER LINES

● = IRRADIANCE STATIONS

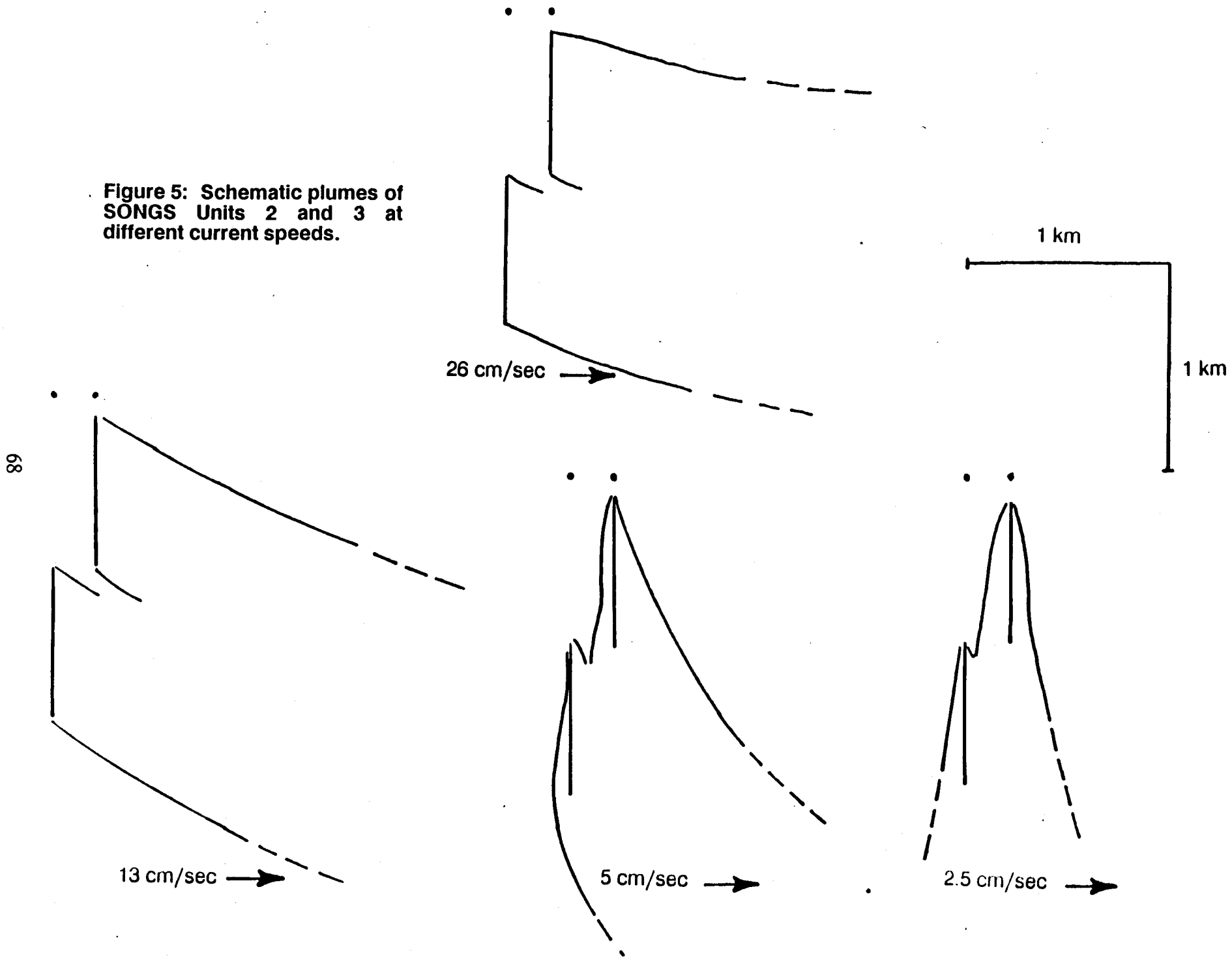

Figure 5: Schematic plumes of SONGS Units 2 and 3 at different current speeds.

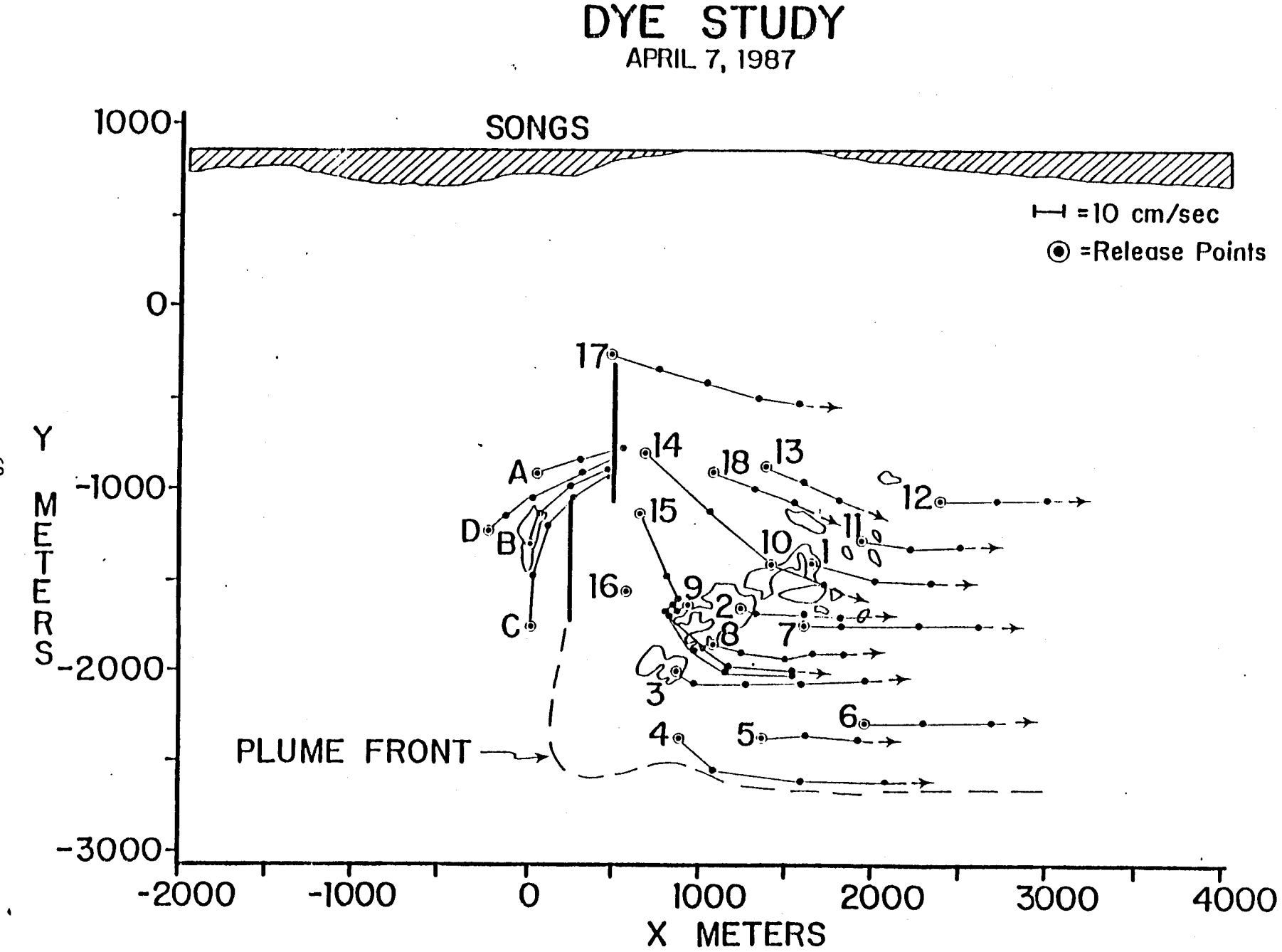

Figure 6: Trajectories of dye-patches in the plume of SONGS

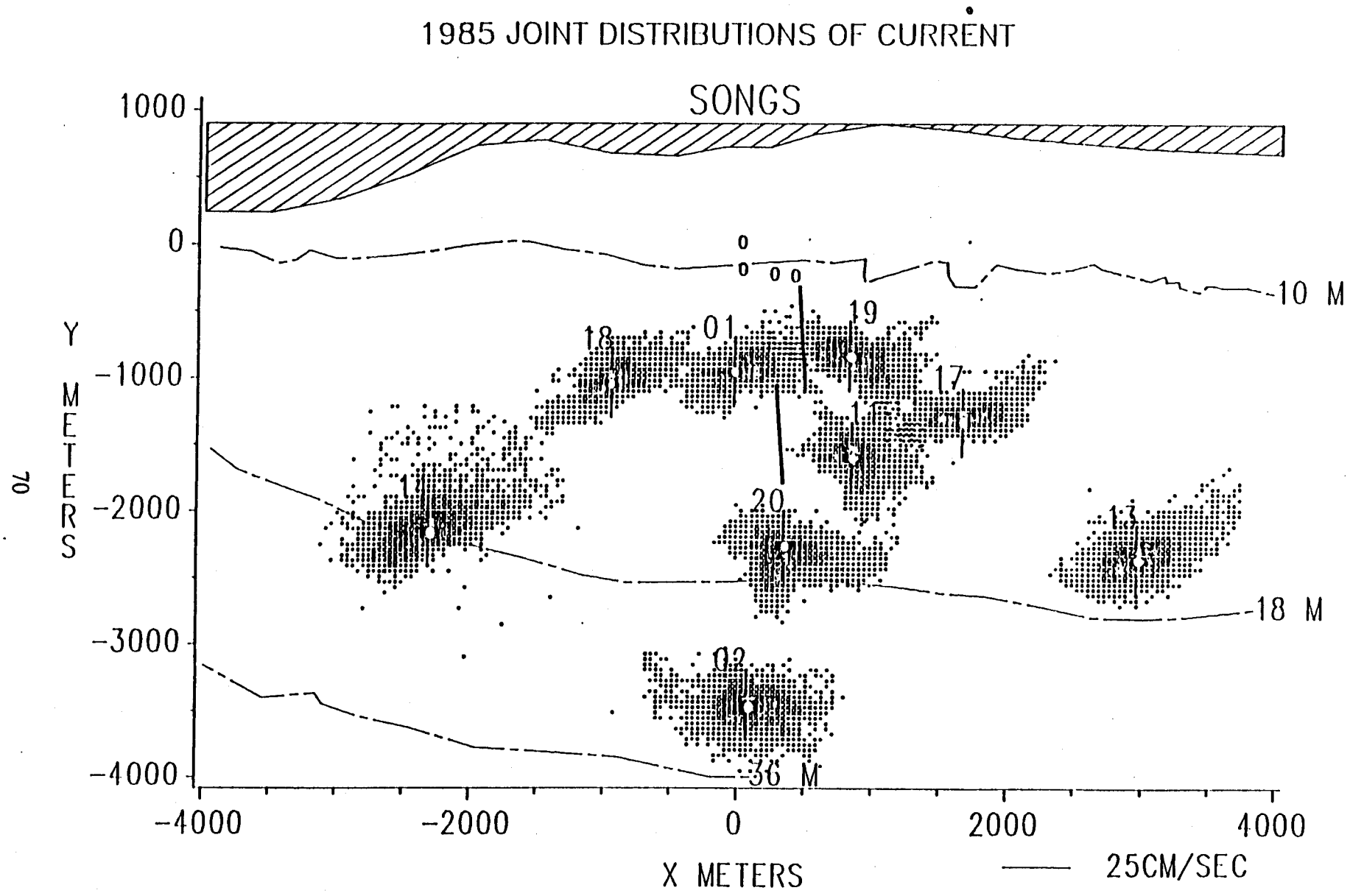

Figure 7: Joint distributions of longshore and cross-shelf current velocities (current roses) off San Onofre, 1985

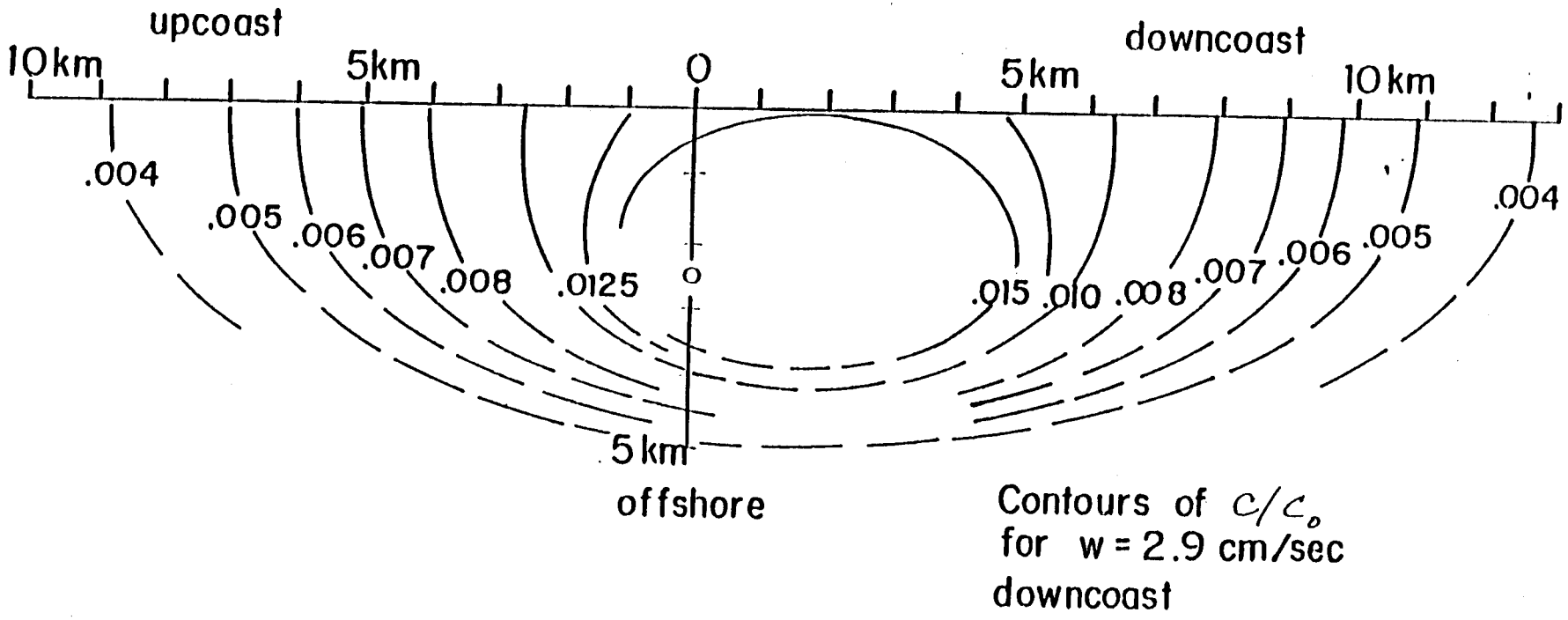

Figure 8: Contours of relative concentration C/C_o for mean current 2.9 cm/sec downcoast

This page intentionally left blank.

APPENDICES

This page intentionally left blank.

APPENDIX A

STATISTICAL ANALYSES OF THE EFFECTS OF SONGS OPERATION ON UNDERWATER IRRADIANCE

1.0 METHODS

1.1 BACIP Analysis

The first method we have used is a variant of the Before-After/Control-Impact Pairs design, called BACIP for short. This design is treated at length by Stewart-Oaten (1986), and will be discussed only briefly here. The BACIP design seeks to detect and estimate a change in mean irradiance that occurred only near the power plant and only after it started operating, separate from natural differences of irradiance between places and times. This is done by setting up an Impact station near the power plant and a Control station at distance, and measuring the instantaneous difference of irradiance ΔI_B (Impact minus Control) between these stations at many times in the Before period prior to start-up of the power plant. By dealing with instantaneous differences, this paired-BACI design subtracts out natural temporal variations that are common to both stations, eliminating a large part of the natural variability. The time-series of ΔI_B may be examined to see if its mean $<\Delta I_B>$ can be taken as a stationary process-mean. If it is stationary, $<\Delta I_B>$ represents a constant natural difference due to location alone, which may be presumed to continue after the power plant starts up.

A similar series of measurements at the same stations in the After period gives a set of differences ΔI_A, similarly free from temporal variations common to both stations, whose mean $<\Delta I_A>$ represents the difference between the locations in the presence of the operating power plant. If $<\Delta I_B>$ was stationary, the difference of means

$$\Delta\Delta I = \langle \Delta I_A \rangle - \langle \Delta I_B \rangle$$

represents a time-location interaction: that is, a change of mean irradiance occurring only near the power plant and only after it started operation.

An important requirement to make this result valid is that the irradiance-differences ΔI_B respond linearly or additively to changes in natural conditions. If they do not, natural changes can masquerade as power plant effects, as shown by the following example. Underwater irradiance varies exponentially with the extinction coefficient K, which is largely a property of the water, so natural changes in K will produce multiplicative rather than additive changes in I. If average irradiance at the Impact station were twice that at Control in the Before period, and if a uniform natural decrease in K doubled both values in the After period, the resulting $\Delta\Delta I$ would be equal to the original irradiance at Control, without any effect of the power plant.

In this particular example, the difficulty could be avoided by dealing with lnI instead of I as the primary variable. This would give the same $\Delta \ln I$ both Before and After (that is, the same ratio of Impact to Control), and $\Delta\Delta \ln I = 0$ in the absence of any real power plant effect. In general, we are not sure in advance what variable may be additive; we try various transformations of the data, such as logarithms, powers, or roots, and test the transformed Before data-sets for non-additivity, seeking a variable that is both additive and physically interpretable. The Tukey test for non-additivity (Tukey 1949), applied to some transformation F(I) of irradiance data from the Before period, looks for a significant regression coefficient of the difference $(F_I - F_C)$ on the sum $(F_I + F_C)$. If the coefficient is statistically significant, we know that the station-differences of F depend systematically on the general level of F, and cannot be additive; if the level of significance is low enough, we can maintain a null hypothesis of additivity.

A calculated time-location interaction $\Delta\Delta F$ may still be an artifact of limited sampling, due to the natural variability of ΔF. If the random fluctuations of ΔF both Before and After were independent and normally-distributed, the significance would be determined by a t-test on $\Delta\Delta F$. In these studies, the fluctuations of ΔF were a time-series showing considerable autocorrelation, so that successive departures from the mean were not independent. This situation was reduced to a situation with independent normal errors by the ARIMA methods of Box and Jenkins (1976), as follows:

The analysis was cast in the form of a linear multiple regression, modelling the time-series of station-differences $F(t) = Y(t)$ as

$$Y'(t) = A + BW(t) + e(t), \text{ with}$$
$$e(t) = C_1e(t-1) + C_2e(t-2) + 0... + \epsilon(t).$$

The indicator variable $W(t)$ is a step-function taking the value 0 for all times in the Before period and 1 for all times in the After period. The function $e(t)$ models the departures of $Y'(t)$ from $A + BW(t)$ as autocorrelated errors proportional to previous departures of Y' from $A + BW$, plus independent normally-distributed random errors $\epsilon(t)$; as many coefficients C are retained as may be needed to free the $\epsilon(t)$ from significant autocorrelation. The coefficients A, B, C_1, C_2,.... are found by an iterative process that starts with the observed values $Y(t)$ in the place of $Y'(t)$. This process uses the SAS procedure PROC AUTOREG with the Maximum Likelihood option (SAS 1984), employing the techniques of Savin and White (1978) to deal with missing values.

This form allows each coefficient to be separately determined and tested for its significance relative to the random errors, in the presence of all the others. The significance of the time-location interaction B found by this method may be considerably

lower than that found by a t-test on a model without autoregressive terms, even if an approximate correction for first-order autocorrelation is applied to the t-statistic.

If the transformed data give an additive set of ΔF_B and a stationary mean $<\Delta F_B>$, and if $\Delta\Delta F$ has an acceptably high level of significance, then the inference can be drawn that $\Delta\Delta F$ is either a real change actually caused by the power plant, or else it is a confounding effect caused by some other localized agent acting at the same place as the power plant and starting work at the same time. Evidence and argument about the presence or absence of such confounding effects is a separate matter from the BACIP analysis itself.

1.2 Plume-Model Analysis

Another method, which we call Plume-Model analysis, deals with the instantaneous differences of irradiance between two stations near the power plant, designated as north (N) and south (S), lying symmetrically on opposite sides of the diffuser lines, averaged over hours when a specified model for the behavior of the plume classifies one station as being in the plume (P) and the other station as being out of the plume or ambient (A). The plume-model is purely kinematic, with the classification of a time and place as (P) or (A) depending on the recent history of the current and the location of the station relative to the diffusers. The current-history may have a natural effect on irradiance, but the part of this effect that is common to both stations is removed by taking the differences. This uniform part of the current-effect is the analogue of the natural BeforeAfter difference in a BACIP analysis; a constant natural location-difference is the same as in BACIP. The difference of mean differences

$$\Delta\Delta I = <I_{NP}-I_{SA}> - <I_{NA}-I_{SP}> = <I_{NP}+I_{SP}> - <I_{NA}+I_{SA}>$$

is twice the mean effect of the model plume minus any effect of the power plant on waters classified as (A), averaged over the two stations, plus the mean of any nonuniform current effect.

The regression-model is $Y'(t) = A + BW(t) + e(t)$ as before, with the same autoregressive $e(t)$. The indicator variable $W(t)$ takes the value 0 for any hour in which the North station is classified as (P) by the plume-model and the South station is classified as (A); it takes the value 1 for any hour in which the South station is classified as (P) and the North station as (A). Hours for which the model classifies neither or both of the stations as (P) are dropped from the analysis.

The coefficient B is the same $\Delta\Delta I$ discussed above, so $B/2$ is the plume-minus-ambient difference of irradiance due to the power plant, averaged over both stations, plus half of any natural nonuniform current effect.

The statistical requirements for validity are the same as in BACIP analysis, but here there is no data-set free of power plant influence that can be tested for non-additivity of natural changes. In this instance, analyses with I and $\ln I$ gave generally consistent estimates of fractional changes in irradiance, as described below in Section 2.2; these changes were small enough to be approximately linear whether transformed or not.

2.0 Data-Sets and Results

2.1 BACIP Analyses of Irradiance off San Onofre

The original data for these BACIP analyses are the recordings of hourly-integrated irradiance on the bottom and two meters above, at three Impact stations within the San Onofre kelp bed (SOKU45, SOKD45, and SOKD35) 500 to 1300 m south of the diffuser lines, and one Control station in the San Mateo kelp bed (SMK45) 5 km north of the diffusers. The bottom depth is 13.7 m at stations labelled 45, and 10.7 m at stations labelled 35. The locations of these stations are shown in Figure A-1. These stations were kept clear of kelp canopy at all times; a fourth station in the San Onofre kelp bed (SOKU35) was not used in BACIP analyses because its irradiance was affected by changes in the density of kelp canopy from Before to After, making a large confounding effect. The Before period includes data from mid-1981 through April 30, 1983; the After period includes data from May 1, 1983 to the end of 1986.

At values of irradiance below 0.01 Einsteins/m^2-hour, such as are often observed in dawn or twilight hours, instrumental uncertainty may be a large part of the reading; in analyses of lnI, dubious values on this order may have a large effect on the means and variances. For this reason, we included only the nine daylight hours between 7am and 4pm of each day in the analyses, plus any other hours with irradiance of 0.01 E/m^2-hr or more, treating all other hours as missing values. The data-sets of hourly station-differences did not generally turn out to be amenable to Box-Jenkins methods, so we dealt instead with the daily means formed by adding hourly irradiances over the included hours, expressing the result in E/m^2-day.

Separate analyses were carried out on these daily means for irradiance at the bottom and at a height of two meters above the bottom, with the three stations in the San Onofre kelp bed combined into one Impact station by averaging the daily mean irradiance from any of the three (usually all three) that were operating on a given day. The set of daily station differences at either height, then, was the set of combined SOK minus SMK45 for all days on which a daily mean was available from both. In general, the differences of irradiance among the three SOK stations at either 0 or 2 m above bottom were much less than the differences between the two levels at any station; we considered it suitable to combine the SOK stations in order to simplify the analysis, but not to combine the two levels.

The Tukey test for additivity was carried out on the Before data by a regression of differences on sums incorporating autocorrelated errors, like the model described in 1.1 above. The stationarity of irradiance-differences was verified by regressions on time to test for trends, and by inspection of successive three-day means and standard deviations, plotted against time and against each other.

BACIP analyses using all the data did not show significant time-location interactions, but the Plume-Model analyses of data within the After period (described in 2.2 below) did show, broadly speaking, that irradiance was on the average significantly less on the downcurrent side of the diffusers than on the upcurrent side at the same time. We suspected that much of the variation within the After period might be due to this interaction of current with the diffusers, so we carried out separate BACIP analyses for the sets of Before and After days when the Impact stations were downcurrent or upcurrent from the diffusers, in order to remove this part of the variability.

Here we report five BACIP analyses: one analysis using all days; two separate analyses using the subsets of days on which the hourly mean current was directed downcoast (towards the south) or upcoast for nine out of nine daylight hours; and two separate analyses using the days on which the current ran downcoast or upcoast for five or more out of nine daylight hours, so that every day fell into one analysis or the other. (The total number of data-points in these last two analyses is less then that in the analysis for all days because the current-direction was not recorded on every day.)

The results of the five BACIP analyses are shown in Table A-I. The successive columns in this Table show:

1) The primary variable, either I or lnI;
2) The height above the bottom, either 0 or 2 meters;
3) The number of Before days b;
4) The number of After days a;
5) The power plant effect on the given data-set: that is, the coefficient B of the Before-After indicator variable, in units of E/m^2-day for analyses of I;
6) The standard deviation of B;
7) The level of significance p of the power plant effect: that is, the probability that B is wholly an artifact of sampling;
8) The level of significance p_A for rejecting the null hypothesis that the Before data-set is additive: that is, the probability that the dependence of ΔI on the sum of I at the two stations is an artifact of sampling (high p_A implies high likelihood that the data-set is additive).

The first thing to look at in Table A-I is p_A, since a result from a non-additive data-set can be seriously misleading. Additivity varies widely among data-sets and variables, but it is clear that lnI tends to be non-additive more often than I: six out of ten analyses of lnI

have p_A of 0.1 or less, but only two out of ten have p_A of 0.5 or more; it is the other way around with I, for which only two out of ten analyses have p_A of 0.1 or less but six out of ten have p_A of 0.5 or more.

This result is contrary to a physical expectation that extinction, and hence lnI, would be additive, as in the hypothetical example given above in 2.1. We should note, though, that any physical process that produces unequal variances for a variable at the two stations will produce a non-zero regression coefficient of the differences on the sums of this variable (the regression coefficient may be written as the difference of the station-variances divided by the variance of the sum). There are many possible reasons, then, why irradiance rather than its logarithm might be additive, and we do not attempt a physical interpretation of this. Whatever the reason, the tendency of I to be more often additive than lnI is a definite characteristic of the BACIP data-sets, so the BACIP estimates of power plant effects B are better expressed as absolute rather than fractional changes in irradiance.

Many of the results in Table A-I are of doubtful additivity or low significance or both (which does not invalidate those results that are both additive and significant). All the results are shown in the Table because there is no set criterion for rejection, though we should certainly mistrust those with very low p_A. For a summary of the most reliable results for the variable I, those with p_A of 0.1 or more are listed below; the results with p_A less than 0.1 are labelled NA for non-additive.

Data-set	Var.	Ht.	B (I in E/m²-day)	s.d.	p	p_A
Downcurrent						
9hr/9	I	0	-0.60	0.23	0.01	0.98
5hr/9	I	0	-0.46	0.21	0.03	0.86
9hr/9	I	2	-0.39	0.32	0.22	0.50
5hr/9	I	2	-0.43	0.29	0.14	0.20
Upcurrent						
9hr/9	I	0	+0.51	0.32	0.11	0.97
5hr/9	I	0	+0.02	0.26	0.93	0.31
9hr/9	I	2	NA			
5hr/9	I	2	+0.41	0.42	0.33	0.82
All Days	I	0	NA			
	I	2	-0.13	0.25	0.61	0.62

The significant and highly additive results for downcurrent days at level 0 compel the conclusion that average irradiance on the bottom at the SOK stations was reduced by approximately 0.5 E/m²-day on downcurrent days by the power plant (in the absence of demonstrated confounding effects). The whole body of BACIP results makes it highly reasonable to conclude that the power plant generally reduced irradiance at and near the bottom in SOK by about 0.4 E/m²-day on all downcurrent days, and probably increased irradiance by a comparable but somewhat smaller amount on upcurrent days.

(The reduction of about 0.4 E/m²-day for all downcurrent days corresponds to a fractional reduction of about 25% at the bottom and 15% at 2 m above, relative to the BACIP estimates of what mean After irradiance at SOK would have been without SONGS; that is, $\langle I_{IB} \rangle + (\langle I_{CA} \rangle - \langle I_{CB} \rangle)$. These numbers are not to be taken as BACIP estimates of mean fractional reductions, which are unobtainable because lnI is not additive in these data-sets.)

Table A-I shows, in reasonable agreement with the overall statistics of the current, that there are more downcurrent days than upcurrent days in these data-sets, in the ratio 59

to 41, so the net effect over all the days is a reduction of irradiance, ranging from about 0.24 E/m^2-day if B for upcurrent days is actually zero, to about 0.08 E/m^2-day if the upcurrent value of B is equal and opposite to the downcurrent value. This accords with the tolerably additive but non-significant BACIP estimate of the net effect as B = -0.13 E/m^2-day for all days at 2 m above the bottom.

2.2 Plume-Model Analyses of Irradiance off San Onofre

The first plume-model that we tried was very simple: it classified a station as in the plume (P) in a given hour if the mean current in that hour ran from the diffusers toward the station, and as ambient (A) if the current ran the other way. This Upstream-Downstream model has obvious deficiencies, and we developed a more elaborate model to take account of the main characteristics of the actual plume, as well as they were known from field observations and hydraulic modelling of the system (Fischer *et al.* 1979). The essential operation of the model was to backtrack water at the station by means of the currents recorded over preceding hours, with allowance for the initial seaward momentum of the plume itself, and for dispersion from the boundaries of the plume. The backtracking computation was continued until the backtrace of the water from the station crossed the diffuser lines, or out to 25 hours. The number of hours, up to 25, from station to diffusers was called the plume age; for all the stations, most of the computed plume ages were either 10 hours or less, or else undefined because the trace did not reach the diffusers within 25 hours; accordingly, we classified a station and hour as (P) if the plume age was 10 hours or less, and otherwise classified the station and hour as (A).

The actual algorithm for plume age used the record of longshore current to find whether the longshore coordinates of water discharged at the beginning and end of the preceding hour bracketed the longshore coordinate of the station. If they did not, the

computation was repeated for the next preceding hour. If they did, say for the n^{th} preceding hour, cross-shelf coordinates of water discharged that hour from the inner and outer ends of the diffuser line were computed from the cross-shelf current history, with two additional kinds of cross-shelf motion: an added seaward velocity of 0.05 m/sec at both ends representing the initial momentum of the plume; and, for the n^{th} preceding hour, a displacement of 10.8 $n^{3/2}$ meters, seaward from the outer end and shoreward from the inner end, representing the mean-square dispersion distance according to the relation of Okubo (1974). If the cross-shelf coordinates of the water from the two ends did not bracket that of the station, the whole computation was repeated for the next preceding hour; if they did, a plume age of n hours was assigned to the station and time. The current-record used for these computations was a composite of several stations some distance to either side of the diffusers, to represent ambient current alone and avoid counting plume-induced velocities twice.

It will be useful at this point to recall from Section 1.2 that the coefficient B found in a Plume-Model analysis represents twice the mean difference of irradiance between (P) and (A) hours, averaged over both stations in the pair, plus any nonuniform natural current-effect. Accordingly, we will tabulate and discuss B/2 as the nominal power plant effect.

The data for Plume-Model analyses are recordings of hourly-integrated irradiance, in E/m^2-hour, at 0 and 2 m above the bottom, at four stations south of the diffusers in SOK and another station called PMRS about 2.5 km south of the diffusers, plus a set of stations north of the diffusers to be paired with the south stations. The names of the paired stations are listed in the tables of results, and the locations of all are shown in Figure A-1. The data-sets of north-south station differences comprise all hours between 7am and 4pm in the years 1985 and 1986 in which both stations of a given pair were operating, plus any other

hours in which both stations had hourly irradiances of 0.01 E/m^2-hr or more. Units 2 and 3 of SONGS were in normal operation, though not wholly uniform or continuous operation, throughout this period.

The statistical tests and procedures on the data-sets were the same as for the BACI analyses, with one exception: Tukey tests for non-additivity were not done because there were no subsets of the data uninfluenced by the power plant in which to test for non-additivity of natural changes. Instead, we analyzed all the data both with I and with lnI as primary variables (dropping any zero irradiances from analyses of lnI), and computed the fractional change in irradiance, relative to the Ambient mean, as $B/2<I_A>$ from the analysis with I, and as $\exp\{B/2\}-1$ from the analysis with lnI. Since the two computations substantially agreed, as shown by the results tabulated below, we concluded that the changes were small enough to remain approximately linear under transformation, and that errors from non-additivity were minor.

The results of the Plume-Model analyses are shown in Table A-II. The successive columns in this Table list the following:

1) The station-pairs (south station first) and their mean distances from the diffusers (half the separation);
2) The height above bottom, 0 or 2 m;
3) The fractions p_S and p_N of all hours, including those dropped from the analysis because both stations were (A), classified as (P) for the south and north stations;
4) The power plant effect B/2 from analysis of I, here called δI;
5) The fractional change δI divided by mean Ambient I, $\delta I/<I_A>$;
6) The power plant effect B/2 from analysis of lnI, here called δlnI;

7) The fractional change $\delta I/I = \exp\{\delta \ln I\} - 1$.

Every analysis of I showed a highly significant negative B/2 representing an average reduction of irradiance on the order of 0.05 E/m^2-hour in the model plume relative to ambient water at the same time, with an average fractional reduction of 24%. Every analysis of lnI showed a highly significant negative B/2, with an average fractional reduction of 28%. The model classified the SOK stations as in the plume (P) for percentages of all hours ranging from 17% to 28%; it classified PMRS as (P) in only 3% of all hours, and PMRN as (P) in 5 or 6% of all hours.

The fractional changes from Table A-II are plotted in Figure A-2 against the mean distance from the diffuser line to the stations in a pair. In this Figure, the symbol I designates an analysis of irradiance and L designates an analysis of lnI, while 0 and 2 refer to height above the bottom. It will be seen from this plot that the nominal power plant effects are somewhat larger for the station-pairs including SOKD stations, at mean distances of about 1000 m from the diffusers, than they are for the pairs including SOKU stations, at mean distances of about 500 m. The effect for the pair PMRS-PMRN, each about 2500 m from the diffusers, is about as large as the effect at 1000 m (though it occurs much less often because the distant stations are rarely in the model plume).

The simplest explanation within the framework of the analysis itself is that there is indeed a differential natural current-effect between the stations of a pair, which increases with the separation between stations out to 2 km. This differential effect must vanish as the separation goes to zero, so it can be eliminated by extrapolating the results toward the diffusers. A rough linear extrapolation from 1100 m to zero on Fig. A-2 would give a mean fractional reduction in the model plume relative to ambient water of something like 15% close to the diffusers, due to the power plant alone. This need not be the true explanation,

of course; the actual plume and make-up flow are obstructed and diverted in a complicated way by the kelp beds themselves, and this may be the cause of the increase of plume-minus-ambient difference with distance.

2.2.1 Upstream-Downstream Analyses

The Plume-Model analyses excluded about half of all hours with recordings at pairs including SOK stations, and 90% of all hours with recordings at PMRS-PMRN. Except for a very few occasions when the model classified both stations in a pair as (P), the excluded hours were times when the model classified both stations as (A). To investigate power plant effects in the large fraction of the time when the plume-model was inapplicable, we analyzed the excluded hours with the original Upstream-Downstream model, which simply classifies a station downcurrent from the diffusers in a given hour as (P) and an upcurrent station as (A). Applied to a pair of stations on opposite sides of the diffusers, this model will always call one station (P) when the other is (A), and no data will be dropped. The results of these Upstream-Downstream analyses are shown in Table A-III, which is arranged like Table A-II. The fractions of hours called (P) are now the fractions of hours analyzed by this method, rather than all recorded hours.

Every analysis of I resulted in a negative B/2 on the order of 0.025 E/m^2-hour, for a fractional reduction averaging 11%. Every analysis of lnI gave negative B/2, with an average fractional reduction of 8%. The Upstream-Downstream model classified the south station in a pair as (P) for a percentage of all analyzed hours ranging from 46% to 69%.

The fractional changes given by Upstream-Downstream analyses are plotted against mean distance from the diffusers in Figure A-3, with the same notation as in Fig. A-2. Like the Plume-Model results, the Upstream-Downstream results showed a tendency for the

nominal power plant effect to increase with distance out to 1000 m or so from the diffusers. Extrapolation of these results to zero separation would give the power plant effect close to the diffusers as a fractional reduction in the neighborhood of 5%, applying to the hours when both stations were classified as (A) by the plume model.

3.0 Comparison of BACIP and Plume-Model Results

BACIP analyses have demonstrated a power plant-induced change in irradiance at Impact stations, relative to an estimate of what it would have been without the power plant, derived from values at a distant Control station and values at the Impact station before the power plant began operating. Plume-Model analyses have demonstrated a power plant induced difference of irradiance between plume water and ambient water, as defined by a specified plume-model, and Upstream-Downstream analyses have done the same with a different plume-model; neither of these two refers to a Control station or to a pre-operational period. There is no way to make a strict comparison among these results, and even the roughest comparison requires a chain of suppositions.

First we must suppose that the Plume-Model and Upstream-Downstream criteria are more or less equivalent. Each is applied to about half the total of hours analyzed, so we can then average their results to say that the average plume-minus-ambient difference over all hours, which we may call <P-A> or <P>-<A>, is about -0.04 E/m^2-hour, or very approximately -0.4 E/m^2-day accumulated over the daylight hours. This round number comes from the averages at the three SOK stations used in the BACI analyses, with no extrapolation to zero separation.

To compare this with the BACI results, we have to suppose next that the mean BACI power plant effect of about -0.4 E/m²-day on downcurrent days represents more or less the same <P> as above, and that the uncertain BACI power plant effect on upcurrent days represents more or less the same <A> as above. With <P> = -0.4 and <P>-<A> = -0.4, we get <A> = 0. This is lower than the highly additive estimates of <A> in Table A-I by about 1 to 1.6 standard errors, so this chain of suppositions brings us to reasonable agreement between BACI and the combined Plume-Model and Upstream-Downstream analyses. If we suppose that half the nominal <P>-<A> is due to a differential current effect, and set <P>-<A> = -0.2, we get <A> = -0.2 instead of zero, lower than the additive BACI estimates of <A> by about 1.5 to 2.2 standard errors, barely at the edge of agreement.

There is no reason to believe that the quantities <P> and <A> actually mean just the same thing in the three different kinds of analysis, but it is reassuring to find by this comparison that the physical meanings of <P> and <A> in the different analyses are not grossly different.

TABLE A-I

RESULTS OF BACI ANALYSES

Var.	Ht.	b	a	B (I in E/m²-Day)	s.d.	p	p_A
<u>All Days</u>							
I	0	377	1101	+0.15	0.17	0.37	0.06
I	2	249	861	-0.13	0.25	0.61	0.62
lnI	0	327	1066	-0.18	0.16	0.25	0.001
lnI	2	238	855	-0.14	0.12	0.27	0.15
<u>Downcurrent Days, 9 hours out of 9</u>							
I	0	83	369	-0.60	0.23	0.01	0.98
I	2	85	295	-0.39	0.32	0.22	0.50
lnI	0	83	369	-0.42	0.23	0.07	0.04
lnI	2	85	295	-0.01	0.16	0.93	0.0001
<u>Upcurrent Days, 9 hours out of 9</u>							
I	0	27	220	+0.51	0.32	0.11	0.97
I	2	16	170	+0.41	0.49	0.40	0.0001
lnI	0	270	220	+0.38	0.28	0.17	0.96
lnI	2	16	170	-0.29	0.26	0.28	0.0001
<u>Downcurrent Days, 5 or more hours out of 9</u>							
I	0	119	590	-0.46	0.21	0.03	0.86
I	2	111	484	-0.43	0.29	0.14	0.20
lnI	0	119	590	-0.31	0.20	0.13	0.34
lnI	2	111	484	-0.06	0.14	0.69	0.0001
<u>Upcurrent Days, 5 or more hours out of 9</u>							
I	0	59	465	+0.02	0.26	0.93	0.31
I	2	30	367	+0.41	0.42	0.33	0.82
lnI	0	59	465	-0.14	0.22	0.53	0.56
lnI	2	30	367	-0.05	0.23	0.82	0.01

TABLE A-II

RESULTS OF PLUME-MODEL ANALYSES 1985-86

Pair	Ht.	p_S	p_N	δI (E/m²-hr)	$\delta I/\langle I_A \rangle$	$\delta \ln I$	$\delta I/I$
SOKU45 (PL45) 600 m	O	0.22	0.37	-0.028	-0.216	-0.231	-0.206
	2	0.17	0.39	-0.042	-0.174	-0.282	-0.246
SOKU35 (PN) 500 m	0	0.27	0.23	-0.037	-0.225	-0.323	-0.276
	2	0.28	0.27	-0.072	-0.237	-0.338	-0.287
SOKD45 (PL45) 1100 m	0	0.22	0.29	-0.054	-0.317	-0.428	-0.348
	2	0.21	0.30	-0.073	-0.257	-0.341	-0.289
SOKD35 (PN) 900 m	0	0.23	0.24	-0.054	-0.253	-0.356	-0.300
	2	0.26	0.23	-0.108	-0.288	-0.378*	-0.315
PMRS (PMRN) 2600 m	0	0.03	0.05	-0.037	-0.231	-0.321	-0.275
	2	0.03	0.06	-0.051	-0.253	-0.364	-0.305

The significance levels of all δI and $\delta \ln I$ are less than $p = 0.0002$, except for *, which is 0.004.

TABLE A-III

RESULTS OF UPSTREAM-DOWNSTREAM ANALYSES 1985-86

Pair	Ht.	p_S	p_N	δI (E/m²-hr)	$\delta I/\langle I_A \rangle$	$\delta \ln I$	$\delta I/I$
SOKU45 (PL45) 600 m	0	0.59	0.41	-0.014	-0.109	-0.042*	-0.041
	2	0.57	0.43	-0.017	-0.075	-0.034**	-0.033
SOKU35 (PN) 500 m	0	0.46	0.54	-0.016	-0.105	-0.129	-0.121
	2	0.51	0.49	-0.021	-0.088	-0.056	-0.054
SOKD45 (PL45) 1100 m	0	0.68	0.32	-0.020	-0.139	-0.097	-0.092
	2	0.69	0.31	-0.033	-0.132	-0.080	-0.077
SOKD35 (PN) 900 m -0.075	0	0.55	0.45	-0.025	-0.135	-0.104	-0.099
		2	0.60	0.40	-0.032	-0.106	-0.077
PMRS (PMRM) 2600 m	0	0.58	0.42	-0.015	-0.114	-0.091	-0.087
	2	0.62	0.38	-0.026	-0.135	-0.105	-0.099

The significance levels of all δI and $\delta \ln I$ are $p = 0.04$ or less (usually much less), except for *, which is 0.12, and **, which is 0.10.

REFERENCES

Box, G., and Jenkins, G. 1976. Time Series Analysis Forecasting and Control, Holden-Day, Oakland, California, 1976.

Okubo, A. 1974. Some Speculations on Oceanic Diffusion Diagrams, Rapp. P.- v. Cons. Int. Explor. Mer, 167, 77-85, December 1974.

SAS Institute, Inc. 1984. SAS/ETS Users' Guide, Box 8000, Gary, North Carolina 27511.

Savin, N., and White, K. 1978. Testing for Autocorrelation with Missing Observations. Econometrica 46: 59-66.

Stewart-Oaten, A. 1986. The Before-After/Control-Impact Pairs Design for Environmental Impact Assessment. Report to Marine Review Committee, June 20, 1986.

Tukey, J. 1949. One Degree of Freedom for Non-Additivity, Biometrics 5: 232-242.

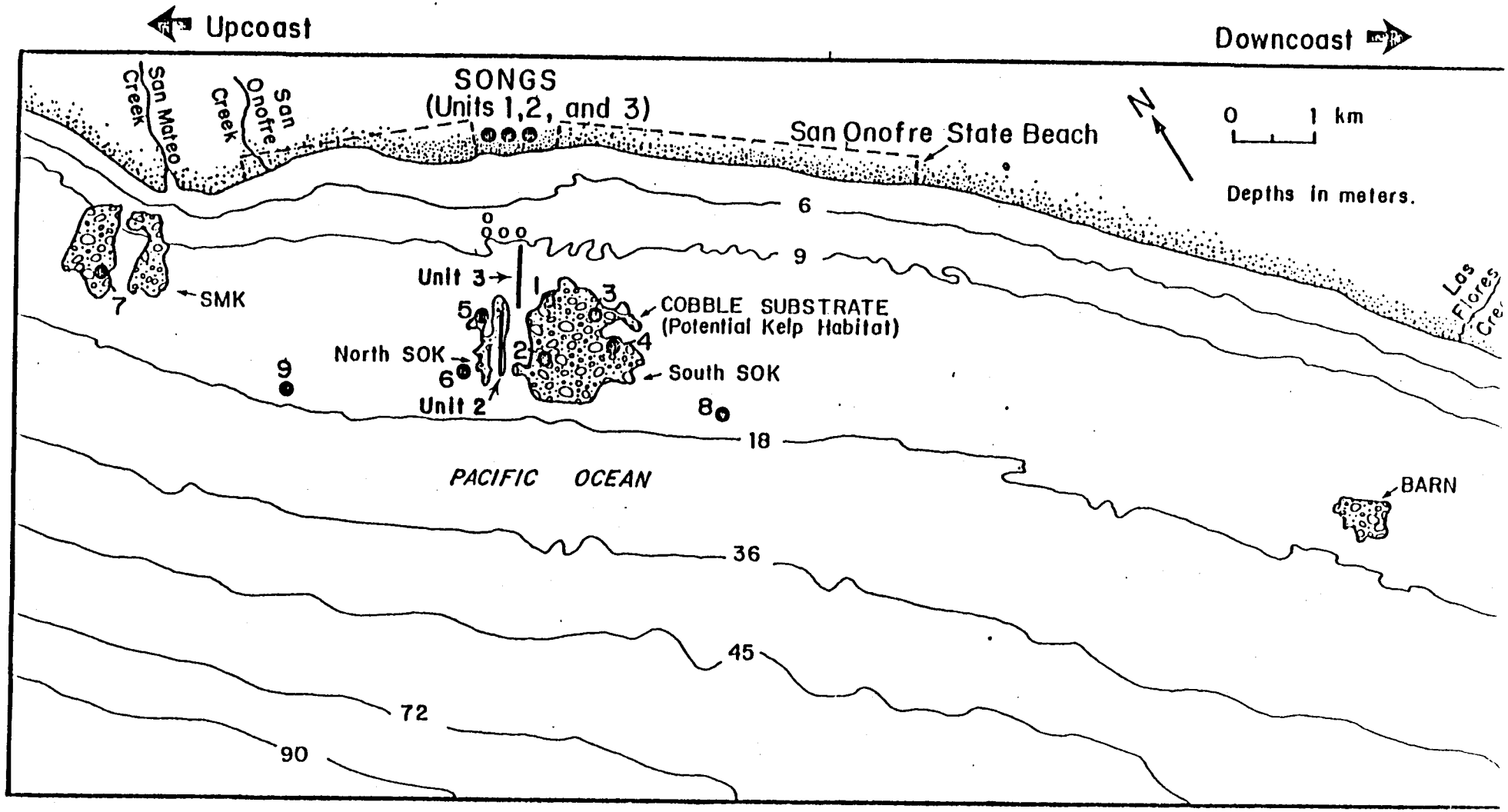

Fig. A-1 Study Site and Locations of Stations

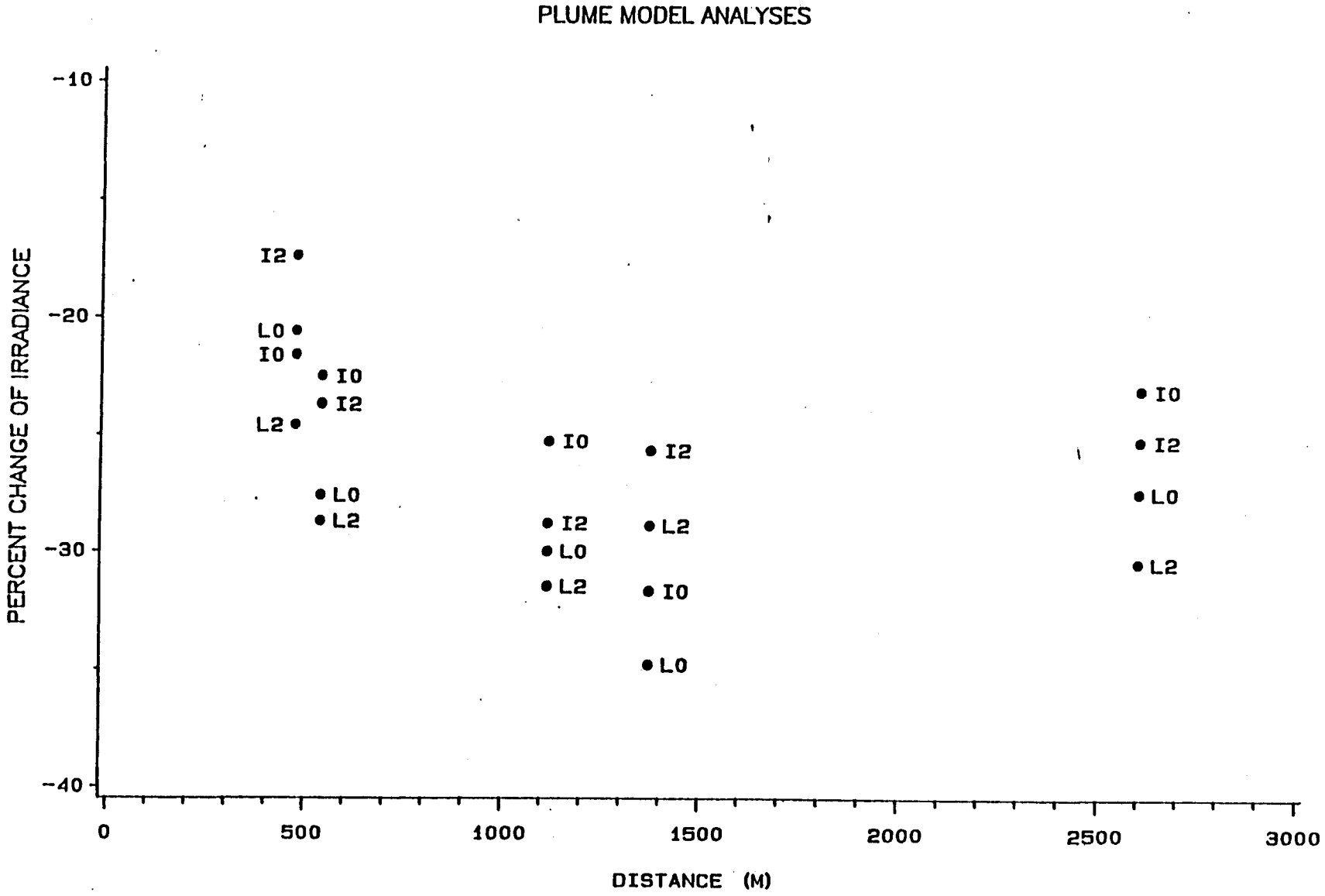

Fig. A-2. Percent Change of Irradiance, Computed From the Plume Model, as a Function of Distance From the Diffusers. I indicates results from calculations using irradiance, L indicates results of calculations using ln(I), 0 and 2 indicate the heights from the bottom.

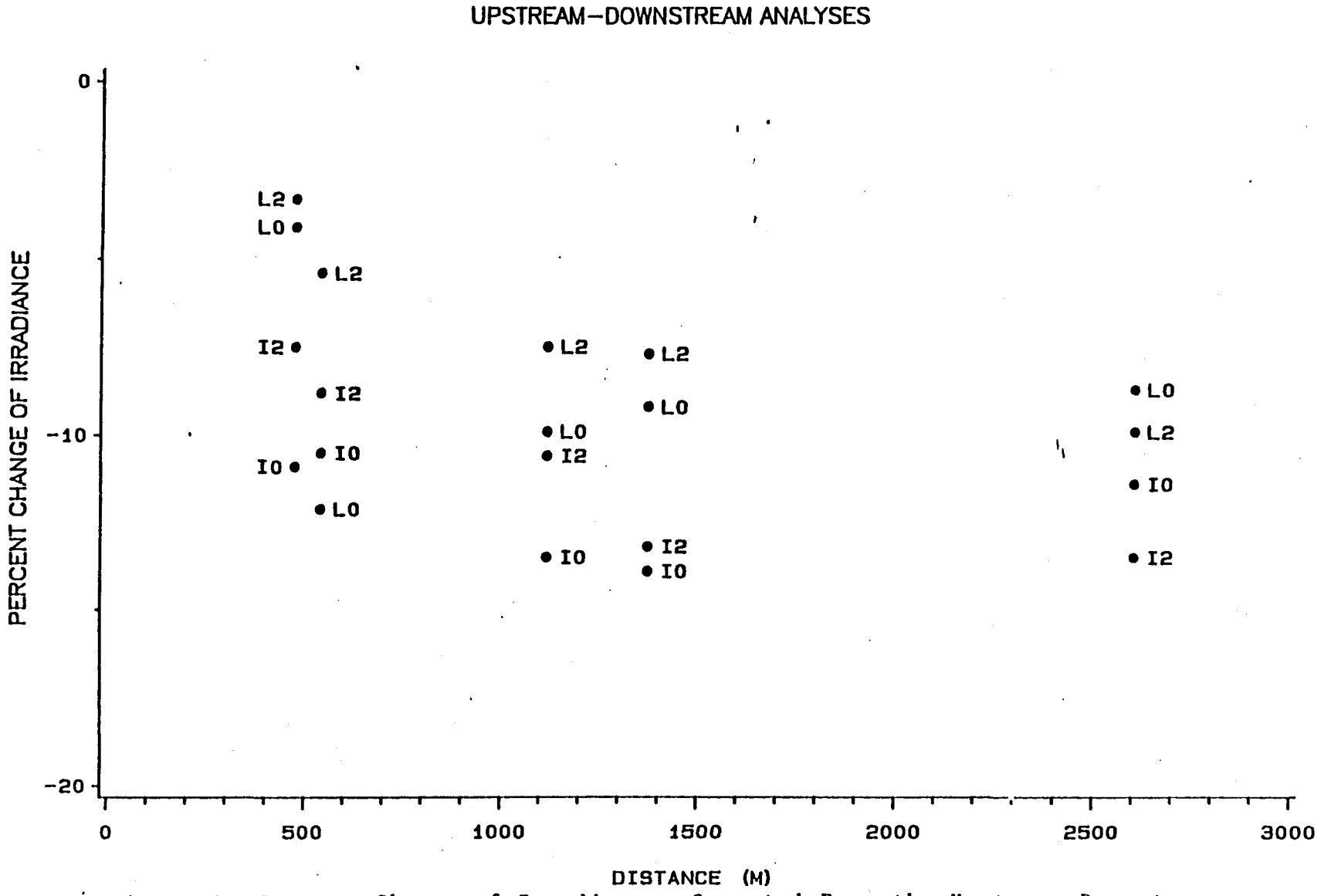

Fig. A-3. Percent Change of Irradiance, Computed From the Upstream-Downstream Model, as a Function of Distance From the Diffusers. I indicates results of calculations using irradiance, L indicates results of calculations using ln(I), 0 and 2 indicate the heights from the bottom.

APPENDIX B

Topics In Mathematical Oceanography

1. Notation

Any vector $\underline{A}$ has components A_i, with the index $i = 1, 2, 3$. The sum convention is used, by which any term containing a repeated index stands for the sum of such terms over all values of the repeated index. For example, the scalar product

$$\underline{A}^*\underline{B} = A_iB_i = A_1B_1 + A_2B_2 + A_3B_3.$$

2. Governing Equations

Consider any quantity S whose concentration (amount per unit volume) in a fluid medium is C and which is produced at a rate q per unit volume. If the local velocity of the medium is $\underline{V}$, the flux of S is $C\underline{V}$, and the net outflow of S from a volume element of unit volume is the divergence of the flux $\nabla^*(C\underline{V}) = \partial(CV_i)/\partial x_i$. The budget of S for a unit volume element is then given by:

{1} $$q = \partial C/\partial t + \partial(CV_i)/\partial x_i.$$

When the quantity S is mass, the concentration is the density ρ; with constant density and no production of mass, the budget equation for mass is the continuity equation:

{2} $$\nabla^* \underline{V} = \partial V_i/\partial x_i = 0.$$

When the quantity S is any component of momentum, the concentration is ρV_i, and by Newton's second law the production rate is F_i, the corresponding component of the resultant applied force on a unit volume element fixed in space. With constant density, the budget equation for a momentum component is the force equation:

{3} $$F_i = \rho \partial V_i/\partial t + \rho \partial (V_i V_j)/\partial x_j.$$

This form of the force equation holds in an unaccelerated frame of reference. For velocities relative to the surface of the earth, which rotates with angular velocity $\underline{\omega}$, the force equation becomes:

{4} $$F_i/\rho = \partial V_i/\partial t + 2(\underline{\omega} \times \underline{V})_i + \partial (V_i V_j)/\partial x_j.$$

The new term $2(\underline{\omega} \times \underline{V})$ is called the Coriolis or geostrophic acceleration, and is directed 90° to the right of the velocity in the northern hemisphere.

The applied force components F_i are given by:

{5} $$F_i = \rho g_i - \partial p/\partial x_i + \partial \tau_{ij}/\partial x_j.$$

Here g is the earth's gravity, which is taken to include the centrifugal force of the earth's rotation and tidal forces; p is fluid pressure and $\partial p/\partial x_i$ is a component of the pressure gradient ∇p; τ_{ij} are shear stresses, with $i \neq j$. The shear stresses due to molecular viscosity within the body of the water column can be neglected, but the

stresses imposed by wind at the surface and friction at the bottom may be important. From {4} and {5} together, we have the force equations, with $\alpha = 1/\rho$:

{6} $$\partial V_i/\partial t + 2(\underline{\omega} \times V)_i + \partial(V_i V_j)/\partial x_j = g_i - \alpha\partial p/\partial x_i + \alpha\partial\tau_{ij}/\partial x_j.$$

3. Hydrostatic Pressure

The positive axis of x_3 or z is taken downward in the direction of g; the level $z = 0$ is set at a reference level near the sea surface, so that the height of the actual surface above $z = 0$ is a small quantity η. Except when the vertical acceleration $\partial V_3/\partial t$ is large, as in the case of gravity waves, the vertical force equation is reduced, for practical purposes of oceanography, to the <u>hydrostatic equation</u> $\alpha(\partial p/\partial z) = g$, because all the terms involving velocities and shear stresses are much smaller than g, about 1000 cm/sec^2. With a uniform density ρ_o, this equation integrates to $p = \rho_o g(\eta + z)$, and the pressure-gradient terms in the horizontal force equations become:

{7} $$\alpha\partial p/\partial x_i = g\partial\eta/\partial x_i.$$

It is important to note that this pressure-gradient force due to a slope $\partial\eta/\partial x_i$ of the sea surface is independent of depth z, so that when this force is dominant the resulting flow will be approximately uniform from top to bottom of the water column.

Stratification of density due to variable temperature and salinity also affects the hydrostatic pressure. Here we need only consider temperature, whose effect on density is roughly given by $(\rho - \rho_o)/\rho_o = -\gamma(T-T_o)$, with the thermal expansion γ

about $2x10^{-4}$ per degree C. Integrating the hydrostatic equation with this variable density gives a more complete expression for the horizontal pressure-gradient force:

{8} $$\alpha\partial p/\partial x_i = g\partial\eta/\partial x_i - g\gamma\partial I/\partial x_i, \text{ with } I = \int_0^z (T-T_o)dz'.$$

4. Coastal Currents And Upwelling

Taking $x = x_1$ alongshore, $y = x_2$ across the shelf, and $z = x_3$ downward, consider a nearshore current with an average velocity directed alongshore, steady in time and horizontally uniform. Taking a time-average of equation {6} and expressing the average product $<V_iV_j>$ as the sum of $<V_i><V_j>$ and the average product of turbulent fluctuations $<v_i'v_j'>$, we find that all the left-hand terms in {6} drop out except $\partial<v_1'v_3'> / \partial x_3$. With no longshore variation of density, {6} and {8}, with $i = 1$, give the longshore force equation:

{9} $$\partial<v_x'v_z'>/\partial z = g\partial\eta/\partial x + \alpha\partial\tau_{xz}/\partial z.$$

Integrating this equation from the surface near $z = 0$ to the bottom at $z = H$, with v_z' vanishing at top and bottom, gives a longshore balance of forces on the whole water column:

{10} $$\tau_{bx} = \rho gH\partial\eta/\partial x + \tau_{wx}.$$

Here τ_{bx} and τ_{wx} are the bottom-stress and wind-stress. This balance applies to shallow nearshore waters for which the average current is constrained by the coast

to flow alongshore and the bottom-stress can rise with the current velocity to balance any forces imposed by slopes or winds.

The velocity profile can be calculated on the supposition that the turbulent vertical flux of x-momentum $\langle v_x' v_z' \rangle$ is proportional to the mean gradient $\partial \langle V_x \rangle / \partial z$ and to $\sqrt{\tau_{bx}}$, and also increases linearly with the height above the bottom $D = H-z$ (see Section 5 on turbulent dispersion below). That is: $\langle v_x' v_z' \rangle = -K \partial \langle V_x \rangle / \partial z$, with $K = ku^*(D+a)$, in which $k = 0.4$ is von Karman's constant, $u^{*2} = \tau_{bx}/\rho$, and a is a characteristic roughness length for the bottom. Substituting this in {9} and integrating leads to the profiles:

{11} $$V_x = (u^*/k)[\ln(1+D/a)-D/H] \text{ when } \tau_{wx} = 0$$

for a slope-driven current, and

{12} $$V_x = (u^*/k)\ln(1+D/a) \text{ when } \partial\eta/\partial x = 0$$

for a wind-driven current. The logarithmic form of velocity profile agrees so well with experience that the supposed form for $\langle v_x' v_z' \rangle$ is generally justified.

For the same longshore current, the force equation for the component in the cross-shelf direction y, from {6} and {8] with $i = 2$, in the absence of cross-shelf velocities and stresses, is:

{13} $$-2(\underline{\omega} \times \underline{V})_y = 2\omega \sin L V_x = g\,\partial\eta/\partial y - g\gamma I/\partial y,$$

in which L is the latitude, positive in the northern hemisphere. Differentiating by the vertical coordinate z, we have the relation:

{14} $$2\omega \sin L \, \partial V_x/\partial z = -g\gamma \partial T/\partial y$$

which gives the cross-shelf temperature gradient corresponding to a given vertical shear in a longshore current.

With $2\omega \sin L$ about 8×10^{-5} sec^{-1} in 33° N. Latitude, g about 10^3 cm/sec^2, and γ about 2×10^{-4} $°C^{-1}$, a steady longshore current flowing downcoast off Southern California with velocity falling from 10 cm/sec at the surface to zero on the bottom at 10 m depth would correspond to a seaward increase of temperature of about 0.4°C per kilometer.

If there is no stratification of temperature, the cross-shelf forces cannot be balanced at every depth by {13}, and the same downcoast current will produce both a surface slope, upward to seaward, and a cross-shelf circulation cell, seaward at the top and shoreward at the bottom.

5. Turbulent Dispersion

In one dimension, consider a set of particles of total mass M released at x=0, t=0, into a fluid medium with spatially-uniform turbulence. If the displacements of particles always keep a normal distribution, so that

$$C/M = (2\pi\sigma_i)^{-1/2} \exp\{(x-\mu_i)^2/2\sigma_i^2\},$$

then the particle-concentration C obeys the advection-dispersion equation

$$\partial C/\partial t = -<V>\partial C/\partial x + K\partial^2 C/\partial x^2,$$

with $<V> = \partial\mu_i/\partial t$ and $2K = \partial(\sigma_i^2)/\partial t$. More generally, a joint normal distribution in three dimensions is a solution of the equation $\partial C/\partial t = -\nabla^*[C<\underline{V}> - \underline{K\nabla C}]$, with K a scalar or tensor. This is a version of the budget equation {1} above (with q = 0), in which $C<\underline{V}>$ represents the particle-flux due to the mean flow and $-\underline{K\nabla C}$ represents the turbulent particle-flux due to correlated fluctuations of C and $\underline{V}$. The postulate of a normal distribution for C/M corresponds then to a postulate that the turbulent flux is linearly related to the gradient of concentration, like the flux in a molecular diffusion process. Either postulate must be taken in a statistical sense, as applicable to a large ensemble of mass-releases rather than to any single release.

A fundamental difference between this postulated process and the process of molecular diffusion is that any diffusivity $K_i = (1/2)\partial(\sigma_i^2)/\partial t$ may vary with the age t of the dispersing mass. The variation of K with t can be expressed in terms of particle-velocity statistics as follows: For any direction x, $\sigma^2 = <x'^2>$, averaged over an ensemble of particles, and $\partial\sigma^2/\partial t = 2<x'v'>$. But $x'(t) = \int_0^t v'(\tau)d = \int_0^t v'(t-\tau)d\tau$, so we can interchange the order of averaging and integration to get

$$(1/2)\,\partial\sigma^2/\partial t = \int_0^t <v'(t)v'(t-\tau)>d\tau = <v'^2>\int_0^t \hat{R}(\tau)d\tau,$$

in which $\hat{R}(\tau)$ is the autocorrelation function of particle-velocity formed by averaging over the ensemble of particles. This will be the same as the autocorrelation function of velocity recorded over time at a fixed point only if the

turbulence is both homogeneous and stationary; in general, the statistic $\hat{R}$ of a velocity-field can only be derived from observations of drifting objects.

The form $K_i = \langle v_i'^2 \rangle \int_0^t \hat{R}(\tau)d\tau$ is very useful, though, to show limiting forms of K for small and large ages t. Since $\hat{R}$ is less than 1 and approaches 1 as t goes to zero, $K_i = \langle v_i'^2 \rangle t$ is a useful approximation for small t and an upper limit for any t. For large t, $\hat{R}(\tau)d\tau$ will approach a limit T, and the diffusivity will approach a constant value $K_i = \langle v_i'^2 \rangle T$. Since both K and σ, the scale of the dispersing mass, are functions of age t, the age-dependence of K can also be viewed as a dependence on scale. The approximation for small age leads to the expression $K_i = \langle v_i'^2 \rangle^{1/2}\sigma$ as an approximation for small σ.

APPENDIX C

AN APPROXIMATE MODEL FOR SONGS' EFFECTS ON PLANKTON POPULATIONS

(This is Appendix C to ECO-M's Final Report on Contract MRC 85-86, May 31, 1986, reprinted with minor corrections.)

AN APPROXIMATE MODEL FOR SONGS' EFFECTS ON PLANKTON POPULATIONS

The central idea of this model is to set up budgets for plankton in a nearshore region and an adjacent offshore region, involving net reproduction rates, net fluxes of plankton into or out of the regions due to advection and turbulent dispersion, and net losses or gains in the regions from mortality and translocation caused by SONGS. The fluxes due to turbulent dispersion are specified by diffusivities K, using the basic definition of diffusivity as the negative ratio of flux to concentration-gradient. If a population has something like a Gaussian distribution of density with distance from shore y, with the inflection point at $y = W$, the concentration-gradient near W is roughly $-C/W$ (C being the mean density inshore of W), and the seaward turbulent flux of plankton is KC/W. This approximation will serve for order-of-magnitude calculations for any reasonable distribution of density.

The regions whose budgets are considered are shown in Figure 1. There is an inshore box of dimensions H (the mean water depth), W (the cross-shelf width of the main habitat for a nearshore species), and L (the longshore extent of any change in population density caused by SONGS). Beside it is an offshore box of depth H, with width W' and length L' that are not specified but are taken to be of the same order as W and L. In a natural steady state, the population density is C_0 offshore from $y = W$ and C_1 inshore. In a new steady state with SONGS in continuous operation, the densities become C_2 inside the inshore box and C_A inside the offshore box, but keep their original values of C_1 and C_0 in the nearshore and offshore zones outside the boxes. All these densities and other quantities are to be taken as means over the regions and over times of months at least.

In the natural steady state, the net of births and deaths in the inshore box is given by $r_1 C_1 LHW$, r_1 being the net reproductive rate (fecundity minus mortality) in the nearshore habitat. The net transfer of individuals to and from the box is all outward through the seaward wall and is given by $-(LHK_y/W)(C_1-C_0)$. These two terms must add up to zero to keep a steady state, which gives the relation

$$r_1 = (K_y/W^2)(1 - C_0/C_1)$$

for the net reproduction rate in the nearshore zone.

A similar balance for the offshore box gives

$$r_o = -(K_y/WW')(C_1/C_o - 1)$$

for the net reproduction rate offshore.

For a truly passive planktonic population that is only viable inshore of W (that is, with $C_o << C_1$) the nearshore relation shows that a very high net reproductive rate may be needed to make up losses due to seaward dispersion from a narrow nearshore habitat. For example, K_y = 1 km²/day (10^5 cm²/sec), W = 4 km, and C_o/C_1 = .5 requires r_1 to be about 3% per day, but the still plausible value K_y = 10 km²/day calls for r_1 close to 30% per day. This argument suggests that strongly zoned nearshore plankton may hold their ground by some kind of behavior, such as seeking the bottom, which greatly reduces the effective cross-shelf diffusivity K_y for the organisms, as compared to that for a passive substance, so that a reasonable reproductive rate can suffice to make up the losses by dispersion.

In the new steady state with SONGS in continuous operation, new balances can be set up in the same way, with new values for r and C in the two boxes, and new terms to take account both of the longshore density-gradients that now exist, and of the effects of SONGS, which are modelled in the following ways for the inshore and offshore boxes. The offshore-directed discharge of SONGS drives water out of the inshore box into the offshore box at a rate Q (about 1000 m³/sec or 0.1 km³/day, representing both the water discharged at the ports and the water entrained in the near-field), removing plankton from the inner box at the rate QC_2 . In a steady state, water must flow back into the inshore box at the same rate; a fraction α of this makeup flow is taken to come through the end-walls of the box, with the original nearshore population-density C_1 , and the remaining fraction $(1-\alpha)$ comes through the seaward wall with the new outer density C_A , so the net rate at which plankton leave the inshore box because of SONGS is given by $QC_2 - \alpha QC_1 - (1-\alpha)QC_A$. Some of the plankton driven from the inner to the outer box are killed by ingestion or entrainment. The fraction surviving is called β , and the rate at which plankton enter the outer box in the discharged and entrained water is βQC_2 . Water must also leave the outer box at the rate Q , with population-density C_A, so the net rate at which plankton enter the outer box because of SONGS is $\beta QC_2 - QC_A$.

A mean longshore current in either direction with speed S will bring plankton into the inner box at a rate $HWSC_1$ and take plankton out of the box at a rate $HWSC_2$, so the net transfer of plankton into the inner box due to the current is $HWS(C_1-C_2)$; similarly, the net transfer into the outer box due to the current is $HW'S(C_0-C_A)$.

With new terms added for the effects of SONGS and mean current, and with dispersion terms specified in the same way as before, the new balance for the inshore box is:

$$r_2 C_2 LHW - (LHK_y/W)(C_2-C_A) + HW(4K_x/L + S)(C_1-C_2)$$

$$- Q[C_2-\alpha C_1-(1-\alpha)C_A] = 0 \quad .$$

For the outer box, the new balance is:

$$r_A C_A LHW' + (LHK_y/W)(C_2-C_A)$$

$$- (4HW'K_x/L' + HW'S + HL'K_y/W')(C_A-C_0)$$

$$+ Q(\beta C_2-C_A) = 0 \quad .$$

From these two new budget equations, we can estimate the new densities C_2 inshore and C_A offshore in terms of the dimensions, diffusivities, and original densities, for different cases corresponding to different ecological hypotheses about the new net reproductive rates r_2 and r_A. There are three tractable cases that fairly well cover the range of likely situations:

1) Behavior-zoned plankton; this is the situation in which both the cross-shelf diffusivity K_y for organisms and the original net reproductive rates r_1 and r_0 are small because the plankton actually resist cross-shelf movement by some kind of behavior. In the extreme, we set K_y and all the r's to zero, leaving only the terms involving K_x, S, and Q.

2) Net reproduction rates independent of density; in this case, it is supposed that $r_2 = r_1$ and $r_A = r_0$, so that the new r's are given by the original budget equations without SONGS. This is an extreme case in which no losses or gains of individuals are compensated to any degree by changes in birthrate or mortality.

3) Net reproduction rates inversely proportional to density; this gives a constant net number of births and deaths in a region per unit of time, regardless of changes in density. This case is not strictly an extreme of compensation, since r could formally change enough to keep density constant no matter what else happened, but we can take it as a practical near-extreme. (One set of runs of the shadow-effects model used this hypothesis for birthrate alone, not for the net reproductive rate.) Here we apply the hypothesis only to the inshore box, setting $r_2C_2 = r_1C_1$. For a nearshore species with negative r_O offshore dominated by mortality, it is not reasonable to expect the mortality-rate to rise as density decreases, so we keep the relation $r_A = r_O$ in the offshore box.

With any of these hypotheses, it is a matter of straightforward algebra to substitute r's from the original budget equations in the new budget equations and to reduce the new equations to pairs of simultaneous equations in the unknown ratios C_1/C_2 and C_A/C_2 . Before setting out the results, we will introduce some convenient notation:

Say $C_O/C_1 = \gamma$, an index of the degree to which a species is zoned across the shelf;

$C_1/C_2 = f$, so the relative depression in nearshore population density is given by

$(C_1-C_2)/C_1 = \delta = 1 - 1/f$; say also

$C_A/C_2 = g$, so the relative increase in offshore density is given by

$(C_A-C_O)/C_O = g/\gamma f - 1$; recall also that

α is the fraction of the makeup flow to the inshore box that comes from the nearshore zone through the ends of the box, and

β is the fraction of plankton transferred by the discharge from the inner to the outer box that survive the process.

With this notation, and some simplifying assumptions, we can write the pairs of simultaneous equations for the three cases compactly as follows, with the equation for the inshore box given first:

1) Behavior-zoning; all r's and K_y are zero; also assume $W' = W$, approximately: then,

$$(T+\alpha)f + (1-\alpha)g = T+1 \quad , \text{ and}$$

$$-\gamma Tf + (T+1)g = \beta \quad , \text{ with}$$

$$T = D + A \quad , \quad D = (4W/L)(HK_x/Q) \quad , \quad A = WHS/Q \quad .$$

2) Density-independent r's ; $r_2 = r_1$ and $r_A = r_0$; also assume $L'/2 = L/2 = W' = W$, and $K_x = K_y$, all approximately: then,

$$(D'+A+\alpha)f + (D'+1-\alpha)g = D'(1+\gamma) + A + 1 \quad , \text{ and}$$

$$-(2D'+A)\gamma f + \{(2+1/\gamma)D'+A+1\}g = \beta + D' \quad , \text{ with}$$

$$D' = 2HK_x/Q \quad \text{and} \quad A = WHS/Q \quad .$$

3) Nearshore compensation; $r_2C_2 = r_1C_1$ and $r_A = r_0$; also assume $L'/2 = L/2 = W' = W$, and $K_x = K_y$, all approximately: then,

$$\{D'(2-\gamma)+A+\alpha\}f + (D'+1-\alpha)g = 2D' + A + 1 \quad , \text{ and}$$

$$-(2D'+A)\gamma f + \{(2+1/\gamma)D'+A+1\}g = \beta + D' \quad , \text{ with}$$

D' and A as above.

The ratios of new densities with SONGS to original densities that can be calculated from these pairs of equations are in terms of the parameters α , β , and γ defined above, and the new parameters D or D' and A , which express the ratios of dispersive and advective transports of water to the transport Q resulting from discharge and entrainment by the SONGS diffusers. The first case, behavior-zoning, is the simplest to deal with, the least restricted by simplifying assumptions, and probably the most realistic for strongly zoned nearshore plankton. Before going into this case, though, we note some common features of all three cases.

In the extreme of very large diffusivity, so that D or D' is very much greater than A , γ , and 1 , all three cases lead to the same result that $f = 1$ and $g = \gamma$; that is, $C_2 = C_1$, $C_A = C_o$, and all is as it was without SONGS.

In the other extreme of very small diffusivity and advection, so that D or D' and A go to zero, all three cases reduce to $g = \beta$ and $\alpha f+(1-\alpha)g = 1$, with the result that the relative decrease of nearshore density is

$$\delta = (C_1-C_2)/C_1 = (1-\alpha)(1-\beta)/\{1-(1-\alpha)\beta\} \quad .$$

The result $g = \beta$ means that the outer box ultimately fills with discharged and entrained water with population density βC_2 of plankton surviving the shocks of ingestion or entrainment. The depression of density in the inner box depends first on α , the fraction of the makeup flow that enters the box from the nearshore zone with the original density C_1 . If $\alpha = 1$, then $\delta = 0$ for any value of β ; if $\alpha = 0$, then $\delta = 1$, meaning that the ultimate inshore density C_2 is zero and no plankton survive in either box. The only exception .is if no plankton at all are killed by SONGS ($\beta = 1$), in which case $\delta = 0$ for any value of α . For a single intermediate example, take $\alpha = .3$ and $\beta = .75$, a value corresponding to 100% ingestion mortality and 20% entrainment mortality with an entrainment ratio of about 10 to 1 . These values give $\delta = .37$, showing that a moderate fraction of makeup flow from alongshore can fairly well offset a high mortality due to SONGS even in the complete absence of natural dispersion. It is to be noted that the original zoning specified by γ does not enter any of these extreme results.

To see what happens at intermediate ratios of natural transports to the SONGS-induced transport, we next consider the first case of behavior-zoning in more detail. Solving the two equations $(T+\alpha)f + (1-\alpha)g = T+1$ and $-T\gamma f + (T+1)g = \beta$ for this case, as given by 1) above, leads to the expression for the inshore depression of density $\delta = 1-1/f$ as

$$\delta = (1-\alpha)\{(1-\gamma)T+(1-\beta)\}/\{(T+1)^2-(1-\alpha)\beta\} \quad .$$

This is hard to portray completely as a function of α, β, γ, and T, so we will bracket the situation by plotting results for $\beta = 0$ (all ingested and entrained plankton killed) and for $\beta = 1$ (no plankton killed).

With $\beta = 0$, we have

$$\delta/(1-\alpha) = \{1+(1-\gamma)T\}/(T+1)^2 \quad ;$$

with $\beta = 1$, we have

$$\delta/(1-\gamma) = (1-\alpha)T/\{(T+1)^2-(1-\alpha)\} \quad .$$

Figure 2 gives plots of these, showing for $\beta = 0$ the regions on a log-log plot of T and γ in which δ exceeds 0.3 for various values of α, and for $\beta = 1$ the regions on a semi-log plot of T and α in which δ exceeds 0.3 for various values of γ. In the worst case $\beta = 0$, we see for strongly-zoned nearshore plankton ($\gamma << 1$) that depressions of density greater than .3 will only occur when the transport-ratio T is less than about 2 for the smallest values of α, and only when T is less than about 0.3 for values of α exceeding 0.6. For weakly-zoned plankton (γ near 1) somewhat smaller values of T are required for a given α, but for strongly-zoned offshore plankton ($\gamma >> 1$) increases of inshore density (negative δ's) exceeding 0.3 can occur over a range of T around 2, whose width increases with γ and decreases as α rises from 0 to 1.

The plot with $\beta = 1$ shows the effects of translocation due to SONGS in the absence of any direct mortality from SONGS. Here we see that δ exceeds 0.3 only when T is less than 1.5 and α is less than 0.2 for any value of γ, and only for T less than 0.3 and α less than 0.05 if γ exceeds 0.3. For unzoned species with $\gamma = 1$, δ is always zero, but as γ rises to several times 1 for strongly-zoned offshore

species, relative increases of nearshore density ($-\delta$) of 0.3 or more become possible for increasingly wide ranges of T and α .

Next we consider the situation with $\beta = .75$ (100% ingestion mortality, 20% entrainment mortality, about 10 to 1 entrainment), which approaches a realistic estimate from the low side. Figure 3 shows contours of δ on semi-log plots of T and α , with $\beta = .75$ and γ taking the values 0 , 1 , and 3 . For strongly-zoned nearshore species, we find that things do not change much from the case with $\beta = 0$: with $\gamma = 0$ it still requires $T < 1.5$ for the smallest α and $T < 0.3$ for $\alpha > 0.33$ to produce inshore depressions of density exceeding 0.3 . For weakly-zoned species, the survival of 75% of translocated plankton, rather than none, makes a good deal of difference: with $\gamma = 1$, δ exceeds 0.3 only if $T < 0.3$ and $\alpha < 0.2$. Offshore plankton with $\gamma = 3$ show increases in nearshore density ($-\delta$) greater than 0.3 over the range of T from 0.3 to 3 for any α less than about 0.33 .

For a quick look at changes in density in the outer box, we examine the single case of $T = 1$, $\beta = .75$, $\alpha = 0$, and tabulate the relative decrease inshore δ and the relative increase offshore $(C_A - C_O)/C_O$ for a range of γ :

γ	0.1	0.3	1.0	3.0	10.0
δ	.35	.29	.08	-.54	-2.7
$(C_A - C_O)/C_O$	2.8	.39	-.15	-.31	-.36

This table shows that the relative changes inshore and offshore are comparable except when zonation is very strong either way. With very strong zonation, the lower density is relatively much increased by admixture of water from the other box.

Before summing up this mass of algebra, we must do something with the neglected cases 2) and 3) above, in which the plankton are taken to be passive and to be zoned because of different net reproductive rates r in the inner and outer boxes. Case 2), we recall, was for no compensation through density-dependence of r , and Case 3) was for strong compensation in the inshore box but none in the outer box, where mortality was not expected to rise as density fell. Since we have seen that the three cases are the same in the one extreme of very high D or D' and in the other extreme of vanishing A and D or D', and since we have also seen that small values of α and γ

are usually necessary to produce large δ's, it will be enough for our purpose to compare the three cases with middling values of the transport-ratios and the fixed values $\beta = .75$, $\alpha = 0$, and $\gamma = 0$.

The order of magnitude of the advection-ratio $A = WHS/Q$ can be estimated, so A need not be left as a wandering parameter. With W about 2500m, H about 20m, S about .03 m/sec (supposing that variations about the long-term mean flow are taken into D or D'), and Q about 1000 m^3/sec, A comes out as 1.5, on the order of unity. By itself, A is near the top of the range of T (the sum of D and A) for which deep depressions in nearshore density can occur under any of the conditions we have looked at, so we now consider only the values 0 and 1 for D or D'.

With D or D' set at 0, A = 1, and other conditions as above, the equations for all three cases reduce to $f + g = 2$ and $2g = .75$, giving $\delta = .38$. With D or D' set at 1, the δ's are .27 for Case 1), .10 for Case 2), and .04 for Case 3). Recalling that $D = (4W/L)(HK_x/Q)$ and $D' = 2HK_x/Q$, we note that D' is larger than D for any given K_x if L is more than 2W, and is unlikely to be smaller than D. This makes Case 1) the worst case in the sense of producing the deepest depression of density for a given K_x, other things being equal.

Now at long last, the conclusions to be drawn from this model can be summarized in a short space, as a set of necessary conditions for producing relative depressions of nearshore density greater than 0.3.

For weakly-zoned species, with γ not very far from 1, D+A must be less than 1 in any circumstances. Over a plausible range for the survival-fraction $.75 < \beta < 1$, D+A must be less than 0.3 <u>and</u> the fraction of makeup flow from the nearshore zone α must be less than 0.2.

For strongly-zoned nearshore species, with γ small relative to 1, D+A must be less than 2 in any circumstances. In the range $.75 < \beta < 1$, D+A must be less than 1.5 <u>and</u> α must be less than 0.4.

It was noted above that the advection-ratio $A = WHS/Q$ is on the order of 1 for a mean longshore drift current of 3 cm/sec, when all variations about this mean are taken into D. Estimating A from the long-term mean current in this way gives the smallest possible value, so A cannot fall an order of magnitude below 1 except in a season for which the mean drift is less than 1 cm/sec. With A not much less than 1, the conditions above mean that D must be much less than 1 to depress the nearshore density of a weakly-zoned species by 0.3, and must be no more than 1 to do the same for a strongly-zoned nearshore species.

We recall that $D = (4W/L)(HK_x/Q)$. With Q about 1000 m^3/sec, H about 20 m, and keeping our assumption that L is about $2W$, we come out with K_x about $25D$ m^2/sec, or a few times $D \times 10^5$ cm^2/sec, or a few times D km^2/day. In terms of K_x, the condition for a depression deeper than 0.3 is that K_x must be less than 10^5 cm^2/sec or 1 km^2/day for a weakly-zoned species and less than a few times this for a strongly-zoned nearshore species.

Offshore species with very strong zoning can show relative increases of nearshore density of 0.3 or more over a wide range of $D+A$ centered around 1. For moderately strong zoning ($\gamma = 3$), $D+A$ must be less than 5, and α must be less than 0.5.

This is an order-of-magnitude model full of approximations, so it is right to consider the force of these conclusions. If $D+A$ is estimated to be two orders of magnitude above the largest value with which the model can explain a statistically-established depression of density, there is definite disagreement giving strong reason to question the estimate of $D+A$ or the statistical basis of the depression in density (or to look for serious omissions or misconceptions in the model). If the estimated $D+A$ is one order of magnitude too high, there is marginal disagreement, suggesting that the data and analyses should be checked and perhaps that more precise modelling should be considered. If estimated $D+A$ is only a few times too high, the discrepancy can reasonably be ascribed to the imprecision of the model, without bringing the other data or analyses into question.

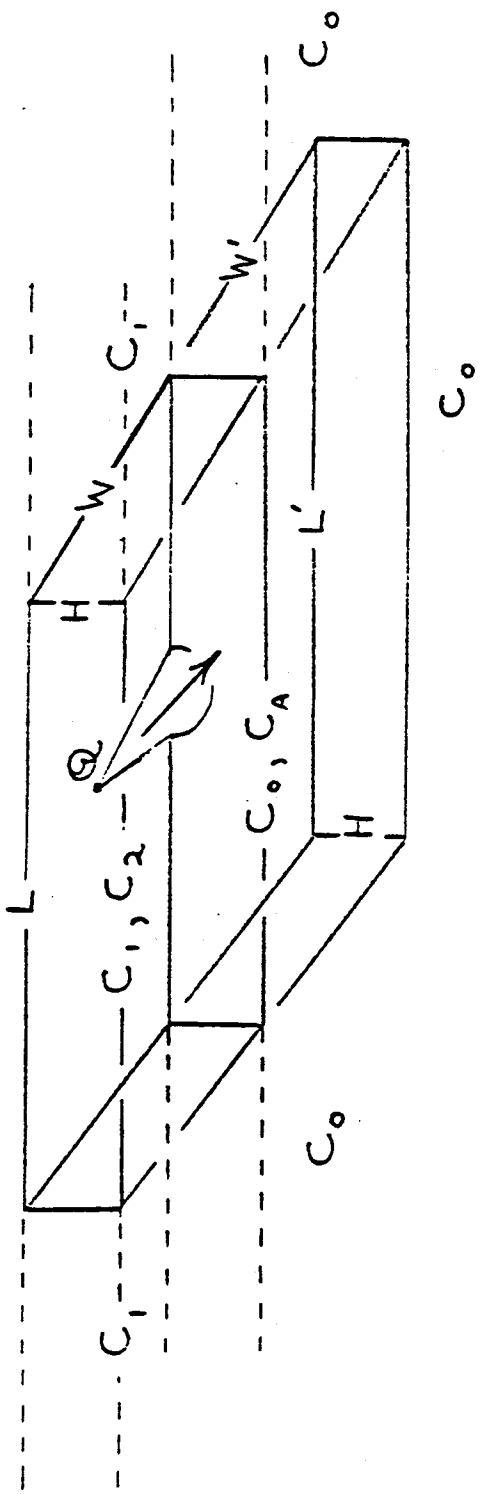

Figure C-1 Two-Box Model

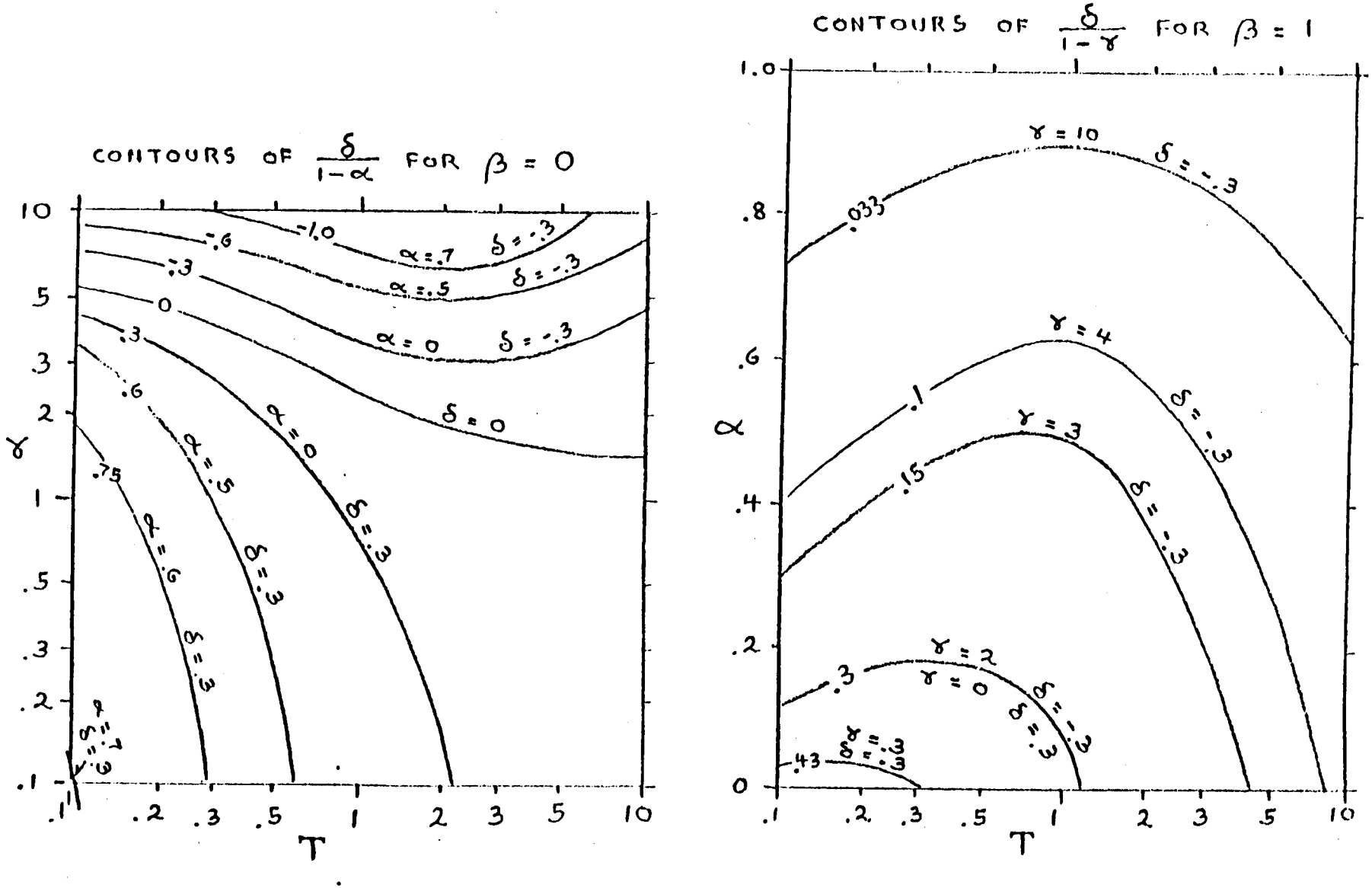

Figure C-2 Contour Plots.

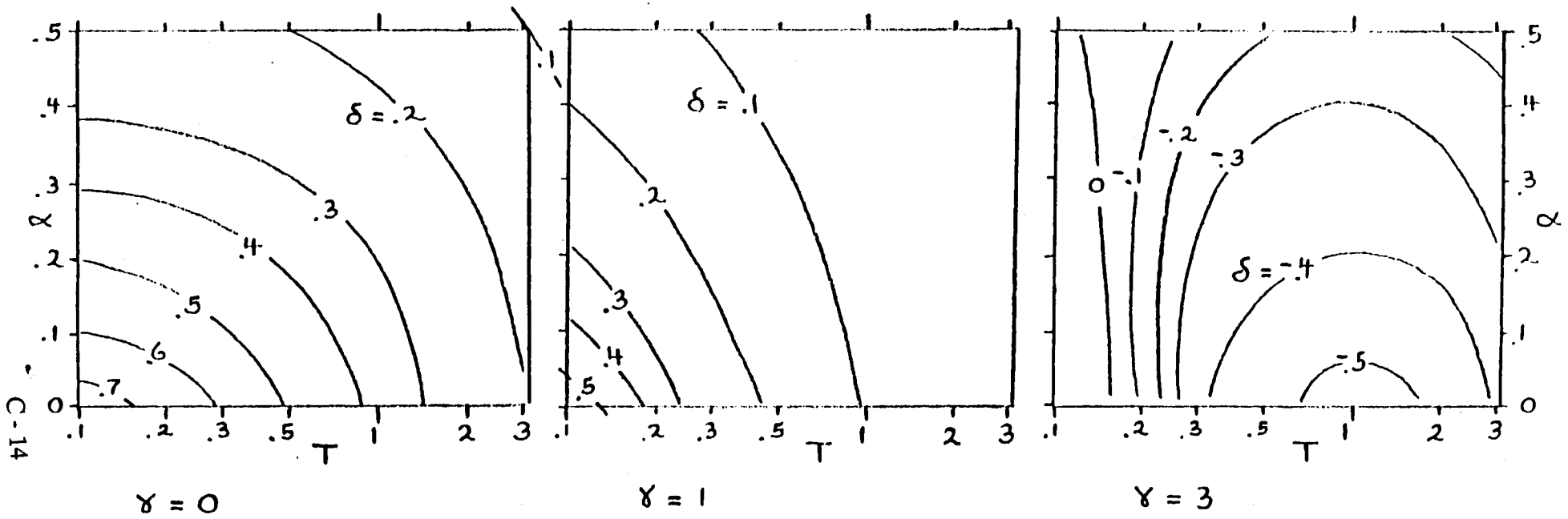

Figure C-3 Contours of δ for $\beta = .75$

APPENDIX D

FINAL REPORT OF THE SHADOW EFFECTS SIMULATION PROJECT

Prepared by:

Daniel Goodman
Scripps Institution of Oceanography
La Jolla, California 92093

For:

MARINE REVIEW COMMITTEE
533 Stevens Avenue, Suite E-36
Solana Beach, California 92075

December 28, 1981

MRC Doc. 81-06

TABLE OF CONTENTS

SUMMARY OF REPORT ON SHADOW EFFECTS SIMULATION MODELING PROJECT

****

OBJECTIVE 1: SIMULATE DEVELOPMENT OF DEPRESSIONS IN ZOOPLANKTON POPULATIONS OWING TO OPERATION OF SAN ONOFRE NUCLEAR GENERATING STATION COOLING SYSTEM

* Three imposed mortality sources in addition to natural mortality: intake primary entrainment mortality,, discharge secondary entrainment shear mortality, and dislocation mortality.

* Model simulates development of depressions over space and time.

APPROACH:

* Three dimensional spatial grid.

* Passive horizontal transport by currents and power plant field.

* Age stratified population model.

* Age and position specific natural mortality rates.

* Birth rates constant (complete compensation, or proportional to population size (density independent).

* Active vertical migration of organisms.

* Natural mortality rates adjusted to reproduce observed population distribution and structure under ambient conditions.

* Waterflow components due to currents and due to power plant field supplied by Marine Review Committee waterflow simulator.

ACCOMPLISHMENTS:

* Construction, debugging and validation of basic simulation model.

* Construction, debugging and validation of mortality rate calibration program.

* Formal interfacing of the Marine Review Committe waterflow simulator and the Shadow Effects model.

RESULTS:

* Natural mortality rates calibrated for Metamysidoposis elongata ages 29-99 days, and Seriphus politus, ages 1-60 days.

* Model indicates rapid development of population depressions on order of 30 to 60% within a few kilometers of the power plant, owing to both sources of entrainment mortality, and with pefect compensation of the birth rate, but without incorporation of the effects of dislocation mortality.

* Depressions on order of 10 to 20% indicated for much greater distances under the same conditions.

REPORTING:

* July 15, 1980. Report to the Marine Review Committee: Shadow effects model, program development and implementation.

****

OBJECTIVE 2: CROSS CHECK EQUIVALENT FISH LOSS CALCULATION

* Need to modify Shadow Model and mortality calibration for special runs intended to provide calculation of equivalent fish loss that could be compared with same quantity calculated in a different manner, using Encounter Model, by Marine Ecological consultants.

* Encounter model, developed in separate program of Marine Review Committee, computes fish loss in units of equivalent adults. This age range is beyond data availability for calibration of natural mortality rates as done in the version of Shadow Model employed for Objective 1.

* Equivalent fish loss calculation returns number for total loss rather than a spatial distribution of loss.

APPROACH:

* Extrapolate natural mortality rates calibrated for age classes 1-60 to age classes 91-105.

* Adjust extrapolated natural mortality rate schedule so as to conform to an empirical survivorship curve based on a modified negative Gompertz curve previously obtained from analysis of age distributions without correcting for water motions
(Barnett, et al., Apr 1980. Predicted larval fish losses to SONGS units 1, 2 and 3 and preliminary estimates in terms of equivalent forage fish. Report to Marine Review Committee)

* Integrate losses over total area, and over area enclosed within the 15% depression contour; and compute instantaneous rates of kill at the power plant structures.

ACCOMPLISHMENTS:

* Mortality rate extrapolation routines constructed, debugged and validated.

* Shadow Model modifications incorporated, debugged and validated.

RESULTS:

* Model indicates rapid development of population depressions on order of 25% for age classes 91-105 days within a few kilometers of the power plant, owing to the primary entrainment mortality alone.

* Population depression on order of 15% indicated for much greater area, extending several tens of kilimeters longshore under the same conditions.

* Total kill compared to the equivalent fish losses as computed by Marine Ecological Consultants.

REPORTING:

* Dec 14, 1980. Memo: Shadow Effects Plankton Model used to estimate loss of fish adult equivalents.

****

OBJECTIVE 3: SENSITIVITY ANALYSIS OF SHADOW EFFECTS MODEL

* Needed to demonstrate that results reported were robust to modest changes in currents and mixing rates.

APPROACH:

* Artifically modify current velocities and mixing rates in test sequences of transition matrices.

* Input modified current and mixing regimes to test runs of the Shadow Effects Model.

ACCOMPLISHMENTS:

* Programs for operator specified modification of current velocities and mixing rates were constructed, debugged and validated.

RESULTS:

* Population depression owing to primary intake mortality or secondary discharge intrainment mortality was not sensitive to changes in currents and mixing rates.

REPORTING:

* Aug 15, 1980. Interim report on plankton population depressions predicted by the Shadow Effects Model.

****

OBJECTIVE 4: EVALUATE ALTERNATIVE GENERATION OF ALTERNATIVE TRANSITION MATRICES DIRECTLY FROM CURRENT METER RECORDS

* Mixing rates obtained from the Marine Review Committee waterflow simulator output were initially too high, so these were adjusted downward in the transition matrices employed in running the Shadow Model for Objectives 1 and 2, but this adjustment was ad hoc.

* Long wavelength coherency implied by repetition of water flow pattern over many tens of kilometers of coastline in the Shadow Model came under question.

APPROACH:

* Simulate ambient waterflow transitions in Shadow Model grid system directly from current meter data.

* Compute power plant flow field using Marine Review Committee waterflow simulator with zero current

* Create new transition matrices by adding power plant flow field to ambient flow field.

* No direct correction for continuity.

* No imposition of theoretically calculated diffusion.

* Compare results of simulation runs using new transition matrices in Shadow Model with runs obtained under the transition matrices employed in Objectives 1 and 2.

RESULTS:

* Directly computed transition matrices obtained in this manner proved inferior to the transition matrices employed for Objective 1 and 2.
Review Committee waterflow simulator.

* Simulated cross-shelf mixing rates excessive.

* Continuity problems worse than before.

REPORTING:

* Oct 13, 1980. Memo: Technical details of generation of the new transition matrices.

INTRODUCTION

Pursuant to a work statement agreed upon by the Marine Review Committe and Dr. Daniel Goodman of Scripps Institution of Oceanography, a model was produced that will simulate formation of depressions of plankton populations as a consequence of operation of unit 1 or of units 1, 2 and 3 of the San Onofre Nuclear Generating Station.

Three types of information went into the model, and these were received from different sources. The data concerning abundances of various size classes and age classes of the organisms of interest were provided by Marine Ecological Consultants. A set of numbers representing a time sequence of water movements off San Onofre was provided by the Marine Review Committee, as an output of their waterflow simulator. The demographic model simulating population growth, death, and movement, was constructed by Drs. Goodman and Gerrodette. Finally, all three components were incoporated into the Shadow Effects Simulation Model by Drs. Goodman and Gerodette.

Three biological populations were modeled. These were larval queenfish (Seriphus politus), juvenile queenfish, and days 29-99 in the life cycle of a mysid shrimp (Metamysidopsis elongata). The current regime employed was computed from current meter records for a two week period of fast currents (often exceeding 12 cm/sec) in April 1979. Two approaches were taken modeling water motion on the basis of these current meter data.

The results indicated the rapid formation of population depressions the intensity of which, in terms of a per cent reduction from the normal population density, for a radius of a few kilometers around the power plant, was 50% for late larval (60 day) Seriphus and 60% for adult Mysids. Lesser effects (but exceeding 20% reduction) extended for tens of kilometers downcurrent from the plant. These predicted reductions, if correct, are significant to the productivity of the coastal ecosystem, but owing to the inherent variability of planktonic sampling, this depression may not be statistically detectable under certain imaginable monitoring programs.

These results are based on model runs where only two out of three sources of mortality were operating (ingestion and shear, but not dislocation), so, to this extent, the predicted population depression is a conservative underestimate.

The original data tapes, and the original Fortran code for the Shadow Effects Model are on file with the Marine Review Committee. In this report, we discuss the background to the problem, describe the operation and validation of the Shadow Effects Simulation itself, and briefly present the major results. More detailed descriptions of the results of the various subprojects are to be found in the four reports and memos associated with the four principal project objectives, as listed in the outline at the beginning of the present document. The purpose of the present report is to provide an overview of the entire project, and to

explain thoroughly the actual functioning of the Shadow Model.

The four reports and memos are

July 15, 1980. Report to the Marine Review Committee: Shadow Effects Model, program development and implementation.

Aug 15, 1980. Interim report on plankton population depressions predicted by the Shadow Effects Model.

Oct 13, 1980. Technical details of generation of the new transition matrices.

Dec 14, 1980. Shadow Effects Model used to estimate loss of fish adult equivalents.

STATEMENT OF THE PROBLEM

Concommitant with the operation of the once-through cooling system of the new units of the San Onofre Nuclear Generating Station, we expect three direct forms of increased mortality to operate at the population level on affected plantonic organisms. The three sources are (1) intake entrainment, wherein we assume that all ingested organisms are killed, (2) discharge entrainment shear mortality, wherein we assume that a fraction of the organisms secondarily entrained in the discharge jets suffer mechanical injury, and (3) dislocation mortality, wherein we assume that the discharge plume will carry some inshore organisms to offshore locations where their natural mortality rate is higher than it would be in their normal inshore habitat.

Obviously, the dislocation mortality (3) can only be assessed in a spatially structured model. The two forms of entrainment model could be treated in a very rudimentary way in a model that did not involve explicit spatial effects, but this would only represent the first transient kills, and not the equilibrium kill.

Given assumptions about the correct fraction for discharge entrainment mortality (i.e., what fraction of the secondarily entrained organisms are actually killed in the process), the initial rate at which the power plant will kill organisms via mechanisms (1) and (2) involves only a simple book-keeping calculation of the volume of water entrained per unit time. Ultimately, however,

the population at risk will itself be reduced due to the prior imposed mortality, and so the number of individuals killed per unit time in this re-entrained water will be a lesser number. The same mixing processes which control re-entrainment will also govern the geometry of the population depression, for the shadow created in the wake of the entrainment mortality will be distributed over a considerable area, at the periphery of which the population is replenished by diffusion-like mixing from areas beyond the reach of the power plant.

Therefore, in order to predict the ultimate rate at which entrainment will be killing planktonic organisms, or to predict the extent and intensity of the ensuing population depression, or to gain some insight into the possible process of dislocation mortality, it became necessary to construct a relatively complicated spatially structured model, which keeps track of the population density at each position, and moves organisms from position to position, as well as representing birth and death processes at each position. To this end, we developed the Shadow Effects Simulation model as a three dimensional compartment model.

The lateral movements of plankton in the model are governed by an input generated by the Marine Review Committee's Waterflow simulator. The position specific natural mortality rates which establish the potential for a dislocation mortality effect, were obtained from a special calibration program which iteratively fits mortality rates that will reproduce, as closely as possible,

the observed distribution of the various age classes in the population along an on-offshore gradient, when used in simulations employing the same waterflow regime as drives the Shadow Model itself. The observed distribution of overall abundances, and the relative abundances of age classes, used in the calibration, as well as for initializing the populations in the Shadow Effects simulation, were provided by Marine Ecological Consultants.

STRUCTURE OF THE SHADOW EFFECTS MODEL

Space

The model treats the region as a three dimensional volume, divided into cubical compartments or cells. Each cell has its own position in terms of depth, offshore position and longshore position. There are processes in the model, such as birth and death, which take place within cells. With respect to these processes, each cell is treated as if it contained its own isolated population. Within the cell, the model does not recognize any spatial structure, so it is as if each cell represents are perfectly mixed tank. Transport processes in the model take place between cells. It is this combination of processes restricted to particular positions, and processes moving organisms from one position to the next, that gives the model its spatial structure. Thus some of the mortality rates, for example, may be position specific: the cells which correspond in position to places where there are diffusers or intakes have mortality rates which of course include the effects of the fraction of that cell's volume which will be entrained in a unit time; and the inshore and offshore cells can have different natural mortaltiy rates also, in order to represent habitat differences which are reflected in observed distributional patterns.

The basic spatial unit, in the horizontal, is a cell which is one kilometer in the offshore and two kilometers in longshore span. The water column is subdivided vertically into three depths which correspond to the positioning of the Marine Review Committee's current meters: 0-6m, 6-15m, and 15m-bottom. Thus, the volume enclosed within a particular cell depends on its depth, and for the bottom layer of cells, the volume increases with distance offshore, for the water depth increases by about 10m with each km offshore. The inshore most row of cells consists only of the 0-6m layer. The next row offshore, corresponding to 1-2km offshore, consists of the top layer and the 6-15m middle layer. At the third row offshore, corresponding to 2-3 km offshore, the bottom layer of cells is added, representing at this position the 15-25m depth.

The cells are organized into modules, each of which forms a grid 20 km longshore (10 cells long) and 10 km offshore (10 cells wide); and consists in the vertical of a stack of three layers. Thus each module requires a computer array of 300 elements for each category of its contents. For example, if there are 5 age classes in the model, the module must store 1,500 elements. The modules formed the basic unit of storage in computer memory, with entire modules being read off disk, and written back to disk, as needed.

Grid modules may be strung together in the longshore dimension, in order to vary the longshore size of the simulated area. Thus, a simulation involving 5 modules represents a

100 km stretch of coast. The linking transport from cells in one module to the next was accomplished with an internal temporary buffer that stored the contents of the extreme longhsore columns of cells, to preserve continuity as that module was read into or out of memory.

Continuity at the offshore boundary of the grid was maintained via a permanent offshore buffer, which operated as an infinite source-sink. Thus the offshore off-grid region always contained a population whose vertical distribution and age distribution and abundances exactly matched the initial reference population. Diffusion or advection from this region always brought in water containing populations with this composition, whereas diffusion or advection into this region did not influence the composition of its contents. At the upshore and downshore extremes of the sequence of modules, permananent buffers of this same nature also serve as infinite source-sinks, preserving vertical, on-offshore, age and abundance distributions of the initial reference population. The rate of transfer in and out of these off-grid regions is governed by the same waterflow mechanisms as operate inside the grid, with continuity constraints on waterflow that will be described in the following section.

Motion

Two forces move organisms within the grid. Lateral motion, representing advection and eddy diffusivity, is determined by a sequence of matrices of position and direction specific transition probabilities, that will be desribed in the next section. Vertical motion is determined by a reference vector which stipulates the fraction of the population that should be found at each of the three depths at that on-offshore position.

It was assumed that plankton are subject to totally passive transport in the horizontal. This assumption could be varied, and indeed there is some evidence suggesting reasonable ranges of assumptions that might be made for Mysids, which exhibit some tendency to maintain their position in the face of slow currents, but which are swept along by rapid currents.

Time

There are four time scales relevant to the workings of the model. The shortest is the simulation's time step. This corresponds to the interval for calculation of lateral motion, vertical redistribution, natural age and position specific mortality, and direct entrainent mortality. Thus, the shortest temporal loop in the Fortran code accomplishes all of those processes once per pass through the loop. In the runs presented in this report, this time step represents 2 2/3 real hours.

The second shortest time scale was a daily cycle. This cycle determined whether it was day or night in the model. On every transition from day to night or night to day, the vertical distribution vector was revised accordingly for those organisms which had different vertical distributions for day and night.

The second longest time scale was the age interval. The age intervals used were 15 days for Seriphus and 14 days for the Mysids. At the end of each segment of time corresponding to an age interval, all organisms "alive" in the model were advanced one age class. Then the individuals became subject to the natural mortality rates and vertical distribution vectors for their new age classes for the duration of the age interval, at the end of which time the survivors would again advance one age class.

The longest time scale was simply the span of the record of transition matrices used to accomplish motion from cell to cell in the grid. The length of this sequence was determined by a budgetary decison based on the quite substantial cost of running the Marine Review Committee waterflow simulator. For Shadow Effects simulations of longer duration than the sequence of transition matrices, the sequence of transition matrices was simply repeated (i,e., "wrapped around"), in the same order as before, as many times as needed.

The runs presented here went for 14 days of physical correspondence beween time in the Shadow Effects Model and time in

the sequence of transition matrices. It was thought that a 14-day segment of the tidal cycle was appropriate to minimize distortion in the frequency distribution of types of motion, owing to wrap around of the sequence of transition matrices. However, no empirical examination was made of the possible bias attendant upon limiting the sample of advective events to a 14 day span.

The current data were drawn from the period of noon on April 12 to noon on April 27, 1979. This was a time of fast currents--often exceeding 12 cm/sec.

Mortality Rates

There were two sorts of entrainment mortality. The primary entrainment was due to ingestion in the intake water. We took it for granted that all ingested organisms were killed in the process. There was less certainty regarding mortality in the secondarily entrained water that was entrained at the discharge jets. A number of values were used, ranging from 20% to zero. Even larger values, for example 50% mortality, were suggested to us as plausible figures for the shear mortality associated with secondary entrainment. In the absence of consensus in this matter, all we could do was present the results obtained with a spectrum of values.

Natural mortality rates were not varied in a direct, deliberate way. Instead, position specific values for natural mortality were arrived at on the basis of a calculation which depended upon the transition matrices supplied by the Marine Review Committee, the age class and abundance distribution data supplied by Marine Ecological Consultants, and on the assumption of passive transport of the plankton. The calculation itself will be described in a later section.

Density Dependence

We built into the Shadow Effects Model two options controling the birth rate. One was for the population (absolute) birth rate to be a constant that did not depend on the population size or composition. The other was for the population birth rate to be proportional to the adult population size at that position. Oddly enough, it is the former that corresponds to what is technically termed density dependence in population biology, whereas the latter corresponds to density independence.

We can understand this in the following way. If the absolute birth rate does not depend in any way on the population size, then the per capita birth rate must be inversely porportional to the adult population density, for we would have a constant numerator (the absolute birth rate) and a denominator that was itself the density measure. The density dependence function would describe a hyperbola; and since the population birth rate remains constant, what we are actually dealing with would be a case of perfect compensation. Perfect compensation cannot be realistic, as the births have to come from somewhere, so to this extent simulations which use the constant birth rate option must underestimate the actual population depression, since they will overestimate the per capita birth rate in places where the population is reduced.

The option of having the absolute number of births proportional to the adult population size results in the

per capita birth rate being constant. In this situation the numerator is proportional to the denominator, so the ratio does not change.

On reflection, the constant birth rate option seems the best starting point for simulations with Seriphus, since it was thought that the action of the power plant cooling system would not immediately affect the adult Queenfish population density, and since the adult population from a considerable distance away could plausibly contribute to a relatively constant "rain" of eggs, regardless of local conditions. The constant birth rate option seemed less realistic for the Mysids, the populations of which are probably more local in character.

In the actual event, we never implemented the genuinely density independent option in simulation runs requested by the Marine Review Committee, for we were directed to concentrate on the Queenfish. The population data on Mysids, supplied by Marine Ecological Consultants, did not allow us to model directly the mortality rates of the youngest age classes. These smallest individuals apparently live, near the bottom, so near shore that they are beyond the reach of the sampling gear. Accordingly, our preliminary model for Mysids begins with age 29 days, and so rather than a birth rate, we were dealing with a rate of appearence of an intermediate age class. Even so, the constant rate of appearance of this age class still must be an overestimate, so it would be well to keep in mind for future work

that there is another option to be explored in the model for Mysids.

INTERFACE OF SHADOW MODEL AND THE WATERFLOW SIMULATOR

The transition matrices used for driving horizontal transport in the Shadow Effects Model were generated by the Marine Review Committee's waterflow simulator. We did not investigate the workings of the waterflow simulator itself. Rather, our requirements for transition matrices were simply presented to the Marine Review Committee and the matrices were calculated as per our directions. Later, when some questions did arise concerning the functioning of the waterflow simulator we did a parallel study, which is described in a following section of this report.

The transition matrices desired for use in the Shadow Effects Model consist of tabulations of the fraction of the water in a given cell that moves into each adjoining cell. This number would have to be recorded for each cell in the grid at every time step in the simulation. Accordingly, a grid corresponding to the geometry of the grid of the Shadow Effects Model was incorporated into a spatial representation in the coordinate system of the Marine Review Committee's waterflow simulator. Then, at each time step, a large number of "particles" were initiated at random positions in the grid. The trajectory of each particle was followed over the course of a time span corresponding to one time step of the Shadow Effects Model. At the end of this time step, each cell in the grid was evaluated, as a source and as a sink, by recording what fraction of the particles which originated

in it had moved to each adjoining cell.These fractions then became the respective transition probabilities, for that time step. The duration of a time step was short enough,that hardly any trajectories crossed more than one cell.

Clearly, proper behavior of the transition matrices would depend both on proper behavior of the waterflow simulator and on using a sufficient number of particles for adequate sampling in the process of generating the matrices in the above described Monte Carlo simulation. Some necessary properties could be enforced after the fact.

Since each cell in the grid has in general eight neighbors (including null cells to represent the shore line), there are nine transitions per cell, counting the fraction that remains behind. By construction, all nine of these transition probabilities summed to one, imposing a conservation constraint on the amount of water leaving a cell or staying behind. But this did not constrain the sum of the amount of water entering a given cell from all of its neighbors. For that, we simply relied upon the continuity properties of the Marine Review Committee's waterflow simulator, which in fact was not equal to the task, and so some eccentricities in behavior ensued, with water piling up unreasonably in some places, and running away from other places. This problem was detected early in the project, but it was decided that the modifications to the Marine Review Committee's waterflow simulator that would be necessary to rectify the

continuity failures were too extensive to be undertaken simultaneously. A proposal for that modification is on file with the Marine Review Committee ("A method for generating a seasonal nearshore San Onofre current regime." Hans Kaspar. 5/23/81).

For purposes of the Shadow Effects project, the faulty transition matrices had to be used, so modifications were made to the Shadow Effects Model to cancel out the effects of continuity failures, wherever possible. These modifications were successful as regards simulation of the geometry of the population depression caused by primary and secondary entrainment mortality. However, no satisfactory way was found to assess dislocation mortality effects with the faulty transition matrices. Since the capability for modeling dislocation mortality effects has been built into the Shadow Model, that too should be investigated in some future study, either by correcting the waterflow simular for its continuity properties or by post-processing of the output of the waterflow simulator to enforce continuity in the transition matrices. The latter approach will require some consensus as to what the resulting mixing rates should be.

Without representation of the effects of dislocation mortality, our predictions regarding population depressions are necessarily biased downward. That is to say, under the present set of modifications, we argue that the Shadow Model reliably represents the effects of primary and secondary entrainment mortality, whereas

dislocation mortality is omitted altogether, so the results are necessarily conservative in the direction of underestimating the severity of the population depression.

The theory of the modification to the Shadow Model for cancelling the effects of continuity failure is as follows. Transition matrices were generated with the waterflow simulator set to ambient conditions (corresponding to power plant off) and with the power plant unit 1 only, and with all 3 units on. The original intention in the Shadow Model (and the correct way to proceed) was to compare plant off simulations (ambient) with simulations with 1 or 3 units on. The population depression would then be measured as the difference between the population maps at the end of the two respective simulations. However, the continuity problems caused the resultant maps to be excessively "lumpy," which made interpretation very difficult. That is, there were large local peaks and valleys in the population that were due entirely to properties of the waterflow simulator, and that had nothing to do with power plant induced mortality (though there was an overall depression produced in any case).

In order to remove these spurious peaks and valleys, a simulation with the power plant on, but with the entrainment mortality rates set to zero, was substituted for the plant-off simulation in the above comparison. Since both sets of simulations would now be utilizing exactly the same set of transition matrices, the discontinuities then cancel exactly, and

the only thing contributing to the observed map of differences is the mortality attributable to primary and secondary discharge entrainment. Since the redistributional effects of the plume are present in both simulations, the effects of dislocation cancel also, so we must stress that the results presented herein are an underestimate of the population depression. They represent only primary and secondary entrainment mortality, and do not include dislocation mortality. Our best understanding is that no other error was introduced by this modification.

Some of the problems encountered with the transition matrices computed with the Marine Review Committee's waterflow simulator were the results of sampling phenomena, as the waterflow simulator treats the trajectories of discrete "particles," and the cost of operation of the waterflow simulator restricted the number of trajectories which could be included in the statistics. Some of the problems originated in the failure of the waterflow simulator itself to incorporate continuity constraints. Those problems which resulted in known quantities having the wrong values were readily corrected, after the fact, by post-processing of the transition matrices before we used them in the Shadow Effects Simulator.

Post-processing of the transition matrices adjusted the volume of intake entrainment and discharge entrainment per unit time, until these matched the correct values supplied independently by the Marine Review Committee. Identification of

the discharge plume was made possible by subtracting plant-off from plant-on transition matrices, but this often was confounded by the "lumpy" topography resulting from the continuity failures, so no attempts were made to adjust the far field properties of the plume to any specific geometry or velocity.

Post-processing of the transition matrices also enforced certain constraints at the boundaries of the grid. The Shadow Effects Model itself exactly balanced the amount of water locally entering the offshore buffer with an amount locally returned to the grid from the offshore buffer. The overall continuity at the longshore extremes was accomplished via a wrap around. Water (but not organisms) leaving at one longshore extreme of the grid was exactly balanced by the amount entering at the same depth and offshore position at the opposite longshore extreme of the grid. These constraints at the boundaries resulted in the total amount of water in the grid remaining constant, even though this obvious continuity property was violated by individual cells.

One final post-processing step before use of the transition matrices as received from the Marine Review Committee was an adjustment of the on-offshore mixing rate. This rate was unrealistically inflated by the same discontinuity problems which caused water to pile up in peaks and retreat from holes. Since the mixing rate was important to the geometry of the population depression, and since it played a role in the calibration of natural mortality rates (to be explained in a later section), we

elected to reduce all the on-offshore transitions proportionately by the application of a simple scale factor, until the mixing rate seemed right, as judged from the rate of spread of a simulated dye patch in the Shadow Model. The longshore transition components were not tampered with in this adjustment.

The value for the scale factor which gave rise to a satisfactory effective mixing rate was 0.1. This resulted in a patch, initiated in one grid cell, spreading to an extent that after 2 days the 10% concentration contour spanned 2 km cross-shelf, the 1% contour spanned 3.5 km, and the 0.1% contour spanned 5 km.

Sensitivity studies showed that the population depressions owing to intake and discharge mortality were not much affected by differences of less than an order of magnitude in the scale factor. Over an eight-fold range of on-offshore mixing, the deepest point of the depression varied over a range of plus or minus 12% of the central value, with or without recalibration of the mortality rates, in test runs evaluating mortality due only to primary and secondary entrainment. We concluded, therefore, that precise adjustment of the on-offshore mixing rate was not critical to the results obtained from the modified version of the Shadow Effects Model. Doubtless this adjustment would have been of greater import to the dislocation mortality, but this was, in any case cancelled out of the runs reported here (in the course of the modifications which we found necessary for smoothing out the peaks and valleys caused by failures of continuity in the Marine Review Committee's waterflow simulator).

SUMMARY OF PROCESSES AS RERPESENTED IN THE SHADOW EFFECTS MODEL

The model computes all quantities separately for each cell. The actual shadow, or population depression, is a pattern that emerges in the relative abundances in the entire array of cells. The mathematical representations of the various processes themselves are very simple.

Advective and diffusive transport move a fraction of the contents of one cell to another, with the fractions being determined by the time and position specific numbers stored in the transition matrices. The advective and diffusive transport is all horizontal. Vertical transport is merely a vertical redistribution of the individuals in each column consisting of the three cells (in a vertical stack) at any one longshore-offshore position, so that the appropriate fraction is then at each depth.

Natural mortality removes from each cell a fraction of the individuals in each age class, with the fraction being age and position specific, but not time specific. The entrainment mortality imposed by the power plant removes a fraction of the individuals in each cell containing an intake or discharge structure, with the fraction removed being proportional to the fraction of the volume of the cell that is ingested or secondarily entrained per unit time step, and the proportionality constant is the intake mortality (100%) or shear mortality

(values between 0 and 20% were used), respectively. Removing the individuals at the intake is equivalent to having the appropriate amount of water, with organisms, enter the intake, and then having the same amount of water reappear, only without organisms, at the discharge.

Ageing is accomplished by moving individuals from one age class to the next; and births (with perfect compensation) are represented simply by adding a constant number of individuals in age class one, with the number depending on the distance offshore and the depth.

The algebraic representations, given in Fortran notation so that the equal sign is a replacement operator and not a statement of equivalence, are as follows:

A. Start of short time scale iteration

Horizontal transport

-Move organisms out of cell, with the water movement

$$N=N-E$$

where N is the number of individuals in the cell, and E is the number of emigrants owing to advection and diffusion. E is given by

E=N*F

where F is the fraction of the cell's volume transported in that direction, as given by the entry in the transition matrix for that position, direction, and time.

-Move organisms into the cell, with the water movement

N=N+I

where I is the number of immigrants owing to advection and diffusion. I is calculated as the sum of the emigrants from all 8 surrounding cells which were moved in directions corresponding to entering this cell.

Vertical transport

-In each horizontal (x,y) position, redistribute organisms over the three depths so that the distribution conforms to a specified pattern appropriate for that species, at that distance offshore, at that time of day.

N(1)=P(1)*N

N(2)=P(2)*N

N(3)=P(3)*N

where N(i) is the number of individuals at depth i; P(i) is the proportion that should appear at depth i; and N is the total number of individuals summed over all depths in the stack of 3 cells at that position (longshore and offshore).

Natural mortality

-Remove a specified fraction of the individuals in each cell, with the fraction removed being determined by species, age, and position offshore.

$$N(j)=N(j)*[1-M(j,k)]$$

where M(j,k) is the natural mortality for age class j at offshore distance k; and N(j) is the number of individuals of age j in that cell.

Entrainment mortality

-In those cells which include an intake or discharge structure, remove a fraction of the individuals in proportion to the fraction of the volume of the cell that is ingested or entrained. For ingestion, the proportion is one; for secondary entrainment mortality, the proportion is an externally specified shear mortality rate.

N=N*(1-R)

N=N*(1-S*Q)

where N is the number of individuals of that age class in the cell, R is the fraction of the cell's volume that gets ingested in one time step, Q is the fraction of the cell's volume that gets secondarily entrained in one time step, and S is the shear mortality rate.

This marks the end of one short time scale iteration.

B. Start of long time scale iteration

When the model has completed a number of short time scale iterations equivalent to one age interval, the following steps are added before resuming the short time scale iterations:

Ageing

-advance the age of each individual by one age class

N(j+1)=N(j)

were N(j) is the number of individuals in age class j in that cell.

Births

-add a position specific number of new individuals to age class one

$$N(1)=B(i,k)$$

where N(1) is the number of individuals in age class one in that cell, and B(i,k) is the birth rate associated with depth i and offshore distance k.

This marks the end of the long time scale iteration. Here the model returns to the short time scale iterations.

INSTRUCTIONS FOR THE OPERATION OF THE SHADOW EFFECTS MODEL

General description

The shadow effects model is a compartment model designed to simulate the reduction in marine planktonic populations due to the operation of the San Onofre Nuclear Generating Station. It combines data on natural distribution and mortality rates of planktonic populations with information on water movement, both in the vicinity of the power plant and far from its influence. The output of the model is a map showing the percentage reduction in planktonic populations within each compartment.

Each compartment or cell is 2 km in the longshore direction and 1 km in the offshore direction. There are 3 depth layers: 0-6 m, 6-15 m, and 15 m to the bottom. In order to use the computer efficiently, the coastline is broken up into several modules, each module being 10 x 10 cells (i.e., 20 km in the longshore direction). In order to compute the percentage reduction of planktonic populations, two loops of the main program are run. On the first loop, no entrainment mortality occurs, though the plant is modeled as "on" and does move water around. On the second loop, the primary and secondary entrainment mortality rates are set to the desired values so these mortalities are added to those of the prior loop. The resulting abundances are compared cell by cell to the first run, and the percentage

reductions are computed and printed. In this fashion, the population reduction owing to primary and secondary entrainment can be mapped, but dislocation mortality is factored out. The reasons for this approach are explained in the section on Interface of the Shadow Model and the Waterflow Simulator.

The Shadow Effects Model is archived on a tape with the Marine Review Committe. The file containing the program itself is named SHADOW.

User's guide to the shadow effects model (SHADOW)

A) Input

The shadow effects model requires, as input, a file describing water movement and a file which specifies the input parameters and options which control the program. Each of these will be described below.

(1) Description of water movement - files TR1, TR2, and TR3.

Files TR1, TR2, and TR3 should be called to the local area before SHADOW is run. These files, one for each of the three depth layers, contain the fractions of water which move from one cell to another during any time step. Each time step constitutes one record.

(2) Input file TAPE1.

A file named TAPE1, containing input parameters and options, should be in the local area when SHADOW is run. TAPE1 has one record, named INPUT, which contains the following variables:

TAPE30 The file name of the reference population of organisms, which file lists abundance per meter squared in an on-offshore "flux plane," by depth layer, position offshore, and age class.

NTAPE32 The file name of the associated survival rates per time step in the flux plane.

NTAPE34 The file name of the birth plane, the number of newborn which appear in the flux plane at the beginning of each age interval.

NM The number of modules (i.e., repeated 20 x 10 km grids) to be included in the run.

IP The position of the module containing SONGS, counted from the upcoast end. If IP=0, there are no power plant effects (ambient conditions). The power plant intake and discharges are located at the longshore center of module IP.

ND The number of days the simulation is to run. Usually this will be some multiple of IC.

NK The number of time steps per day, currently 9.

NC The number of age classes in the reference population.

IC — The length of an age interval (the number of days individuals remain in a given age class). IC=15 for queenfish; IC=14 for mysids.

MAXT — The maximum number of time steps (records) in TR1, TR2, and TR3; currently 126. After MAXT time steps, the file resumes reading from the first record.

NAD — The number of days already elapsed in the current age interval when the simulation begins, normally set to 0.

PKV — A vector giving fractional intake mortalities on each loop, normally set to 0 on first loop.

SKV — A vector giving fractional discharge mortalities on each loop, normally set to 0 on first loop.

KVRT — Control parameter for vertical redistribution of organisms at each time step:

-1=no vertical redistribution

0=redistribute vertically according to proportions in reference population, as with queenfish

+1=alternating day and night vertical distribution patterns, as with mysids

KBRT — Control parameter for birth process:

0=local absolute birth rate constant (perfect compensation)

1=local percapita birth rate constant (actual density independence; no compensation)

NL — Number of loops (1 or 2) of main program, normally set equal to 2.

IPLV — Vector of SONGS plume control: 0=off,+=on. Normally on.

IPRV Vector controlling printing of results after each loop:

0=no printing of interim run

1=print results (abundance maps) of run.

Normally set to 0,0 and then only the maps of percentage reduction are printed.

ISM Parameter to control smoothing of results:

-1=print results, smooth, then print smoothed results

0=print without smoothing (normal setting)

+1=smooth results, then print

KPACK Control parameter for output format:

0=normal, full output

1=compressed output; results are collapsed to a single depth and the matrix of abundances is printed as a map corresponding to the actual topology of the coast (otherwise the matrix appears as a mirror image).

The user may consult files IN or BOOTIN as guides in forming this input file.

B) Output

The output of the shadow effects model is written on file TAPE2.The heading echoes back many of the parameters in TAPE1 and lists the reference population, the survival rates, and the birth plane. The maps of abundance follow, if specified by IPRV, listed by X-Y position, depth and age class. The maps of percentage

reductions between loop 1 (ambient) and loop 2 (with power plant) are listed next.The percentage reductions themselves are saved on TAPE10, TAPE11, and TAPE12, for depths 1, 2, and 3, respectively.

C. Submitting the job

Because of the large number of computations involved in a normal run, SHADOW has been written to operate in a batch mode. To submit a batch job, a submit file must be created. After the accounting information, the important steps are:

1. Reset the field length to 100000.

2. Reset the time limit. Production runs in the past have used from a few minutes to nearly an hour of CPU time. Set limits accordingly (in seconds).

3. Get files TAPE1, TR1, TR2, TR3, and SHADOW from permanent storage.

4. Compile and execute.

5. Save the output file TAPE2.

6. Request that the output file be printed and delivered.

D) Comments on the survival rates in NTAPE32.

The survival rates in file NTAPE32 are used as an input to the shadow effects model.These may simply be specified by the user or they may be computed from some other data.Our approach was to estimate the survival rates by a "calibration" program, CLBRT. The calibration program (described in a following section of this report) involves a search for the set of survival rates which, when used to project the population, gives a population which most closely matches the reference population.The actual operation of the calibration procedure is not automatic, however, and requires judgments and some mathematical understanding by the operator. The survival rates must have been calculated with the same files describing water movement as will be used in SHADOW.

STRUCTURE OF THE MORTALITY CALIBRATION PROGRAM

The mortality calibration program provides a means for estimating appropriate natural mortality rates. It does this by iteratively fitting mortality rates to a simulation, until the simulation duplicates, as nearly as possible, the age distributions and patterns of abundance with distance from shore and with depth that have been observed in the region off San Onofre for the organisms in question.

The mortality calibration program duplicates all the processes of the Shadow Model, but on a reduced dimensionality. Since we are concerned here only with the on-offshore-depth pattern, we way dispense with the longshore. Accordingly, the transition matrices were averaged over the longshore for on-offshore transport, and these matrices were stored as records of transport in the on-offshore dimension only, for later use in calibration runs. In the calibration runs, these matrices were applied to a model of a population representing an on-offshore transect, to simulate the average on-offshore passive movements.

Two mortality regimes were posited for each age class of each organism. An inshore mortality and an offshore mortality. The positions in space corresponding to the demarcations between the places where the inshore mortality rates operate and the places where the offshore mortality rates operate, were determined by inspection of plots of the abundances of each age

class, by distance offshore and depth. The demarcation for a given age class was placed just inshore of the transition from high to low abundance of that age class relative to the next younger age class, or just inshore of the transition from high to low abundancy for that age class, whichever transition was more marked. In the actual event, these transition points were quite obvious.

Then the mortality rates applying in the two regions were estimated, age class by age class, through a non-linear least squares fitting algorithm that searched for a minimum in the residual obtained from comparing the reference population's age distribution and pattern of abundance, over depth and distance offshore, with a population projected using those mortality rates. The projection was calculated by starting with the reference population (initial) and running it through the reduced dimension Shadow Model simulation using the reduced dimension transition matrices, described above, and using the same processes (except without a power plant) as described for the Shadow Model itself. A perfect fit would be obtained if the projected population, at the end of the simulation, was an exact duplicate of the starting population, for this would be indicative of a perfect ability of the model to reproduce the ambient conditions with those parameters.

Some mathematical insight into the calibration process may be gained from comparing it with the more familiar computation of mortality rates from a population's age distribution. That operation presumes that the observed age distribution is an equilibrium age distribution (called the stable age distribution) which corresponds to the dominant eigenvector of the projection matrix (called a Leslie matrix) associated with the population's life history. This information, in conjunction with knowledge of the population's overall growth rate (which is the dominant eigenvalue of the projection matrix, and which is usually assumed to have the value one, corresponding to a stationary population), is sufficient for calculation of the mortality schedule. When this mortality schedule is applied to any arbitrary starting population, the projected population age distribution will converge ultimately to the equilibrium age distribution from which the mortality rates were calculated. When this mortality schedule is applied to a population which is already in equilibrium age distribution, the age distribution will remain constant.

Three properties distinguish the population dynamics in the Shadow Model from the linear mathematics employed above in computing mortality rates from an eigenvector. (1) We have no assurance that the observed population distribution we used as a reference population really is an equilibrium, so this particular population composition may not be exactly feasible as an eigenvector, though it may well be approximatable.

(2) The effective projection matrix we apply to the population includes currents as well as age specific dynamics, and the currents are time dependent, so there does not in general exist a single matrix, which if raised to the appropriate power, will correctly project the starting population to the corresponding time, and so we cannot exactly refer to the eigenvector of this non-existent matrix. (3) The density dependent birth rate model we employed (perfect compensation) cannot be represented simply by the application of a matrix to the population vector, for the time constant birth rate is a non-linear feature.

Peculiarities (2) and (3) are dealt with in our calibration process by applying a time dependent transition matrix to the population vector at each time step and by explicitly building a non-linear birth rate into the projection. The simulation does what we want, but owing to the non-linearities the mortalities cannot be calculated analytically (as they could for the simple population dynamics problem) and must be fit by trial and error. As regards peculiarity (1), we simply assume that the average population distribution computed from the data provided by Marine Ecological Consultants is an equilibrium, but we are still left with the question of how we wish to allocate the error in the event that this distribution really cannot be duplicated exactly by the constrained projection process.

The essence of this latter question has to do with the time horizon for which we would like the discrepancy between the reference population and the projection population to be minimal. Had the reference population been an actual eigenvector, this question would not arise, because the discrepancy would go to zero with the first application of the matrix, and it would stay at zero thereafter. But with our problem, we need to consider the time course of the discrepancy: if we minimize the error after say one application of the matrix, and that error is not zero, we would then expect, from the multiplicative nature of the projection process, that the error will increase with successive applications of the matrix using rates fit in this manner. In fact this was the case only up to a point--the discrepancy did not continue to grow exponentially. The reason for this is that the birth rates, under the perfect compensation model, were unaffected by the mortality calibration and so the spatial distribution of births, and their quantity per unit time, was always "correct" in the projection. For this reason, the projected error rapidly stabilized, and so, in practice, calibration for a time horizon of one generation was quite adequate.

Since our actual simulations with the Shadow Model were themselve of a duration on the order of a generation or so, and since the greatest influence of mortality rates was on dislocation mortality, which we were forced to cancel out in any case, the time horizon of the mortality calibration

was not critical to the outcome. If, at some time in the future, the Marine Review Committee's waterflow simulator is corrected to the extent that evaluation of dislocation mortality becomes a possibility, then it will be more important to calibrate mortality rates precisely to the time horizon corresponding to the Shadow Effects simulation.

The non-linear least squares fitting algorithm employed in the mortality calibration was a variant of Marquardt's algorithm modified to so as to estimate partial derivatives implicitly by infinitesimally incrementing the free variables (rather than explicitly calculating derivatives, which of course would in practise be impossible in this complex simulation). This version of the Marquardt algorithm was obtained from the IMSL subroutine package. In actual use, the algorithm proved sensitive to initial estimates, sometimes blowing up, or at other times converging on physically impossible values (e.g., mortality rates greater than 100% or less than zero).

There were two possible sources of the difficulty, one being actual inconsistencies in the fixed parameters of the simulation, the other being discontiuities in the parameter space through which the fit was searching. Inconsistencies in the fixed parameters would have generated conditions of simulation such that the model literally could not reproduce the desired pattern with physically real mortality rates. One example of this was detected when the on-offshore mixing rate input to the simulation

was much too high. Under these conditions, the mixing would smear out the spatial structure in the simulated population regardless of how great the difference between the inshore and offshore mortality rates (within the aforementioned physical limits) so the algorithm could not arrive at a parameter set that would reasonably reproduce the observed pattern of high inshore abundance and low offshore abundance. This problem was relieved by reducing the on-offshore mixing rate, as described with reference to post-processing of the transition matrices.

The second source of difficulty was encourtered when either the correct value of the free parameter, or a trial value of that parameter, was too near to a boundary beyond which physical interpretability was lost, or where the model itself exhibited discontinuous behavior. Two approaches were employed to ease this difficulty. One was mathematically to transform the free variable in the calculations so as to bound it away from forbidden values (e.g., the absolute value transform to keep it from going negative, or the relation P=X/(A+X), where P is one minus the mortality rate, X is the free variable acted upon by the fitting algorithm, and A is a positive parameter which then keeps the ratio P smaller than one, regardless of how high a positive value X takes on).

The second approach was simply to begin the search with a trial value close enough to the correct value that the search never enters the troublesome portions of the parameter space.

This was accomplished by building up solutions in an incremental strategy. The first step was to start with very short age intervals in a calibration for one age class , and then raising the result to the appropriate power to find the starting value for the free parameter with a longer age interval, until the age interval used in the actual Shadow Model was reached. Finally when solutions had been obtained for each age class separately, the calibration was carried out on the entire set of age classes simultaneously.

In this manner, we arrived at sets of natural mortality rates which would allow runs of the Shadow Model to reproduce a fair similitude of the known reference distribution of age classes and abundances over depth and distance offshore with the power plant off (ambient). It must be noted, however, that this calibration procedure was not fully automatic, since it required some judgement and intervention of the operator whenver the algorithms stopped converging. This does not lessen the objectivity of the result, for when convergence did occur it would be unmistakable; but it does lessen the ease with which the entire procedure can carried out. Finally, we must point out that, with the non-linearities in the system, we are not in a position to be absolutely certain that any given solution for the mortality rates is unique. In the actual event, we felt confident that the incremental strategy of fitting rates first for one age class at a time, and then using these as

starting values for a complete calibration, did keep the system in the correct domain of attraction, but here too the operator's judgement must be involved in exploring the convergence behavior in some reasonable sample of the parameter space.

INSTRUCTIONS FOR OPERATION OF THE MORTALITY CALIBRATION PROGRAM

General description

The mortality calibration programs are designed to compute a set of mortality rates which will best account for the observed spatial distribution and age structure of a planktonic population. This is accomplished by using Marquardt's algorithm to search for a set of survival rate schedules which, when used to project a starting population under a specified current regime, will lead to a final population structure which matches the initial population as closely as possible. The programs fit survival rate schedules that are position specific, one applying to the inshore positions, the other applying offshore. The boundary between the inshore and offshore regions is user specified for each age class. Births are added at each age step according to a specified pattern that is not dependent on the present population (in effect, with perfect density compensation in the birth rates). The final output of the program, on a successful run, is the best fit set of survival rate schedules.

The population is modeled in spatial and age class compartments. The number of age classes depends on the population in question. The spatial subdivision is into cells 1 km offshore, 2 km longshore, and with three depths, corresponding to 0-6m, 6-15m, and 15m to bottom. The system consists of just one flux

plane of such cells (no repetition longshore), out to 10km offshore, per age class.

There is no longshore motion. Cross-shelf motion is governed by a set of time varying transition matrices which represent mean on-offshore motions for that time period and position in the flux plane, with the average being taken over all longshore positions. Organisms migrate vertically according to species specific patterns. The horizontal motion of organisms is presumed to be strictly passive.

User's guide

A) Inputs and parameter specification for program operation

The mortality calibration programs require a reference population to which the survival rates will be fit, a time sequence of transition matrices describing mean on-offshore water movement, and six additional control parameters. In the 1980 runs of the Shadow Effects Model, the sequence of cross-shelf transitions was calculated by averaging longshore in the full transition matrices (time step by time step) as modified by us after receipt as output of the waterflow simulator of the Marine Review Committee. This sequence was stored as file OFBAR, and was called from permanent tape storage to file 7 at the beginning of each run.

The mortality calibration programs are written to be used interactively. The computer will display the current values of the input parameters, and query the operator to set any new values as desired. The input parameters are:

NC The number of age classes in the simulation.

IC The length of the age interval in days (we used 15 for queenfish and 14 for mysids).

NK The number of time steps per day (determined by the resolution of the sequence of transition matrices--this was 9 steps per day in our reported runs).

NCD The duration of the run in age interval units.

NTI The number of time steps already elapsed at the beginning of the run, relative to noon=0. (This is to maintain phase for the day and night distributions in mysids--it is irrelevant for queenfish).

NF Control parameter to permit option of fitting rates for one age class at a time. For non-xero NF, the value of NF is the age class for which the rates are to be fit. For NF=0, all age classes are fit simultaneously.

After specifying these parameters, the computer will query the operator for the file name of the reference populaton (which serves both as a starting population for the projections and as a reference to which the simulations are fit by adjusting mortality rates). This file does not have to be in the local area before being called, as the program can bring it there. At present, there are two reference populations in storage: SERIFUS for queenfish, and MYSID for the mysids.

Next the computer will query the operator to supply the initial guesses at the inshore and offshore survival rate schedules, arrays PIN and POUT, respectively, where the number of elements corresponds to the number of age classes. The fitting algorithm may be sensitive to these initial guesses, and fail to converge unless the initial guess is close to the correct value. A variety of initial guesses should be tried, in order to explore the behavior of the program in each situation.

The boundary between inshore and offshore mortality regimes is specified by the array IYPCUT, where the i'th element gives the position of the boundary for the i'th age class. In the case of mysids, there is an additional survival rate, POFF, which applies beyond 5 km offshore (in order to adjust for the fact that no mysids of this species are expected beyond 5 km). When POFF is specified, it remains fixed for the duration of the run; only PIN and POUT are adjusted by the algorithm.

The computer will echo the values of the input parameters, and query the operator whether it should proceed or abort. During the fitting procedure, the current values of the survival rates are displayed on the terminal, so that execution can be terminated if it becomes clear that the computation is entering a biologically unreasonable region of parameter space, or if it appears that the computations are blowing up. There are several convergence criteria which must be satisfied before the program will exit normally from the fitting loop. The run will abort automatically after MAX iterations if convergence has not yet been achieved.

C) Output

The main output is written to file 2. This output consists of an echo of the input parameters, the initial guesses at the survival rates, the distribution of the reference population, the number of births added to each compartment at each age step, and, in the case of diurnal migrators, the nighttime vertical distribution (where the daytime distribution is already given by the reference population). The convergence criteria employed are displayed, and the manner in which the run terminated will be indicated. If the convergence criteria were met, the best fit survival rates will be printed, as will the final population resulting from projection with these rates. If the procedure has worked well, the final population will look recognizably like

the reference population in age and spatial distribution. If convergence was not achieved, a diagnostic message will be printed.

In the event of a successful run, the fitted survival rates are also written to file 32, in a form in which they can be used as input for program SHADOW.

C) Submitting the program

There were a number versions of the calibrate program stored, all with names beginning with the letters CLBRT. The version described here, which is the most flexible, is CLBRTMX. A simpler version, CLBRTX, could be used where diurnal vertical migration is not involved. As the program is interactive, there is little formal set up required. The program calls subroutine ZXSSQ of the IMSL package, which must be linked to the program before execution.

APPENDIX E

Dispersion and Settling of Organic Detritus from SONGS

The water discharged from SONGS contains organic detritus (from the plankton killed during their passage through the plant) that settles out from the plume. The consequent enrichment of the bottom is one possible mechanism explaining the increased abundance of bottom fish and soft benthos near SONGS. This Appendix presents some rough calculations of (1) the distance and direction the organic detritus is likely to travel before settling to the bottom and (2) the fallout rate. In particular, we are interested in whether the organic detritus from SONGS could settle to the bottom as far as 6 km downcoast and 1.7 km offshore of the diffusers, where BACIP analyses have shown increased abundance of soft benthic organisms.

We can get an order-of-magnitude estimate of how far detritus will spread, starting from the estimates of long-term mean concentrations of effluent from SONGS in ECO-M's Final Report (Vol. II-2, 10/15/87). Getting detritus out to 6 km downcoast or 1.7 km offshore from the diffusers will mainly be done by natural dispersion, since the plume momentum is largely diluted or lost at these ranges. A simplified version of the dispersion model used for effluent concentrations represents the distribution of an instantaneous release as a normal distribution in two dimensions, with the standard deviations of x and y given as $\sigma_x = \nu_y t$ for offshore distance from SONGS, where t is the time since release. The dispersion velocities used in the effluent calculations were ν_x = 7.2 cm/sec and ν_y = 2.8 cm/sec.

A set of particles with settling-rate s released a height D above the bottom would sink to the bottom in a time t = D/s, and the normal distribution with this value of t would give the distribution of these particles on the bottom. A continuous or intermittent release of similar particles would accumulate similar distributions, without changing the shape. The center of the distribution will be displaced a distance Vt downcoast from SONGS, V being the long-term mean velocity of 2.9 cm/sec. Most of the particles will reach the bottom within two standard deviations in any direction from this center.

For a round number, let us take the initial height D as 7 m; even if the jets initially carry detritus from SONGS to the surface at 10 - 15 m above the bottom, the particles will mix back downward to some extent as they disperse. This gives $\sigma_x \sim 1/2s$ and $\sigma'_y \sim 1/5s$, in centimeters when s is given in cm/sec.

This would be the place to put in any observed values of actual settling-rates for dead plankton and detritus of various sizes and shapes. Lacking these, the next best is to go by Stokes' Law; taking the density contrast as 0.1 for another round number, this will give $s \sim 500d^2$ for the settling-rate in cm/sec of a particle with diameter d in centimeters. The table below shows the displacement Vt, σ_x and σ_y, all in kilometers, for particle diameters in microns (10^{-6} m).

D	Vt	σ_x	σ_y
10 μ	50 km	100 km	40 km
30 μ	5 km	10 km	4 km
100 μ	0.5 km	1 km	0.4 km

APPENDIX E

Dispersion and Settling of Organic Detritus from SONGS

The water discharged from SONGS contains organic detritus (from the plankton killed during their passage through the plant) that settles out from the plume. The consequent enrichment of the bottom is one possible mechanism explaining the increased abundance of bottom fish and soft benthos near SONGS. This Appendix presents some rough calculations of (1) the distance and direction the organic detritus is likely to travel before settling to the bottom and (2) the fallout rate. In particular, we are interested in whether the organic detritus from SONGS could settle to the bottom as far as 6 km downcoast and 1.7 km offshore of the diffusers, where BACIP analyses have shown increased abundance of soft benthic organisms.

We can get an order-of-magnitude estimate of how far detritus will spread, starting from the estimates of long-term mean concentrations of effluent from SONGS in ECO-M's Final Report (Vol. II-2, 10/15/87). Getting detritus out to 6 km downcoast or 1.7 km offshore from the diffusers will mainly be done by natural dispersion, since the plume momentum is largely diluted or lost at these ranges. A simplified version of the dispersion model used for effluent concentrations represents the distribution of an instantaneous release as a normal distribution in two dimensions, with the standard deviations of x and y given as $\sigma_x = \nu_y t$ for offshore distance from SONGS, where t is the time since release. The dispersion velocities used in the effluent calculations were ν_x = 7.2 cm/sec and ν_y = 2.8 cm/sec.

A set of particles with settling-rate s released a height D above the bottom would sink to the bottom in a time t = D/s, and the normal distribution with this value of t would give the distribution of these particles on the bottom. A continuous or intermittent release of similar particles would accumulate similar distributions, without changing the shape. The center of the distribution will be displaced a distance Vt downcoast from SONGS, V being the long-term mean velocity of 2.9 cm/sec. Most of the particles will reach the bottom within two standard deviations in any direction from this center.

For a round number, let us take the initial height D as 7 m; even if the jets initially carry detritus from SONGS to the surface at 10 - 15 m above the bottom, the particles will mix back downward to some extent as they disperse. This gives $\sigma_x \sim 1/2s$ and $\sigma'_y \sim 1/5s$, in centimeters when s is given in cm/sec.

This would be the place to put in any observed values of actual settling-rates for dead plankton and detritus of various sizes and shapes. Lacking these, the next best is to go by Stokes' Law; taking the density contrast as 0.1 for another round number, this will give $s \sim 500d^2$ for the settling-rate in cm/sec of a particle with diameter d in centimeters. The table below shows the displacement Vt, σ_x and σ_y, all in kilometers, for particle diameters in microns (10^{-6} m).

D	Vt	σ_x	σ_y
10 μ	50 km	100 km	40 km
30 μ	5 km	10 km	4 km
100 μ	0.5 km	1 km	0.4 km

The oversimplification of these estimates is large and obvious, but it doesn't take away the main conclusion that organic particles can go many kilometers before they first settle, if they are small enough. The result does suggest that most of the zooplankton killed by SONGS reach the bottom before they get 6 km downcoast or 1.7 km offshore from the diffusers. The mass of phytoplankton killed by SONGS is most probably several times greater than that of zooplankton, though, from the usual food-chain arguments. If a good fraction of these dead phytoplankton are about 30 μ or less in diameter, they provide a reasonable source for long-range effects of SONGS on benthic organisms and bottom-feeding fish.

The same line of argument also supplies equally rough order-of-magnitude estimates of the fallout rate r for given ranges of x and y, given the rate q at which SONGS produces organic detritus. This fallout rate will be the normal distribution

$$r = (q/2\,\sigma_x\sigma_y)\exp\{-(x-Vt)^2/2\sigma_x^2\}\exp\{-y^2/2\sigma_y^2\}$$

For an example, suppose SONGS produced 1000 tons dry weight per year of dead phytoplankton about 30 microns in diameter. At 6 km directly downcoast (y = 0), r is on the order of 40 kg per hectare per year. At 1.7 km directly offshore (x = 0), r is also on the order of 40 kg per hectare per year. If the particles were 100 microns in diameter, the fallout rate would be on the order of 2 kg/Ha-yr at 6 km downcoast but would still be on the order of 40 kg/Ha-yr at 1.7 km directly offshore.

Besides being crude by nature, this model also takes no account of the kelp bed, which will certainly affect natural dispersion as well as the plume in the region

we are talking about. So "on the order of" means what is says: the confidence limits on a result are something like a factor of 10 either way.

Note that these rates have no relation to the relative concentration of a non-settling tracer given in the ECO-M report cited above. The only feature in common is that both are calculated with the same dispersion velocities ν_x and ν_y. Mean tracer concentration from a continuous source can reach a steady state because the tracer is dispersing into an ocean that is practically infinite compared to the strength of the source. But particles continually settle out on a finite region of the bottom, and will accumulate except as they are dispersed by high waves or eaten by organisms.

APPENDIX F
FLOW CHARTS OF DATA ANALYSIS

5.0 SONGS EFFECTS ON IRRADIANCE

5.1 BACIP ANALYSES

A. Results for I and ln I downcurrent and upcurrent days, Appendix A, Table 1.

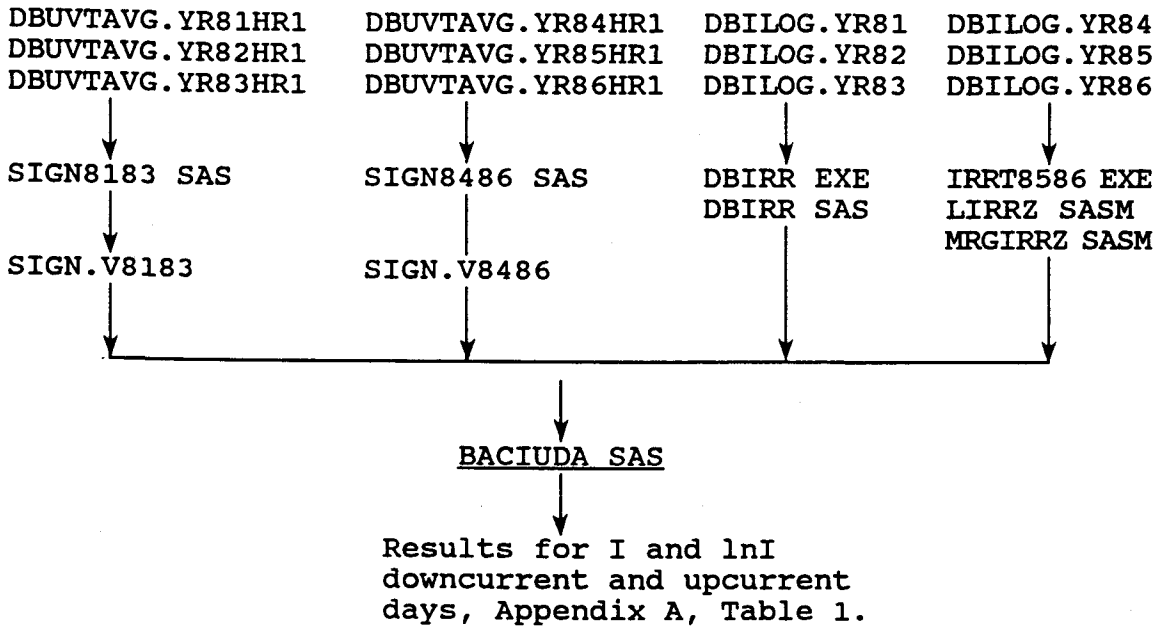

B. Results for I all days, Appendix A, Table 1.

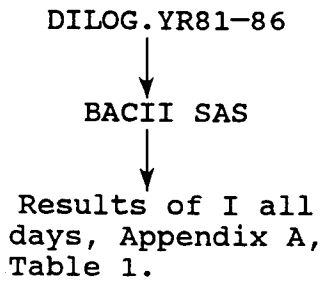

C. Results for I all days, Appendix A, Table 1.

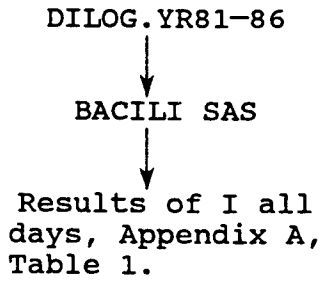

5.2 Plume-model and Upstream-Downstream Analyses.

A. Creating PLUMEAGE.YR8486 data base

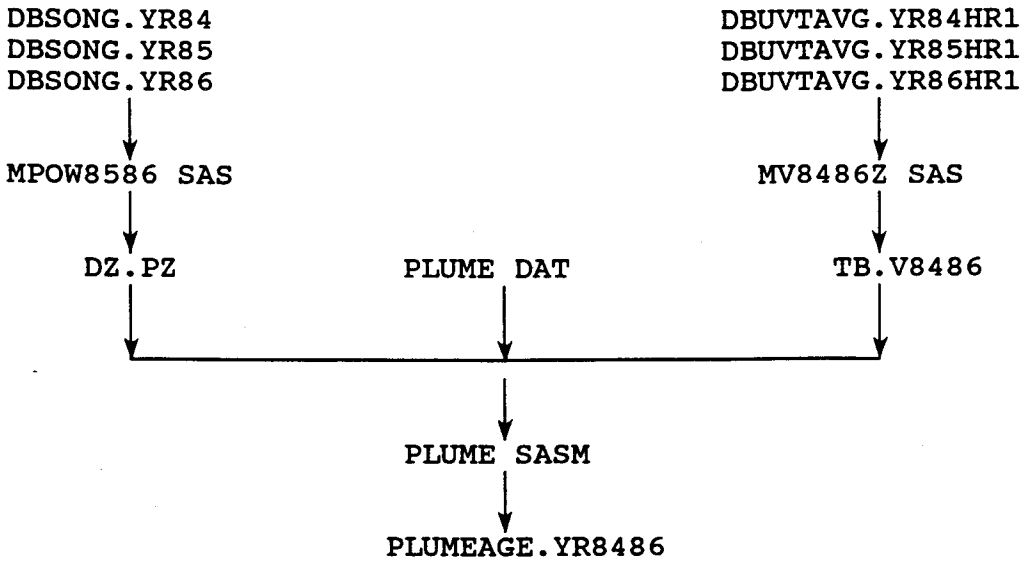

B. Results of Plume model, Appendix A, Table 2.

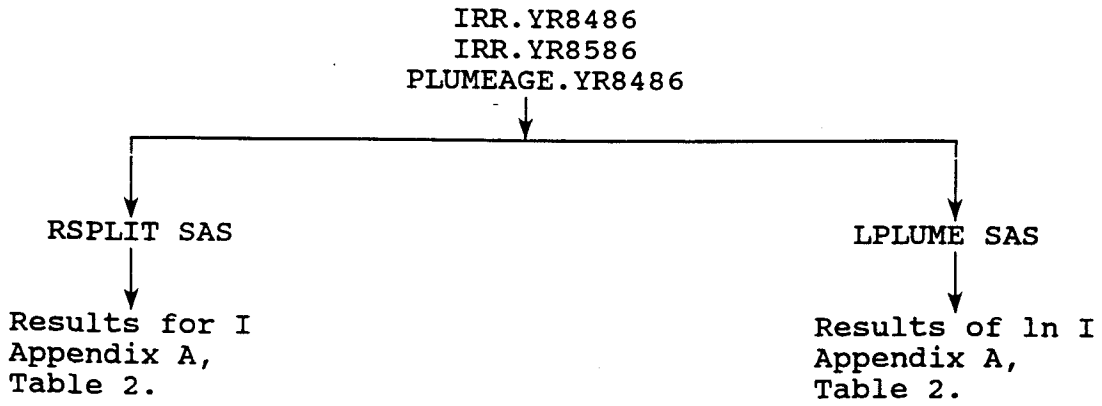

C. Results of UPstream-Downstream analyses, Appendix A, Table 3.

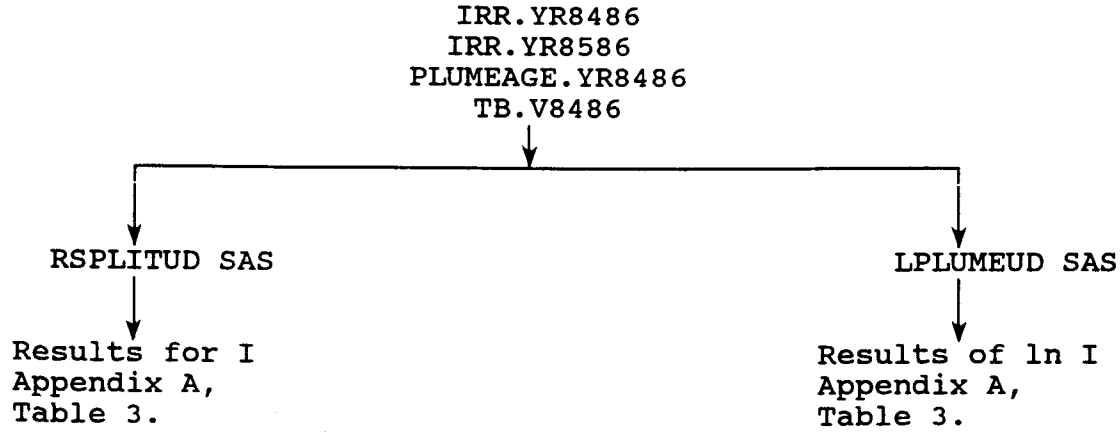

6.0 EFFECTS OF SONGS ON TEMPERATURE AND SUSPENDED PARTICLES.

6.1 Compliance with Thermal Standards

A. Plume model analyses of temperature at 3m depth for four stations UVT01, UVT17, UVT18 AND UVT19.

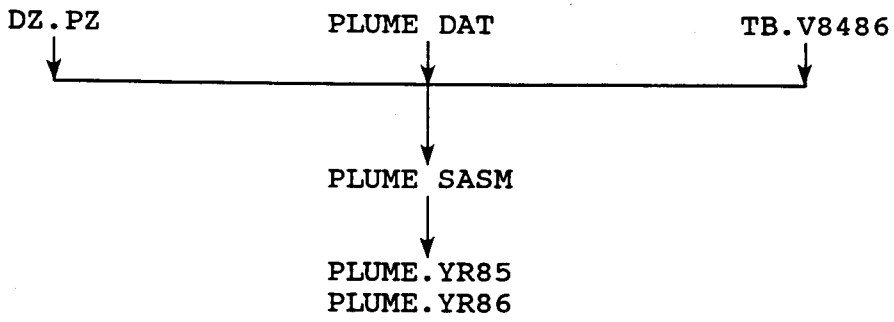

B. Creating temperature data bases in format suitable for program Trsplit SAS

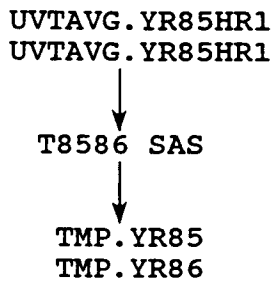

C. Plume model results on temperature.

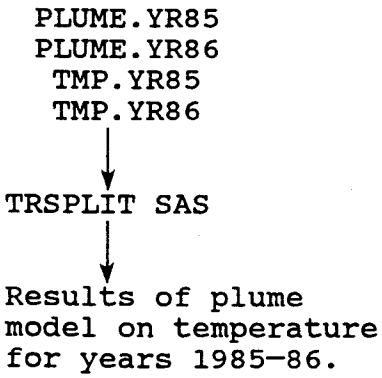

D. Descriptive statistical results on temperature difference.

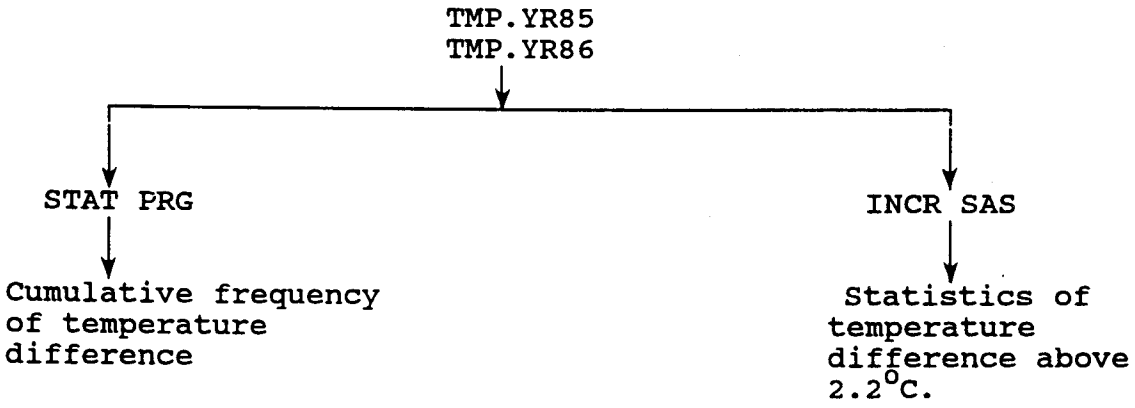

6.2 SONGS-induced Upwelling, BACIP analyses of bottom temperature

A. Creating T.YR8183 and T.YR8486

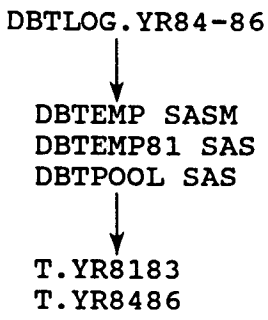

B. BACIP results of bottom temperature

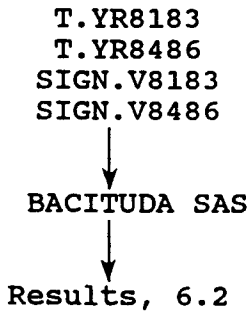

6.3 Suspended Particles

A. Results for untransformed data, 6.3. This is one of several analyses of seston flux that reported, with flow charts, in Technical Report K.